INTEGRATED FIELD OPTIMIZATION ON UNISIM-I-D BENCHMARK CASE

A Thesis

by

CHAIYAPORN SURANETINAI

Submitted to the Office of Graduate and Professional Studies of
Texas A&M University
in partial fulfillment of the requirements for the degree of

MASTER OF SCIENCE

Chair of Committee,	Eduardo Gildin
Committee Members,	John Killough
	Maria A. Barrufet
Head of Department,	Daniel Hill

August 2017

Major Subject: Petroleum Engineering

ABSTRACT

Integrated field optimization is known to be a useful tool to evaluate oil and gas asset performance and maximize asset's value. However, it is not an easily achievable task due to its complexity. This study aims to assess the potential of the integrated optimization on UNISIM-I-D benchmark case, and a surface network model. The objective of the optimization is to maximize the asset's Net Present Value by choosing the optimal surface facilities capacity. The integration of the model or being called as coupling is carried out in INTERSECT field management software while the reservoir is modeled in ECLIPSE reservoir simulator and the surface network is modeled in PIPESIM steady-state flow simulator. MATLAB codes are used to operate all the commercial software and automatically analyze the results obtained from them. Optimizations are performed on MATLAB Optimization Toolbox™.

The reservoir is treated as a black oil model while the surface network is a steady-state simulation. The partially implicit coupling scheme is selected to be used to optimize the computational effort and maintain the accuracy of the results. The purpose of having MATLAB codes executing the commercial software is that these codes will be able to be directly applied to the industry's working resources.

Simulations are run in both uncoupled and coupled fashion. Surface facilities limits from UNISIM-I-H model are used in a base case. Base case results from the uncoupled and coupled cases are identical which confirm the accuracy of the coupled simulations and

signify that at the base case conditions, effects from the surface network are not significant.

The optimal results show 3-7% improvement in the asset's Net Present Value while optimizing the oil processing capacity, water processing capacity, and water injection capacity. Although some cases may have the same oil recovery at the end of production period, the asset's Net Present Values are different. Cumulative water production, cumulative water injection, and production timing affect the final asset's value in the economic point of view. The optimal surface facilities capacity ends up at the pre-defined lower boundary which can be implied that there is a bottleneck in the well performance.

ACKNOWLEDGEMENTS

First of all, I would like to thank my advisor, Dr. Eduardo Gildin for all the guidance, supports, and encouragement. My work would not be completed without his kind and supportive advices. I would also like to thank Dr. John Killough and Dr. Maria A. Barrufet for being my committee members and for their constructive and insightful recommendations throughout this study. All of them have inspired me to continuously develop myself.

I would like to thank PTT Exploration and Production Public Company Limited, my employer, for the graduate study scholarship and for all the opportunities they have been giving to me. Thanks to Texas A&M Petroleum Engineering department and IFP School, France for having me in their dual degree program.

Thanks also go to my friends, colleagues, faculty and staff both at Texas A&M University and IFP School for making my graduate study a memorable experience. I would like to extend my appreciation to Texas A&M Thai Student Association for being like a family, and for the generous helps and supports throughout these years.

Finally, I would like to express my gratitude to the most important people in my life, my family and my boyfriend, Danai. Thanks for always being here for me through good and bad times. Without their love, encouragement, understanding, patience, and support, I wouldn't have made it this far, and I wouldn't have achieved this study.

CONTRIBUTORS AND FUNDING SOURCES

This work will not be completed without supports from a thesis committee consisting of Dr. Eduardo Gildin and Dr. John Killough of the Department of Petroleum Engineering and Dr. Maria A. Barrufet of the Department of Chemical Engineering.

All work for the thesis was carried out by the student, under the supervision of Dr. Eduardo Gildin of the Department of Petroleum Engineering.

Graduate study was sponsored by a scholarship from PTT Exploration and Production Public Company Limited, Bangkok, Thailand.

NOMENCLATURE

A	Pipe Cross-sectional Area
AC	Abandonment Cost
API	American Petroleum Institute Gravity Unit
B	Formation Volume Factor
B_o	Oil Formation Volume Factor
B_w	Water Formation Volume Factor
B_g	Gas Formation Volume Factor
BHP	Bottomhole Pressure
C_{p_o}	Oil Processing Capacity
C_{p_w}	Water Processing Capacity
C_{i_w}	Water Injection Capacity
d	Pipe Diameter
d	Discount Rate
DEIM	Discrete Empirical Interpolation Method
f	Friction Factor
g	Gravitational Acceleration
g_c	Conversion Factor for Gravitational Acceleration
GOR	Gas-Oil Ratio
h	Reservoir Thickness
Inv	Total Investment on Equipment and Facilities

Inv_{plat}	Investment on Platform
Inv_{drill}	Investment on Drilling and Completion
Inv_{conn}	Investment on Well-Platform Connection
IAM	Integrated Asset Modeling
ICV	Inflow Control Valve
IPR	Inflow Performance Relationship
J^{-1}	Jacobian Matrix
J	Optimization Objective Function
J^n	Objective Function at Timestep n
k	Permeability
k_{ro}	Relative Permeability to Oil
k_{rw}	Relative Permeability to Water
k_{rg}	Relative Permeability to Gas
k_x	Permeability in the x-direction
k_y	Permeability in the y-direction
$\widetilde{m}$	Mass Flux per Volume Unit
n_w	Total Number of Wells
N_c	Newton Iteration Number
N_t	Total Number of Calculation Timestep
NCF	Net Cash Flow
NLP	Nonlinear Programming
NPV	Net Present Value
OC	Operational Cost

OPR	Outflow Performance Relationship
p	Pressure
p_o	Oil Phase Pressure
p_w	Water Phase Pressure
p_g	Gas Phase Pressure
p_b	Bubble Point Pressure
p_{cow}	Oil-Water Capillary Pressure
p_{cgo}	Gas-Oil Capillary Pressure
p_{wc}	Pressure of Grid Block Containing Well
p_{wf}	Bottomhole Flowing Pressure
p_{sep}	Separator Pressure
p_{t1}	Tubing Pressure at the Bottomhole
PID	Proportional, Integral, Derivative Control
POD	Proper Orthogonal Decomposition
PVM	Parallel Virtual Machine
PVT	Pressure, Volume, Temperature Relationship
$\tilde{q}_o$	Oil Phase Mass Flow Rate
$\tilde{q}_w$	Water Phase Mass Flow Rate
$\tilde{q}_g$	Gas Phase Mass Flow Rate
q_o^*	Oil Phase Volume Flow Rate
q_w^*	Water Phase Volume Flow Rate
q_g^*	Gas Phase Volume Flow Rate

r_o	Equivalent Grid Block Radius
r_w	Wellbore Radius
R	Residual Vector
R_{sur}	Residual Vector of Surface Flow Equation
R_{res}	Residual Vector of Subsurface Flow Equation
R_{ro}	Residual Vector of Oil Discretization Equation
R_{rw}	Residual Vector of Water Discretization Equation
R_{rg}	Residual Vector of Gas Discretization Equation
R_{Wo}	Residual Vector of Well Oil Flowing Equation
R_{Ww}	Residual Vector of Well Water Flowing Equation
R_{Wg}	Residual Vector of Well Gas Flowing Equation
$R_{sur,o}$	Residual Vector of Tubing/Piping Oil Flowing Equation
$R_{sur,w}$	Residual Vector of Tubing/Piping Water Flowing Equation
$R_{sur,g}$	Residual Vector of Tubing/Piping Gas Flowing Equation
$R_{sur,p}$	Residual Vector of Energy Conservation Equation
R_{BHP}	Residual Vector of Bottomhole Pressure Equation
R_{bc}	Residual Vector of Boundary Condition Equation
R_s	Solution Gas Ratio
Re	Reynolds Number
R	Gross Revenue from Oil Selling
Roy	Royalties
s	Skin Factor

S	Saturation
S_o	Oil Phase Saturation
S_w	Water Phase Saturation
S_g	Gas Phase Saturation
SQP	Sequential Quadratic Programming
ST	Social Taxes
t	Time
T	Corporate Tax Rate
THP	Tubing Head Pressure
U_{res}	Unknown Subsurface Parameters
U_{sur}	Unknown Surface Parameters
v	Fluid Velocity
v_m	Gas/Liquid Mixture Velocity
v_x	Fluid Velocity in x-direction in the Cartesian Coordinate
V_G	Gas Volume
V_o	Oil Volume
V_{res}	Fluid Volume at Reservoir Conditions
V_s	Fluid Volume at Surface Conditions
V_{seg}	Volume of Pipe Segment
VFP	Vertical Flow Performance Relationship
w	Fluid Mass Flowrate
WI	Peaceman's Well Index
WAG	Water-Alternate-Gas Injection

x	Distance in x-direction in the Cartesian Coordinate
y	Distance in y-direction in the Cartesian Coordinate
y_l	Liquid Holdup
y_g	Gas Holdup
z	Distance in z-direction in the Cartesian Coordinate
Δp_{pipe}	Pressure Loss across Piping and Flowline
Δp_{choke}	Pressure Loss across Choke Valve
Δp_{tubing}	Pressure Loss across Production Tubing
Δp_{valve}	Pressure Loss across Valves and Fittings
∂x	Solution Vector of Newton-Raphson Linearization
∂x_{sur}	Solution Vector of Newton Linearization of Surface Flow
∂x_{res}	Solution Vector of Newton Linearization of Subsurface Flow
ρ	Fluid Density
ρ_o	Oil Density
ρ_w	Water Density
ρ_g	Gas Density
ρ_{Go}	Solution Gas Density
ρ_m	Gas/Liquid Mixture Density
ρ_l	Liquid Density
ϕ	Porosity
μ	Viscosity
μ_o	Oil Viscosity
μ_w	Water Viscosity

μ_g	Gas Viscosity
μ_{Go}	Solution Gas Viscosity
μ_m	Gas/Liquid Mixture Viscosity
μ_l	Liquid Viscosity
λ	Mobility Ratio
λ_o	Oil Mobility Ratio
λ_w	Water Mobility Ratio
λ_g	Gas Mobility Ratio
γ_o	Oil Hydrostatic Gradient
γ_w	Water Hydrostatic Gradient
γ_g	Gas Hydrostatic Gradient
θ	Pipe Inclination Angle
δU	Correction Vector of Newton - Raphson's Linearization
$\left(\frac{dp}{dz}\right)$	Total Pressure Gradient
$\left(\frac{dp}{dz}\right)_{pe}$	Pressure Gradient from Hydrostatic
$\left(\frac{dp}{dz}\right)_{f}$	Pressure Gradient from Friction
$\left(\frac{dp}{dz}\right)_{a}$	Pressure Gradient from Acceleration

TABLE OF CONTENTS

Page

Page

Page

LIST OF FIGURES

Page

Page

Page

LIST OF TABLES

Page

1. INTRODUCTION

The oil and gas industry comprises of major elements, from the subsurface to surface to the end consumer and the stakeholders. Each part of the industry has developed modeling tools to work with its functionality - reservoir simulators, network pipeline simulators, surface processing facilities simulators, and economic models. As a result of different backgrounds and disciplines, each element of the business has limited knowledge on how changes in its model would influence each other. As an example, upstream and downstream parts are being treated in separate domains.

Managing and operating complex assets requires a comprehensive view of the whole value chain. An integrated model will help every discipline to identify dependent and dynamic parameters those are not being determined while using individual models. Although a multidisciplinary culture which improves communications between teams has been promoted in the industry, the integration of all the models still poses technical challenges due to the complexities of the problems. In this project, we tackle integration by investigating the interplay between a reservoir model (subsurface), a well and network model (surface), and an economic model.

Integrations of these models can be carried out by a method called coupling. The general concept of subsurface and surface coupling is to connect both models by exchanging their parameters. Subsurface and surface coupling is being performed in the industry by means of three main schemes; explicit coupling, implicit coupling, and fully implicit coupling.

The differences of these schemes are, firstly, how subsurface and surface models are being treated, secondly, how models exchange their controlled parameters, and lastly, how the models' convergence takes place. If the subsurface and surface models are solved sequentially, depended only on the convergence of reservoir equations, and the coupling is being performed at the beginning of the timestep, then the scheme is explicit. The implicit scheme works similarly to the explicit method, but the coupling is being operated at Newton iteration level. If subsurface and surface models are being treated as a single model and the convergence of both reservoir and surface facilities equations is taking place simultaneously, the scheme is fully implicit. While being able to provide more accurate results, tighter coupling such as fully implicit scheme is the most numerically complicated and computationally expensive. Therefore, optimizing how efficient the coupled algorithms are is one of the keys to achieving practical solutions.

To cope with the volatility of the oil price, optimization is one of the approaches to gain more oil and gas recovery and reduce investment and production costs. Integrated field planning and optimization studies in the past have revealed the potential of reservoir and facilities management improvement which leads to a maximization of asset's economic value. Optimization of the integrated model will enable one to understand effects of controlled variables on the project's objective and can be applied to various stages of field life resulting in, an initial field development plan, an advanced operational control, production strategy changes in a mature field, etc. There exist several optimization techniques that can be employed to the integrated model but, due to different applicability, selection of the optimization techniques is crucial to get the optimal results.

1.1. Literature Review

According to Rahmawati et. al. (2012), integrated field optimization has been in an interest of the industry in recent years. Methods have been continuously developed on both areas of models integration and optimization techniques. Iemcholvilert (2013) presented that the model integration started from earlier researchers combining more complex well models into a reservoir simulator, was expanded to include pipeline networks and surface facilities. Currently, the whole petroleum production value chain is taken into account. The models combining the petroleum production system from reservoir sand face to the points of sales is called an Integrated Asset Modeling (IAM) (Serbini et. al. (2009)).

With a benefit of an advanced integration, several pieces of research presented significant improvements in petroleum field management, planning, and operation while imposing optimization techniques on the integrated model comparing to independent optimization approach. To provide a background to this project, we briefly review some of the published works on models integration and optimization in this section.

1.1.1. Integration of Surface Network Simulator and Reservoir Simulator

Hepguler et. al. (1997) and Hepguler and Dutta-Roy (1997) suggested an ability of tightly integrated reservoir and surface simulators using Parallel Virtual Machine (PVM) interface for field development and planning purposes. Two commercial models, namely, ECLIPSE and NETOPT, were used and converged successfully while changes in both models were taken into account representing more realistic field behavior than separately used simulators. Trick (1998) used the same interface but different surface network

simulator with Hepguler et. al. (1997). The highlight of the study was an application of implicit coupling which the models were converged at Newton iteration level rather than timestep level. The study also improved the computational time from the previous studies.

Güyagüler and Ghorayeb (2006) presented a field management workflow combining reservoir simulators, surface network models, process modeling simulators, and economic packages from the same vendor with utilities to produce cases to assist field development planning, facilities design, and optimization. Some commercial software's have also been launched to provide an integration of various models using in the petroleum industry; however, there was a limitation on the compatibility from different vendors. Juell et. al. (2009) used an integration and optimization software to simulate the optimization of two gas-condensate reservoirs producing to a common process facility. Rahmawati et. al. (2010) extended Juell et. al. (2009) works by adding one miscible WAG reservoir. Gas from surface facilities was reinjected to the reservoirs leading to more interactions between all individual models; thus, an optimization on the tightly coupled model showed significant improvement in net present value. Iemcholvilert (2013) and Gao (2014) implemented a production optimization with simple production constraints on the various level of coupled subsurface and surface model. The outcomes of the projects demonstrated the importance of coupling scheme selection on the optimal results. Both commercial software and a MATLAB open-source code for reservoir simulation developed by SINTEF (Knut-Andreas Lie (2016)) were utilized. Rahmawati et. al. (2014) introduced an integrated model between reservoir simulators and network simulators from three different vendors. The coupling was successfully carried out at a timestep level (explicit coupling) with an expansion from only black oil PVT model to compositional model.

1.1.2. Field Development Optimization

With an advantage of the developing model integration, optimization to obtain the best return-on-investment becomes a vital task, especially in the relatively low oil price scenario. To minimize an investment by optimal placement and selection of production facilities, Ding and Startzman (1996) reported algorithms using mathematical programming with a concept of model reduction and preprocessing. The system saved several million dollars in investment. Schiozer and Mezzemo (2003) developed a new field development planning approach regarding economic constraints. The proposed methodology gave a set of good decision-making alternatives as a result of optimization.

Litvak et. al. (2007) proposed an in-house field development technology with an ability to handle multiple reservoir and surface facilities models in a probabilistic approach. Results from the optimization showed significant improvement in oil recovery, sweep efficiency, and asset's net present value. Serbini et. al. (2009) performed an explicitly integrated asset modeling study using seven reservoirs, more than one hundred production wells, and four surface facilities network models. The results identified the bottleneck of the system and proposed a debottlenecking scenario. Production losses that might have occurred from suboptimal design were evaluated.

Temizel and Tiwari (2016) outlined advantages of next-generation reservoir simulators which are used to perform Integrated Asset Modeling (IAM). By having those simulators running simultaneously, they achieved the faster run time and more robust results.

1.1.3. Optimization Techniques

Apart from a strong focus on optimization application to the field, there are a lot of optimization techniques that are being developed and used in the oil and gas industry. Each technique suits a particular type of problems. Some of the applications on the field development and production optimization problems are shown here as examples. Wang et. al. (2007) pointed at the drilling of the wells at optimal locations to extract more hydrocarbons at a lower cost. The paper presented an idea to convert well placement optimization problem from discrete non-gradient-based into continuous gradient based optimization that is being used in the industry. The results provided a good start in developing more robust and efficient optimization algorithms.

Li and Jafarpour (2011) used a gradient-based method to solve well control optimization problem while coupling with a well placement optimization problem. The results showed the improvements on recovery performance and economic value. Echeverría Ciaurri et. al. (2012) integrated the massive amount of data obtained by the Intelligent Fields (Smart Fields, Closed-Loop Reservoir Management, etc.) with mathematical optimization and decision making algorithms, thus, added more robustness into the earlier optimization methodologies. Sampaio Pinto et. al. (2015) proposed a new framework using proper orthogonal decomposition (POD) with the discrete empirical interpolation method (DEIM) to perform an optimization in gradient-based approach using forward and adjoint model. Computational efforts to obtain the optimal solution of the complex reservoir were reported to be significantly reduced. However, using gradient-based optimization techniques with gradient computed using adjoint model is time-consuming, Moraes et. al.

(2017) presented a workflow that combines multi-scale (MS) forward simulator and stochastic gradient computation for well controls optimization. The improvement in speed and accuracy obtained from the workflow allows users to be able to tackle a large-scale optimization problem.

Most of the abovementioned studies were performed by using gradient-based optimization and faced the challenge of obtaining the accurate gradient information. Echeverría Ciaurri et. al. (2012a) demonstrated the applicability of derivative-free optimization methods on generally constrained production optimization problems while comparing the results with a gradient-based algorithm. Due to the complexity of a mixed-integer nonlinear programming problem, Obiajalu (2013) also suggested the noninvasive derivative-free generalized field development optimization be applied to the real cases where there is no available gradient information.

1.1.4. Benchmark Cases

Benchmark cases were widely developed to evaluate the performance of developing integration and optimization methodologies. In this thesis, we develop an optimization framework applied to one of the benchmark cases developed in the literature. In particular, we will use the UNISIM-I-D case generated by a research group in State University of Campinas, Brazil (Avansi and Schiozer (2013)). Avansi and Schiozer (2013) introduced how the synthetic UNISIM-I-R model was generated from data of Namorado Field, Campos Basin, Brazil to represent a real reservoir. The UNISIM-I-R contains high-resolution data from well logging, core samples, and 3D seismic resulting in more than 3

million active grid cells. The UNISIM-I-R model was later upscaled for production strategy selection study and was named as UNISIM-I-D model. The study also simulated a base production strategy to compare results of UNISIM-I-R and UNISIM-I-D. The results are used as a benchmark of this project. Garpar et. al. (2014) extended Avansi and Schiozer (2013) by explaining more details on a benchmark model, UNISIM-I-D. UNISIM-I-D is a medium numerical grid resolution model with about 37,000 active grid cells. The purpose of the UNISIM-I-D model is to serve as a study case for oil field development and production strategy selection. Physical restrictions were included. The expected result of this benchmark case is an oil production development strategy stating key parameters.

Field development and production forecast require proper knowledge on the dependency between subsurface reservoir behavior and surface facility constraints. Earlier, reserves and production were predicted by using only reservoir simulations and material balance calculations. This approach led to inaccurate results since most of the production parts were neglected. Management of produced fluids was also not able to be performed, and reservoir management was improperly posed. With no effect from other wells and surface equipment, all the wells oil production is often overestimated while having excessive water production. Here presents the gap of the field development case that can be fulfilled by the integration of the surface network. The surface processing capacities optimization and rate allocation will be carried out to minimize investment, maximize the oil production and minimize unwanted fluids; thus, having the maximum asset's net present value.

1.2. Thesis Objectives

This project aims to assess the potential of the integrated field optimization with different available coupling techniques. A UNISIM-I-D benchmark case will be optimized in the field development phase to demonstrate the effects of surface facilities and operational parameters on economic values.

1.3. Scope of Study

To assess the potential of the integrated optimization and exhibit the adaptability to the industry, subsurface and surface coupling is performed mainly on the commercial software. Commercial simulators that are being used in this project are ECLIPSE reservoir simulator, INTERSECT field management system, and PIPESIM steady-state network simulator. On the other hand, MATLAB is being used as a programming language for data management and optimization. The UNISIM-I-D benchmark case is used in this study. Proposed commercial simulators have an ability to perform two partial coupling schemes, i.e. explicit coupling, and partially implicit coupling. Effects of coupling schemes and frequency on production performance will be demonstrated. Optimal coupled model will be further used in integrated field optimization.

The construction of the optimization model, parameters, and constraints follow the conditions stated in the benchmark. Although there can be several possible objectives for each project, the optimization objective of this study is a maximization of asset's net present value (NPV), and the optimization is carried out in the field development phase.

In this case, producing each fluid at the minimum investment and at the right point in time is paramount to gain maximum return. In this project, the controlled variables (i.e. decision variables) selection focuses on the interface between reservoir and production facilities. Influences of the production tubing, pipeline size, and capacity of surface facilities will be investigated. Restrictions and limitations provided with UNISIM-I-D case will be utilized as the constraints. This project's problem will be treated as a nonlinear programming problem.

1.4. Thesis Organization

Apart from this introductory section, this thesis contains five more sections. The second, and third sections discuss the brief fundamental theories on subsurface/surface modeling, and subsurface/surface coupling, respectively. The fourth section exhibits the model development, the use of numerical simulations and related software while the fifth section shows the results of the optimization. Conclusion and recommendation are summarized in section six.

2. SUBSURFACE AND SURFACE MODELING

Petroleum production system consists of two main parts which are subsurface and surface. The simplified petroleum production system taken from Economides et. al. (2013) is shown in Figure 1 where the system comprises of the reservoir, the well, and the surface facilities. We will use Figure 1 as a reference to briefly explain the petroleum production system in this section.

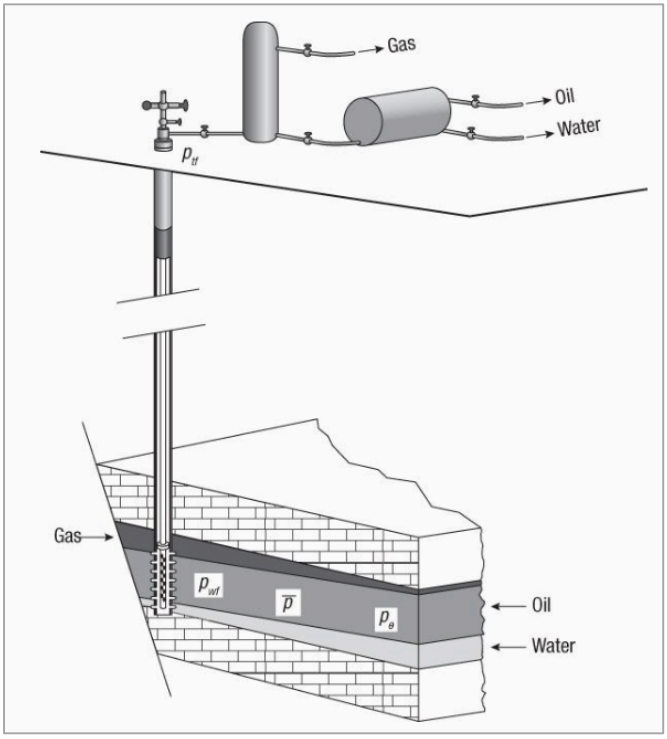

Figure 1 Petroleum production system

Source: Reprinted with permission from Economides et. al. (2013)

Fluids are initially present in the reservoir pore space in an equilibrium condition with reservoir pressure p_e, and average pressure $\bar{p}$. Once field development started, wells are drilled into the reservoir causing pressure difference between reservoir and wellbore. The pressure at the bottom part of the well is called the bottomhole pressure and denoted as p_{wf}. The pressure difference $(p_e - p_{wf})$, also called pressure drawdown, then becomes a driving force for fluid to flow in the reservoir porous media. Flow of fluid in the reservoir depends upon several parameters, including reservoir parameters, and fluid characteristics. Reservoir thickness, reservoir permeability, and fluid viscosity are among the most important parameters. We can present the relationship between flow in the reservoir and bottomhole pressure by assuming constant reservoir pressure in terms of equation and call it an inflow performance relationship (IPR) (Economides et. al. (2013)).

Once fluid reaches the well, it needs to be lifted up to the surface. The energy used to lift the liquid up is from the pressure of the fluid at the bottomhole p_{wf}. This pressure needs to overcome the pressure loss along the well to achieve the required tubing head pressure p_{tf}. This tubing head pressure is normally set by the requirement of surface facilities. It acts as a boundary of a simple production system evaluation; hence, in the single well model, we can present the relationship between flow in the well and the bottomhole pressure by assuming constant tubing head pressure and call it an outflow performance relationship (OPR). It is noted that the outflow performance relationship is not limited to the conditions affected by only the well but can be extended to cover the transportation of the fluid from the distant well to the separation facility.

To produce oil and gas, one must find a relationship between how fluids flow in the reservoir to the well and how those fluids are being transported to the surface. The subsurface inflow performance relationship (IPR) determines what the reservoir can deliver while surface outflow performance relationship (OPR) or sometimes called as vertical flow performance (VFP) determines what well and surface network can deliver. Their graphical representation is depicted in Figure 2. The graphical intersection of those two relationships provides us the well deliverability as an expression of what we will get from the well at the given conditions.

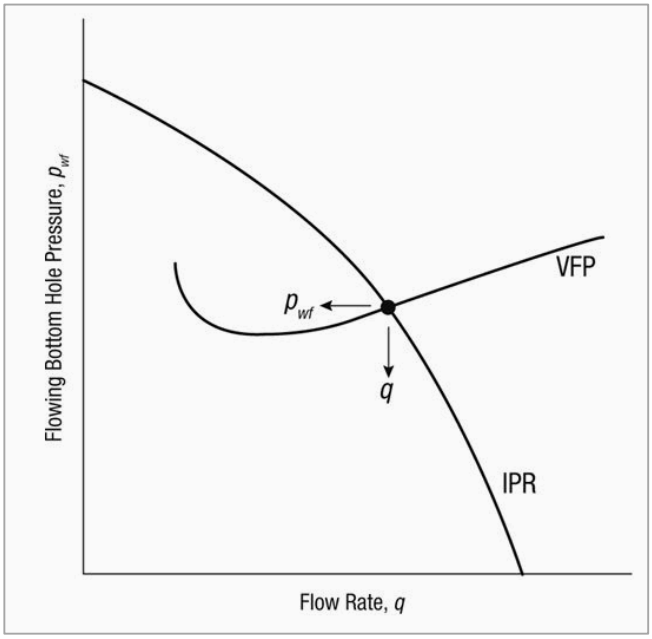

Figure 2 Combination of IPR and VFP

Source: Reprinted with permission from Economides et. al. (2013)

Due to different functions, subsurface and surface models are built and utilized separately. They are being treated as two separate domains, and the exchange in controlled parameters (for example, bottomhole flowing pressure and flowrates) are occasionally carried out. The subsurface model consists of reservoir and well models while the surface model consists of production gathering system, processing facilities, and exporting network. Subsurface and surface simulations and system design are based on the fixed wellhead pressure. Although the bottomhole flowing pressure and flowrates change with production time, dynamics of both systems are not considered together which makes the production operations and optimization less efficient.

Given the separation between subsurface and surface simulations and the fact that both have different sets of constraints, integration between them is crucial for determining the correct set of control inputs to both reservoir and surface network models. To exchange controlling parameters between subsurface and surface simulations, we use the process called coupling. The primary objective of subsurface and surface coupling is to predict an accurate oil production with respect to reservoir conditions e.g. pressure, and saturations, and the surface facilities limitations e.g. tubing head pressure.

In this section, we briefly explain the theories behind reservoir and network simulations and the two sets of equations; reservoir material balance and surface process calculation, that need to be solved. Three coupling schemes are being used in the industry. The differences in the coupling methods, and the advantages and the disadvantages of each method will be presented in the next section.

2.1. Subsurface Modeling

Subsurface model in the production engineering point of view is the model that predict inflow performance relationship. It defines fluid flow in porous media with changes in pressure and fluid properties. Subsurface model in this study refers to the black oil multiphase reservoir model with a built-in function to solve well equations. The model simulates flow of three fluid phases i.e. oil, gas, and water. The black oil formulation is a derivation of Darcy's equation and material balance equations. The governing equations for reservoir modeling are exhibited by nonlinear partial differential equations. Discretization and linearization are carried out by using finite difference method to solve for pressure and saturation of each grid cell. Fluid flows in porous media equations presented in this section refer to Chen et. al. (2006).

2.1.1. Material Balance Equations

Material balance or mass conservation equation shows that the mass accumulation is a difference between mass inflow and mass outflow which can be stated as:

$$Mass_{inflow} - Mass_{outflow} = Mass_{accumulation} \tag{1}$$

External sources and sinks also have an effect on the overall mass balance so equation 1 can be rewritten by including the external source and sink term as:

$$Mass_{inflow} - Mass_{outflow} = Mass_{accumulation} \pm Source/Sink \tag{2}$$

To derive flow in porous media equations, we need to have a reservoir model. In the reservoir model, each grid cell has its properties; permeability, k, porosity, ϕ, and saturations, S, while each fluid has its density, ρ, and viscosity, μ. Flow in porous media is driven by pressure differences. Fluid flow through each grid cell affects the properties of the porous media. Also in the view of material balance, there is a mass interchange between oil and gas phases; thus, the mass conservation is not performed in each phase but the total hydrocarbon components. The general partial differential for fluid flow continuity equation derived from Darcy's equation and material balance equations are shown as:

$$-\nabla \cdot (\rho v) = \frac{\partial}{\partial t}(\rho \phi S) - \widetilde{m} \tag{3}$$

Where v is fluid's velocity, and $\widetilde{m}$ is mass flux per volume unit. Equation 3 is a general equation that needs to be applied to each fluid phase. In what follows, we present the equations for each fluid phase, i.e. oil, water, and gas. They are defined by the subscripts and are represented respectively (Chen et. al. (2006)).

$$\nabla \cdot \left[\frac{\rho_o k_{ro} k}{\mu_o}(\nabla p_o - \rho_o g \nabla z)\right] = \frac{\partial(\rho_o \phi S_o)}{\partial t} + \tilde{q}_o \tag{4}$$

$$\nabla \cdot \left[\frac{\rho_w k_{rw} k}{\mu_w}(\nabla p_w - \rho_w g \nabla z)\right] = \frac{\partial(\rho_w \phi S_w)}{\partial t} + \tilde{q}_w \tag{5}$$

$$\nabla \cdot \left[\frac{\rho_{Go} k_{ro} k}{\mu_{Go}} (\nabla p_o - \rho_o g \nabla z) + \frac{\rho_g k_{rg} k}{\mu_g} (\nabla p_g - \rho_g g \nabla z) \right] = \frac{\partial((\rho_{Go} S_o + \rho_g S_g)\phi)}{\partial t} + \tilde{q}_g \tag{6}$$

It is noted from equation 6 that fluid flow equation for gas phase is more complicated than oil and water phase since there are two sources of gas; e.g. free gas and dissolved gas. ρ_{Go} stands for the partial density of gas dissolved in oil phase.

Since mass of each phase is not conserved due to the interchange between oil and gas phase, the solution gas ratio R_s is used to determine the gas fraction dissolved in the oil. The R_s is the volume of gas at the standard conditions dissolved in stock tank oil volume at any pressure:

$$R_s = \frac{V_G}{V_o} \tag{7}$$

The volume of each phase changes with pressure and temperature. Formation Volume Factor B is used to relate the phase volume at the surface conditions and the reservoir conditions:

$$B = \frac{V_{res}}{V_s} \tag{8}$$

Relating phase at surface conditions and the relationship between volume, mass, and density, phase densities at reservoir conditions become:

$$\rho_o = \frac{R_s \rho_{G,s} + \rho_{o,s}}{B_o} \tag{9}$$

$$\rho_w = \frac{\rho_{w,s}}{B_w} \tag{10}$$

$$\rho_g = \frac{\rho_{g,s}}{B_g} \tag{11}$$

Mobility ratio λ is a ratio derived from a momentum conservation equation. It is defined as the ratio of effective permeability to the phase viscosity and formation volume factor:

$$\lambda = \frac{k_r k}{B\mu} \tag{12}$$

Substitute solution gas ratio, formation volume factor, and mobility ratio of each phase into equation 4 to 6 yields:

$$\nabla \cdot [\lambda_o (\nabla p_o - \rho_o g \nabla z)] = \frac{\partial}{\partial t}\left(\frac{\phi S_o}{B_o}\right) + \ q_o^* \tag{13}$$

$$\nabla \cdot [\lambda_w(\nabla p_w - \rho_w g \nabla z)] = \frac{\partial}{\partial t}\left(\frac{\phi S_w}{B_w}\right) + \ q_w^* \tag{14}$$

$$\nabla \cdot [\lambda_g(\nabla p_g - \rho_g g \nabla z) + R_s \lambda_o(\nabla p_o - \rho_o g \nabla z)] = \frac{\partial}{\partial t}\left(\frac{\phi R_s S_o}{B_o} + \frac{\phi S_g}{B_g}\right) + \ q_g^* + q_o^* R_s \tag{15}$$

In the porous media, the pressure of each phase related to the capillary pressures. While water is assumed to be the wetting phase, oil is the intermediate wetting phase, and gas is the non-wetting phase, relationships between phase pressures capillary pressures are shown in equation 16 and 17.

$$p_{cow} = p_o - p_w \tag{16}$$

$$p_{cgo} = p_g - p_o \tag{17}$$

It is also known that all the void space is filled with fluids. The general equation of fluid saturation constraint is:

$$S_w + S_o + S_g = 1 \qquad \text{where} \qquad p_o \leq p_b \tag{18}$$

Equation 2.18 applies when the pressure of oil phase is less than the bubble point pressure p_b leading to an existence of free gas and a system with three phases. The reservoir is called as a saturated reservoir. On the other hand, if the pressure of oil phase is higher than the bubble point pressure, the reservoir is regarded as a undersaturated reservoir

with no free gas and constant solution gas ratio. The model becomes a two-phase flow model, and the saturation constraints are:

$$S_w + S_o = 1, \quad S_g = 0, \quad R_s = constant \qquad \text{where} \qquad p_o > p_b \tag{19}$$

2.1.2. Discretization

Since we cannot solve nonlinear conservation equations obtained from the previous section directly, we need to perform a discretization to transform the nonlinear partial differential equations to nonlinear algebraic equations. The discretization is carried out by using a block-centered finite difference method. The discretization in this subsection is based on Ertekin et. al. (2001).

As mentioned earlier, the reservoir model is divided into small grid cells. We use 3D Cartesian grids in the discretization. Figure 3 shows grid blocks which the cube's faces are parallel to the Cartesian axes (i, j, k) and having a centroid denoted as (x, y, z) with a dimension of Δx, Δy, and Δz.

From Figure 3, we observe a fluid flow across the grid blocks. The mass flux across the interface in x-direction are expressed as:

$$(\rho v_x)_{x-\frac{\Delta x}{2},y,z} \quad , \quad (\rho v_x)_{x+\frac{\Delta x}{2},y,z} \tag{20}$$

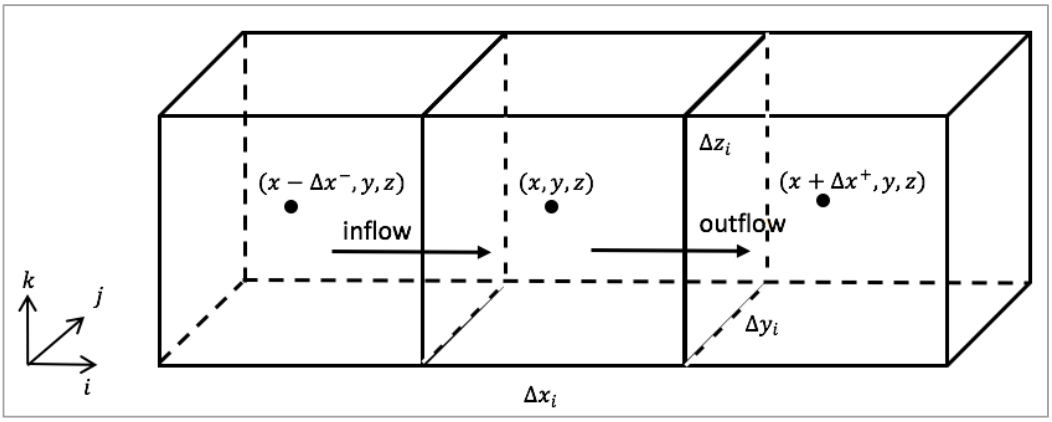

Figure 3 Flow across Cartesian grid block in x-direction

Source: Adapted from Gao (2014)

And the pressure differences in the x-direction are:

$$\frac{p_{o_{x+\Delta x^+,y,z}} - p_{o_{x,y,z}}}{\Delta x^+} \quad , \quad \frac{p_{o_{x-\Delta x^-,y,z}} - p_{o_{x,y,z}}}{\Delta x^-} \tag{21}$$

It is noted that the plus and minus signs in the subscription show the properties of the adjacent blocks. The minus sign $(i-1, j, k)$ indicates the properties of the block in the negative x-direction and the plus sign $(i+1, j, k)$ indicates the properties of the block in positive x-direction. The plus and minus one-half also report the average properties of two adjacent grid blocks. The minus subscription $(i-\frac{1}{2}, j, k)$ stands for the average properties at the interface of two grid blocks in the negative x-direction while the plus subscription $(i+\frac{1}{2}, j, k)$ indicates the properties on the positive x-direction.

In order to perform discretization, we apply the concepts of equation 20 and 21 into the mass conservation equation and obtain the discretization of mass flux in x, y, and z directions. Two types of discretization need to be done; in space, and in time. The final discretization of each phase is shown in this section. The details of each phase discretization can be found in Ertekin et. al. (2001). The discretization of oil phase conservation shown in equation 22.

$$
\begin{aligned}
&\frac{1}{\Delta x_i}\left(\lambda_{o_{i+\frac{1}{2},j,k}}\frac{p_{o_{i+1,j,k}}-p_{o_{i,j,k}}}{\Delta x_i^+}+\lambda_{o_{i-\frac{1}{2},j,k}}\frac{p_{o_{i-1,j,k}}-p_{o_{i,j,k}}}{\Delta x_i^-}\right)\\
&\quad+\frac{1}{\Delta y_i}\left(\lambda_{o_{i,j+\frac{1}{2},k}}\frac{p_{o_{i,j+1,k}}-p_{o_{i,j,k}}}{\Delta y_i^+}+\lambda_{o_{i,j-\frac{1}{2},k}}\frac{p_{o_{i,j-1,k}}-p_{o_{i,j,k}}}{\Delta y_i^-}\right)\\
&\quad+\frac{1}{\Delta z_i}\left(\lambda_{o_{i,j,k+\frac{1}{2}}}\frac{p_{o_{i,j,k+1}}-p_{o_{i,j,k}}}{\Delta z_i^+}+\lambda_{o_{i,j,k-\frac{1}{2}}}\frac{p_{o_{i,j,k-1}}-p_{o_{i,j,k}}}{\Delta z_i^-}\right.\\
&\quad\left.-\lambda_{o_{i,j,k+\frac{1}{2}}}\gamma_{o_{i,j,k+\frac{1}{2}}}\frac{z_{i,j,k+1}-z_{i,j,k}}{\Delta z_i^+}-\lambda_{o_{i,j,k-\frac{1}{2}}}\gamma_{o_{i,j,k-\frac{1}{2}}}\frac{z_{i,j,k-1}-z_{i,j,k}}{\Delta z_i^-}\right)\\
&\quad=((1-S_w-S_g)^n(b_o^{n+1}\phi'+\phi^n b_o')\Delta p_o)-((\phi^{n+1}b_o^{n+1})(\Delta S_w+\Delta S_g))\\
&\quad+WI_o({p_o}_{wc}^{n+1}-p_{wf})
\end{aligned}
\tag{22}
$$

where $\gamma=\rho g$, $b=\frac{1}{B}$, $b'=\frac{b^{n+1}-b^n}{p^{n+1}-p^n}$, $\phi'=\frac{\phi^{n+1}-\phi^n}{p^{n+1}-p^n}$, $\Delta p=\frac{p^{n+1}-p^n}{\Delta t}$, and $\Delta S=\frac{S^{n+1}-S^n}{\Delta t}$. The superscript indicates the time step of the properties; n indicates the current time step while $n+1$ indicates the next time step. These parameters apply to all three phases discretization by using each phase's properties. A simplified well model is added to the equation by using Peaceman's equations (Ertekin et. al. (2001)). It is noted that

the equations are not applicable to the complex wellbore conditions; i.e. fractured reservoir. A relationship between flow of source/sink q^* and well index WI is:

$$q^* = WI(p_{wc}^{n+1} - p_{wf}) \tag{23}$$

where subscript wc indicates the location of the grid block containing the well. Well index WI can be calculated as:

$$WI = -\frac{(2\pi k_r \sqrt{k_x k_y} h)}{\left(\mu B \left[\ln\left(\frac{r_0}{r_w}\right) + s\right]\right)} \tag{24}$$

where k_x is permeability in x-direction, k_y is permeability in y-direction, h is grid block thickness, r_w is wellbore radius, and r_0 is the equivalent wellbore radius. The equivalent wellbore radius r_0 is the grid block radius which the reservoir pressure equals to well block pressure at steady state, which is defined as:

$$r_0 = 0.28 \frac{\sqrt{\left[\left(\frac{k_y}{k_x}\right)^{\frac{1}{2}} \ (\Delta x)^2\right] + \left[\left(\frac{k_x}{k_y}\right)^{\frac{1}{2}} \ (\Delta y)^2\right]}}{\left(\frac{k_y}{k_x}\right)^{\frac{1}{4}} + \left(\frac{k_x}{k_y}\right)^{\frac{1}{4}}} \tag{25}$$

The discretization of water phase conservation was obtained in the same steps as the oil equation and is exhibited in equation 26.

$$
\begin{aligned}
&\frac{1}{\Delta x_i}\left(\lambda_{w_{i+\frac{1}{2},j,k}}\frac{p_{o_{i+1,j,k}}-p_{o_{i,j,k}}}{\Delta x_i^+}+\lambda_{w_{i-\frac{1}{2},j,k}}\frac{p_{o_{i-1,j,k}}-p_{o_{i,j,k}}}{\Delta x_i^-}\right)\\
&\qquad+\frac{1}{\Delta y_i}\left(\lambda_{w_{i,j+\frac{1}{2},k}}\frac{p_{o_{i,j+1,k}}-p_{o_{i,j,k}}}{\Delta y_i^+}+\lambda_{w_{i,j-\frac{1}{2},k}}\frac{p_{o_{i,j-1,k}}-p_{o_{i,j,k}}}{\Delta y_i^-}\right)\\
&\qquad+\frac{1}{\Delta z_i}\left(\lambda_{w_{i,j,k+\frac{1}{2}}}\frac{p_{o_{i,j,k+1}}-p_{o_{i,j,k}}}{\Delta z_i^+}+\lambda_{w_{i,j,k-\frac{1}{2}}}\frac{p_{o_{i,j,k-1}}-p_{o_{i,j,k}}}{\Delta z_i^-}\right.\\
&\qquad\left.-\lambda_{w_{i,j,k+\frac{1}{2}}}\gamma_{w_{i,j,k+\frac{1}{2}}}\frac{z_{i,j,k+1}-z_{i,j,k}}{\Delta z_i^+}-\lambda_{w_{i,j,k-\frac{1}{2}}}\gamma_{w_{i,j,k-\frac{1}{2}}}\frac{z_{i,j,k-1}-z_{i,j,k}}{\Delta z_i^-}\right)\\
&\qquad=S_w^n(b_w^{n+1}\phi'+\phi^n b_w')\Delta p_w+(\phi^{n+1}b_w^{n+1})\Delta S_w+WI_w({p_w}_{wc}^{n+1}-p_{wf})
\end{aligned}
\tag{26}
$$

For the discretization of gas conservation, terms representing the gas solution in oil phase were added. The derivation was also done in the same manner as oil and water. The discretization of gas conversation is:

$$
\begin{aligned}
&\frac{1}{\Delta x_i}\left((R_s\lambda_o)_{i+\frac{1}{2},j,k}\frac{p_{o_{i+1,j,k}}-p_{o_{i,j,k}}}{\Delta x_i^+}+(R_s\lambda_o)_{i-\frac{1}{2},j,k}\frac{p_{o_{i-1,j,k}}-p_{o_{i,j,k}}}{\Delta x_i^-}\right)\\
&\quad+\frac{1}{\Delta y_i}\left((R_s\lambda_o)_{i,j+\frac{1}{2},k}\frac{p_{o_{i,j+1,k}}-p_{o_{i,j,k}}}{\Delta y_i^+}+(R_s\lambda_o)_{i,j-\frac{1}{2},k}\frac{p_{o_{i,j-1,k}}-p_{o_{i,j,k}}}{\Delta y_i^-}\right)\\
&\quad+\frac{1}{\Delta z_i}\left((R_s\lambda_o)_{i,j,k+\frac{1}{2}}\frac{p_{o_{i,j,k+1}}-p_{o_{i,j,k}}}{\Delta z_i^+}+(R_s\lambda_o)_{i,j,k-\frac{1}{2}}\frac{p_{o_{i,j,k-1}}-p_{o_{i,j,k}}}{\Delta z_i^-}\right.\\
&\quad\left.-(R_s\lambda_o)_{i,j,k+\frac{1}{2}}\gamma_{o_{i,j,k+\frac{1}{2}}}\frac{z_{i,j,k+1}-z_{i,j,k}}{\Delta z_i^+}-(R_s\lambda_o)_{i,j,k-\frac{1}{2}}\gamma_{o_{i,j,k-\frac{1}{2}}}\frac{z_{i,j,k-1}-z_{i,j,k}}{\Delta z_i^-}\right)\\
&\quad+\frac{1}{\Delta x_i}\left(\lambda_{g_{i+\frac{1}{2},j,k}}\frac{p_{o_{i+1,j,k}}-p_{o_{i,j,k}}}{\Delta x_i^+}+\lambda_{g_{i-\frac{1}{2},j,k}}\frac{p_{o_{i-1,j,k}}-p_{o_{i,j,k}}}{\Delta x_i^-}\right)\\
&\quad+\frac{1}{\Delta y_i}\left(\lambda_{g_{i,j+\frac{1}{2},k}}\frac{p_{o_{i,j+1,k}}-p_{o_{i,j,k}}}{\Delta y_i^+}+\lambda_{g_{i,j-\frac{1}{2},k}}\frac{p_{o_{i,j-1,k}}-p_{o_{i,j,k}}}{\Delta y_i^-}\right)\\
&\quad+\frac{1}{\Delta z_i}\left(\lambda_{g_{i,j,k+\frac{1}{2}}}\frac{p_{o_{i,j,k+1}}-p_{o_{i,j,k}}}{\Delta z_i^+}+\lambda_{g_{i,j,k-\frac{1}{2}}}\frac{p_{o_{i,j,k-1}}-p_{o_{i,j,k}}}{\Delta z_i^-}\right.\\
&\quad\left.-\lambda_{g_{i,j,k+\frac{1}{2}}}\gamma_{g_{i,j,k+\frac{1}{2}}}\frac{z_{i,j,k+1}-z_{i,j,k}}{\Delta z_i^+}-\lambda_{g_{i,j,k-\frac{1}{2}}}\gamma_{g_{i,j,k-\frac{1}{2}}}\frac{z_{i,j,k-1}-z_{i,j,k}}{\Delta z_i^-}\right)\\
&\quad=\Delta p_o\Big\{(1-S_w-S_g)^n\Big[\Big(b_o^{n+1}\phi^{'}+\phi^n b_o^{'}\Big)R_S^n+R_S^{'}(\phi b_o)^{n+1}\Big]\\
&\quad+S_g^n\Big[b_g^{n+1}\phi^{'}+\phi^n b_g^{'}\Big]\Big\}-R_S^{n+1}(b_o\phi)^{n+1}\Delta S_w+\big[(b_g\phi)^{n+1}-R_S^{n+1}(b_o\phi)^{n+1}\big]\Delta S_g\\
&\quad+WI_g\left(p_{g_{i,j,k}}^{\;n+1}-p_{wf}\right)\\
&\qquad+R_S^{n+1}WI_o\left(p_{g_{i,j,k}}^{\;n+1}-p_{wf}\right)
\end{aligned}
\tag{27}
$$

We can see the relationship between reservoir pressure, reservoir saturations and the bottomhole flowing pressure in oil, water, and gas discretization equations. Equation 23 is one of the most important equations in this study. It shows the relationship between bottomhole flowing pressure, reservoir pressure at the grid cell containing the well, and flowrates. These bottomhole pressure and flowrates are the control parameters that are sent back and forth from the subsurface simulation to the well and surface model. As

mentioned at the beginning of this section that well will be able to flow when the relationship between subsurface and surface conditions match i.e. both systems have the same flowrates and bottomhole pressure.

All the equations presented in this subsection are loaded in the reservoir simulators. In this study, ECLIPSE and INTERSECT reservoir simulators developed by Schlumberger are used. The reservoir model is treated as a Black Oil model that ECLIPSE 100 software uses the fully implicit method to solve the set of linear equations. Since the physical properties are depicted in the nonlinear partial differential equations, Newton-Raphson linearization is used to linearize those discretized equations; thus, enables them to be solved by linear solvers. ECLIPSE also has an ability to model and control individual well; thus, the bottomhole flowing pressure and flowrates are transferred to the network model as control parameters. (Schlumberger (2014)). Details of Newton-Raphson linearization is presented in the next section. We now have some idea on how flow in subsurface reservoir contributes those parameters. In next subsection, we will talk about how to evaluate the well and surface network part by having bottomhole pressure and flowrates from the reservoir as inputs.

2.2. Surface Modeling

Once we obtained the subsurface equations representing fluid flow in the reservoir, we need to have a production system to deliver the fluids to the selling point. The section from the well to the point of sales is always regarded as surface facilities or can be considered as an outflow performance of the wells. Surface model in this study refers to a

multiphase flow in pipe model since in most instance; the petroleum production contains all three phases; oil, gas, and water. The model calculates pressure as a function of distance in the production network with the converged flowrate from subsurface model with respect to changes in holdups, and fluid properties. A brief concept of multiphase flow refers to Economides et. al. (2013), Hasan and Kabir (2002), and PIPESIM User Guide Version 2015.1 – Technical Description.

The major task of network modeling in petroleum industry is to obtain the accurate wellhead pressure which is strongly related to the pressure losses in the system. The fundamental of the pressure losses can be presented with a conservation of momentum equation. When fluid flows through the production system, fluid pressure reduces as a result of several forces acting on it. While the forces that are acting on the fluid element will be discussed later in this section, we show here in equation 28 the general equation for bottomhole pressure estimation with an accounting of pressure losses in the production system.

$$p_{wf} = p_{sep} + \Delta p_{pipe} + \Delta p_{choke} + \Delta p_{tubing} + \Delta p_{valve} \tag{28}$$

where p_{wf} in the left-hand size indicates the bottomhole flowing pressure which connects to the reservoir performance and all the terms in the right-hand size indicate the surface separator pressure p_{sep} as the entrance to the processing facilities and pressure losses along the system. The pressure loss terms in equation 28 consist of pressure loss across piping and flowline Δp_{pipe}, pressure loss across choke valve Δp_{choke}, pressure loss along the production tubing Δp_{tubing}, and pressure loss across valves and fittings Δp_{valve}. In

sample production network modeling, the separator pressure is fixed while the pressure losses contain only two main components which are pressure losses in tubing and flowline. This basis is used in this study.

2.2.1. Material Balance Equations

Similar to subsurface modeling, the surface modeling equations are based on the material and energy balances or conservations of mass and momentum. Tubing, piping, and flowlines are divided into small segments in the same manner as grid blocks in the reservoir modeling. The fluid flow in piping and flowline also follows the mass balance equation (equation 1).

$$Mass_{inflow} - Mass_{outflow} = Mass_{accumulation} \tag{1}$$

The general partial differential equation and material balance equations for liquid and gas are shown in equation 29, and 30, respectively.

$$\widetilde{q}_{l,in} - \tilde{q}_{l,out} = V_{seg}\frac{\partial}{\partial t}(y_l \rho_l) \tag{29}$$

$$\tilde{q}_{g,in} - \tilde{q}_{g,out} = V_{seg}\frac{\partial}{\partial t}(y_g \rho_g) \tag{30}$$

where $\tilde{q}$ terms stand for inflow and outflow of liquid and gas into the pipe segment with the volume V_{seg}, y indicates hold up of the specific phase while ρ is the density of the

phase. In the typical environment of liquid and gas production, the lighter phase will be moving faster than the denser phase leading to a slippage of two phases and a difference of pipe occupied by the phase and the overall volumetric fraction. This phenomenon is called the holdup. Liquid holdup depends on how the two phases distributed in the pipe; thus, requires a more complicated calculation than the material balance. The state of fluid phase can be calculated using a multiphase flow simulator or empirical and model-based correlations. The multiphase flow calculation will be discussed later in this section.

As mentioned earlier, the pipe is divided into small segments which each segment has its pressure and fluids flow across it. We present the pipe as cylindrical segments where the flowrates are measured at the pipe connection (subscripted with j), and the segment pressures are subscripted with i. Figure 4 shows flow in pipe segments with a length of Δx and a volume V_{seg}.

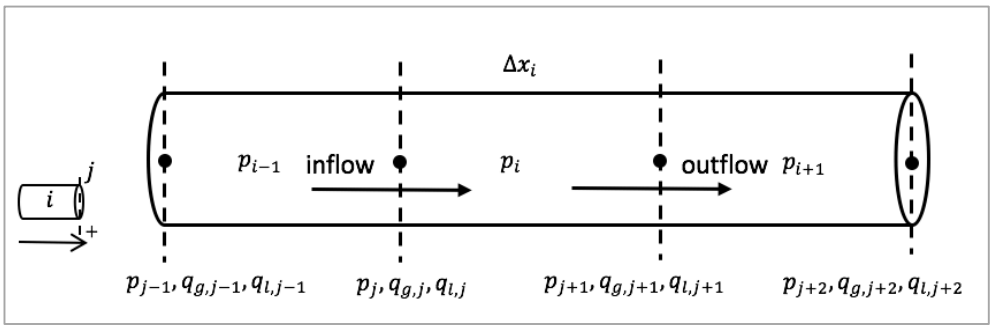

Figure 4 Flow across pipe segments

Source: Adapted from Gao (2014)

Taking time-scale discretization on equation 29, and 30, the mass conservation equations of oil, gas, and water are:

$$q^*_{o,j} - q^*_{o,j+1} = \frac{\Delta x_i A_i}{\Delta t}[(y_o b_o)^{n+1}_i - (y_o b_o)^n_i] \tag{31}$$

$$q^*_{w,j} - q^*_{w,j+1} = \frac{\Delta x_i A_i}{\Delta t}[(y_w b_w)^{n+1}_i - (y_w b_w)^n_i] \tag{32}$$

$$q^*_{g,j} - q^*_{g,j+1} = \frac{\Delta x_i A_i}{\Delta t}[(y_g b_g)^{n+1}_i - (y_g b_g)^n_i + (R_s y_o b_o)^{n+1}_i - (R_s y_o b_o)^n_i] \tag{33}$$

As can be seen in equation 31 – 33, the flowrates change with time (timestep n to $n+1$). The changing flow in time is a characteristic of transient flow which occurs at the beginning of the well production, however, in this study, we consider that the flowrates are not changing with time and the system is in a steady-state condition. Appling steady-state condition into equation 31-33, we obtain mass conservation equations in pipe segment as:

$$q^*_{o,j} - q^*_{o,j+1} \approx 0 \tag{34}$$

$$q^*_{w,j} - q^*_{w,j+1} \approx 0 \tag{35}$$

$$(q^*_{g,j} - q^*_{g,j+1}) + R_s(q^*_{o,j} - q^*_{o,j+1}) \approx 0 \tag{36}$$

2.2.2. Mechanical Energy Balance

From above section on material balance, we consider that our system is in steady-state and assume that the pressure in the plane normal to flow is constant; thus the pressure between the two interfaces of the segment equals to the fluid pressure losses. We get a simplified momentum balance equation as sum of forces acting to the fluid equals to the change in fluid's momentum. The main elements affecting fluid momentum are pressure, friction, and gravity. Those elements are depicted in Figure 5: momentum balance for a fluid element.

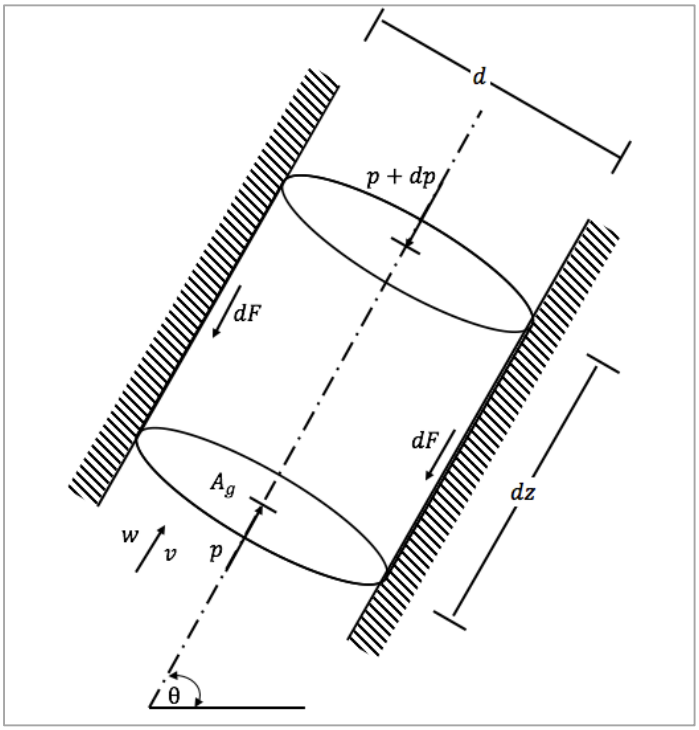

Figure 5 Momentum balance for a fluid element

Source: Adapted from Hasan and Kabir (2002)

The conservation of momentum equation for a fluid element can be written as:

$$pA - (p + dp)A - df - A(dz)g\rho sin\theta = (w + dw)(v + dv) - wv \tag{37}$$

The left-hand side shows the forces acting on the fluid where p is pressure of fluid, f is friction on the pipe wall, A is pipe cross-sectional area, $A(dz)g\rho sin\theta$ term represents hydrostatic effect with an inclination θ. While the right-hand side shows fluid momentum change where w is fluid mass flowrate and v is fluid velocity.

By having the constant mass flow ($dw = 0$), we obtain the total pressure gradient equation from the momentum conservation equation:

$$\frac{dp}{dz} = \left(\frac{dp}{dz}\right)_{pe} + \left(\frac{dp}{dz}\right)_{f} + \left(\frac{dp}{dz}\right)_{a} \tag{38}$$

where $\left(\frac{dp}{dz}\right)_{pe}$ is hydrostatic gradient, $\left(\frac{dp}{dz}\right)_{f}$ is frictional gradient, and $\left(\frac{dp}{dz}\right)_{a}$ is the acceleration gradient. However, in the system that no significant change in the cross-sectional area, the pressure loss caused by changing in fluid velocity (acceleration term) is generally negligible. Hydrostatic pressure gradient represents pressure loss due to the potential energy or elevation change. It is calculated by using:

$$\left(\frac{dp}{dz}\right)_{pe} = \frac{g}{g_c}\rho_m sin\theta \tag{39}$$

where ρ_m is the mixture density at the point of calculation. ρ_m can be calculated by using gas and liquid hold up obtained from the multiphase flow calculation as described in the next subsection.

Frictional pressure gradient represents pressure loss from the friction between fluid and the pipe surface. It is calculated by using:

$$\left(\frac{dp}{dz}\right)_f = \frac{f v_m^2 \rho_m}{2 g_c d} \tag{40}$$

where f is Moody's friction factor, d is pipe diameter, ρ_m is fluid mixture density, and v is fluid velocity. As same as ρ_m, these parameters can be determined by using different multiphase flow correlations. It can also be concluded that the calculation of the total pressure gradient depends on the liquid holdup calculation, how the phases distribute in pipe while flowing and the friction factor. As mentioned earlier that the multiphase liquid holdup and pressure losses can be both in empirical approaches and model-based correlations, it was found that the empirical methods potentially give an inaccurate result when applied to various scenarios (Hasan and Kabir (2002)). In this study, the flow-related parameters will be identified using flow pattern and related correlations.

2.2.3. Multiphase Flow Patterns

Gas and liquid flow separately and simultaneously in the pipe at different velocities, and properties. They can create a number of flow patterns from the effects of physical

interactions; for example, surface tension effect, liquid droplet stability, etc. The flow patterns are used to represent the phase distribution in the pipe at each flowing conditions. The flow patterns differ from vertical system to deviated and horizontal system since pipe configurations lead to complexity in dynamics. Four patterns are used in identifying vertical upward concurrent two-phase flow and are shown in Figure 6.

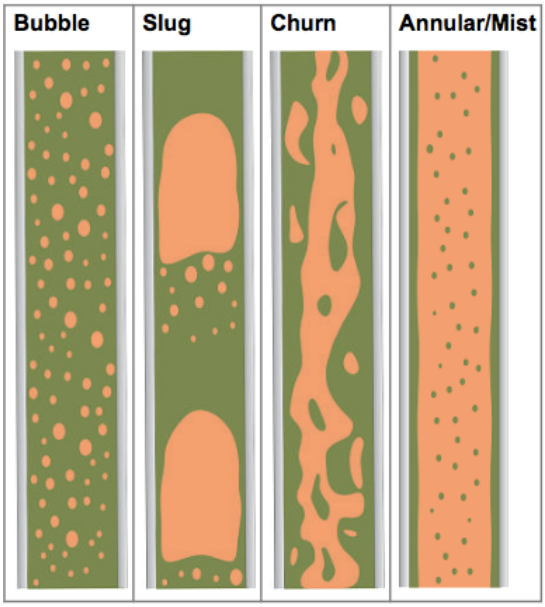

Figure 6 Flow patterns in vertical upward two-phase flow

Source: Reprinted from PIPESIM User Guide (Schlumberger (2015))

The four patterns consist of bubble flow, slug flow, churn flow (or slug-mist transition flow), and annular flow (or mist flow) (Economides et. al. (2013)). Each flow pattern has its distinct characters which are briefly described as:

- Bubble flow represents dispersed gas flowing the continuous liquid. The example of bubble flow is the liberation of the solution gas from the undersaturated oil when the pressure is less than bubble point pressure.
- Slug flow represents the condition that gas flow at higher velocity than the bubble flow. Gas bubbles form into bigger bubble and occupy the pipe cross-sectional area leading to a blockage in liquid flow and a discontinuous of each flowing phase. In this condition, both gas and liquid significantly contribute to the pressure gradient.
- Slug-mist transition or churn flow represents an instability of large gas bubbles due to high gas velocity. Gas bubbles collapse and turbulently disperse in flowing liquid.
- Annular or mist flow represents a flowing condition at very high gas velocity. Gas phase becomes continuous and flows through the central core of the pipe while liquid droplets are entrained in the gas and deposit on the pipe wall as a liquid film. Annular flow is a common flow pattern in a gas-condensate well.

Prediction of liquid holdup in horizontal system has a minor contribution to the pressure losses calculation comparing to the computation in the vertical or inclined system since there is no potential energy effect. However, knowing how fluid flow in pipe will benefit design and operations of receiving and processing facilities; for example, sizing of inlet separator and slug catcher. Too high slug volume may lead to riser liquid build up and the blockage of gas production to the processing facilities. As in vertical flow system, the two-phase horizontal flow can be categorized into four patterns as shown in Figure 7.

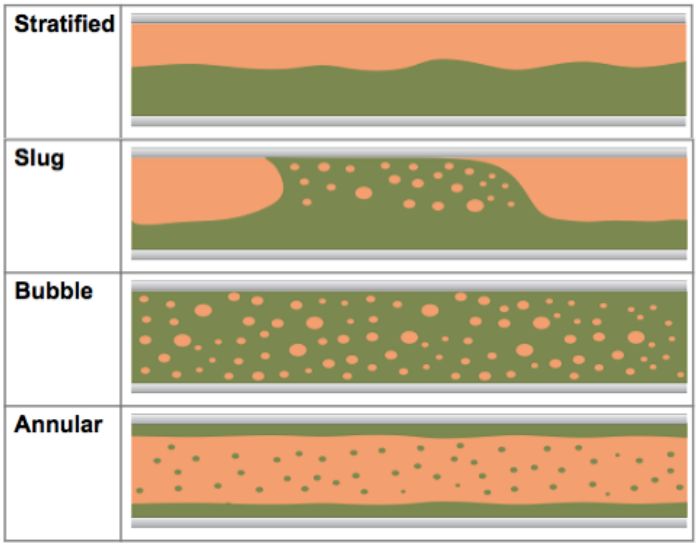

Figure 7 Flow patterns in two-phase horizontal flow

Source: Reprinted from PIPESIM User Guide (Schlumberger (2015))

The four patterns consist of stratified flow (segregated flow), slug flow (intermittent flow), bubble flow, and annular flow (mist flow) (Economides et. al. (2013)). Each flow pattern has its distinct characters which are briefly described as:

- Stratified flow represents a segregation of gas and liquid by their density. Both phases flow separately where gas flows at the top of the pipe and liquid flows at the bottom.
- Slug flow represents an intermittent flow when the gas velocity is high. The liquid slug alternates the large gas bubbles that fill a significant portion of the pipe area.
- Bubble flow in horizontal system occurs when the gas velocity is very high. Gas disperses in liquid asymmetrically due to the effect of gravity and density.

- Annular flow shows that gas flows at the center of the pipe while liquid forms a film on the pipe surface. The annular flow pattern in horizontal flow is similar to the one in vertical flow except that the liquid film is asymmetrical and thicker at the bottom of the pipe.

2.2.4. Multiphase Flow Correlations

Numerous models and correlations were developed to represent the multiphase flow in particular conditions. Selecting the models to calculate the holdups and pressure gradient poses a challenge in applicability and suitability. However, several models are widely used in the industry and have better performance than most of the available correlations. We use the modified Hagedorn and Brown correlation for the vertical system and Beggs and Brill correlation for the horizontal system (Economides et. al. (2013) and Hasan and Kabir (2002)).

The modified Hagedorn and Brown correlation is an empirical two-phase flow correlation developed from the original Hagedorn and Brown with an accounting of the no-slip holdup and modification in a bubble flow determination. Most of the calculations are performed with dimensionless numbers. Detailed calculation can be found in Economides et. al. (2013), and Hasan and Kabir (2002). Liquid holdup calculated from the modified Hagedorn and Brown correlation plotted as a function of fluid properties displayed in a dimensionless number is shown in Figure 8. Two-phase mixture viscosity defined by modified Hagedorn and Brown correlation is:

$$\mu_m = (\mu_l^{y_l})(\mu_g^{y_g}) \tag{41}$$

where y_l is liquid holdup, and $y_g = 1 - y_l$ is gas-volume fraction.

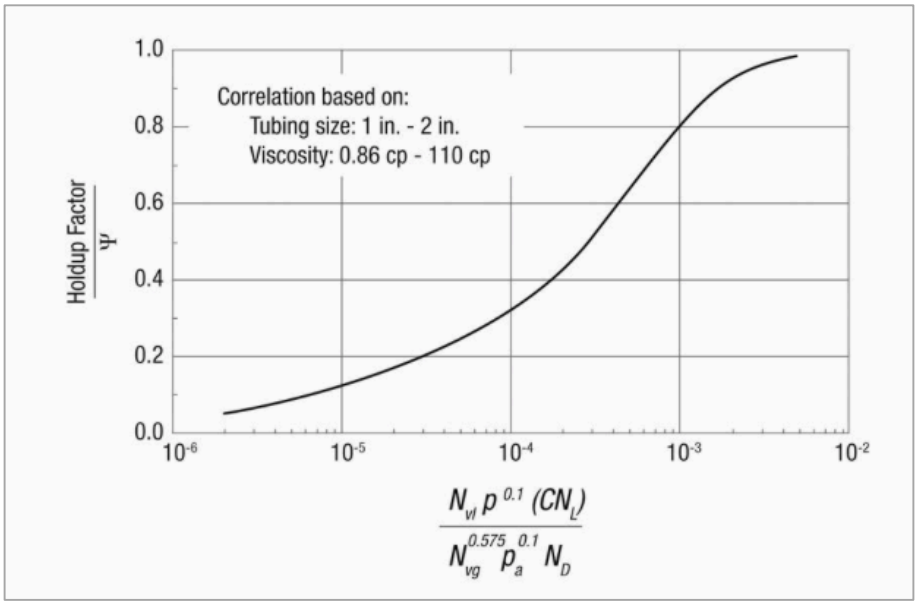

Figure 8 Hagedorn and Brown correlation for holdup

Source: Reprinted with permission from Economides et. al. (2013)

Beggs and Brill correlation was developed from horizontal system then applying some corrections for the vertical and inclined system. It includes flow pattern determination into the calculation. It utilizes the general mechanical energy balance equation and the in-situ average density to calculate the pressure gradient. The horizontal flow pattern map used in Beggs and Brill correlation is shown in Figure 9. The map plots the Froude number which is a dimensionless number calculated from mixture velocity and pipe diameter versus the input liquid content.

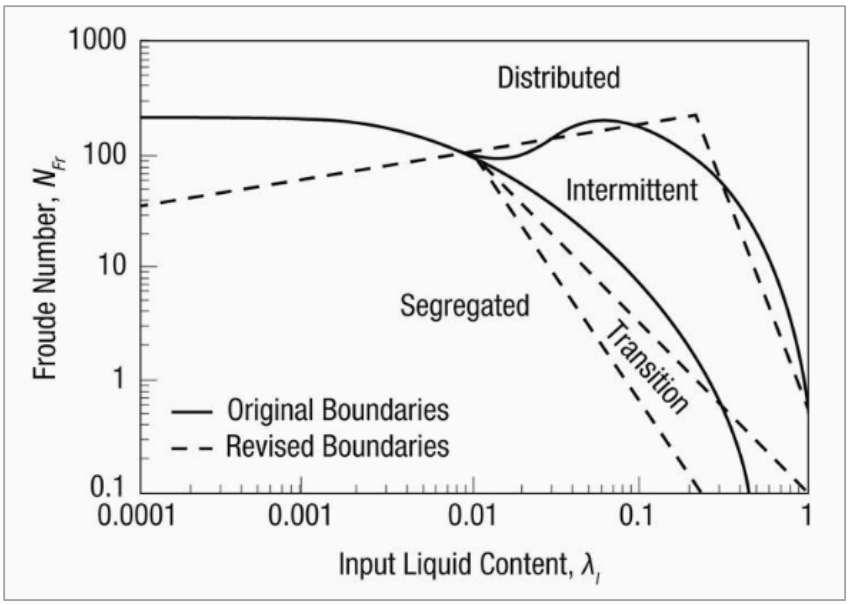

Figure 9 Beggs and Brill flow regime map

Source: Reprinted with permission from Economides et. al. (2013)

2.2.5. Pressure Gradient Calculation

Different correlations have different definitions of a mixture density ρ_m, mixture viscosity μ_m, and friction factor f. Once we obtain those values from the correlations, the pressure gradient can be calculated by using equation 38 – 40.

Since total pressure gradient consists of pressure loss from hydrostatic head (potential energy), pressure loss from friction, and pressure loss from acceleration as shown in equation 38. The acceleration term is generally negligible, so the calculation is not shown in this section. The potential energy term is a result of the weight of the fluid column; thus, strongly relates to fluid mixture density and can be calculated by:

$$\left(\frac{dp}{dz}\right)_{pe} = \frac{g}{g_c}\rho_m sin\theta$$

(39)

Once having mixture velocity v_{m}, mixture density ρ_{m}, and mixture viscosity μ_m from the correlations, Reynolds number can be calculated using:

$$Re = \frac{dv_m\rho_m}{\mu_m}$$

(42)

Friction factor f can also be calculated in many ways. Friction factor equations depend on Reynolds number range showing that fluid is flowing in laminar, transition, or turbulent flow. We use Moody diagram here in Figure 10 as one of the most common methods to get the friction factor value. Once having Reynolds number and pipe properties, we can read the friction factor from the chart. The pressure loss from friction depends on mixture velocity and average density as shown in equation 40. More gas fraction in the fluid reduces the hydrostatic loss while increasing the frictional loss; thus, selecting the suitable pipe and network is one of the crucial components to obtain the optimal well deliverability.

$$\left(\frac{dp}{dz}\right)_f = \frac{fv_m^2\rho_m}{2g_c d}$$

(40)

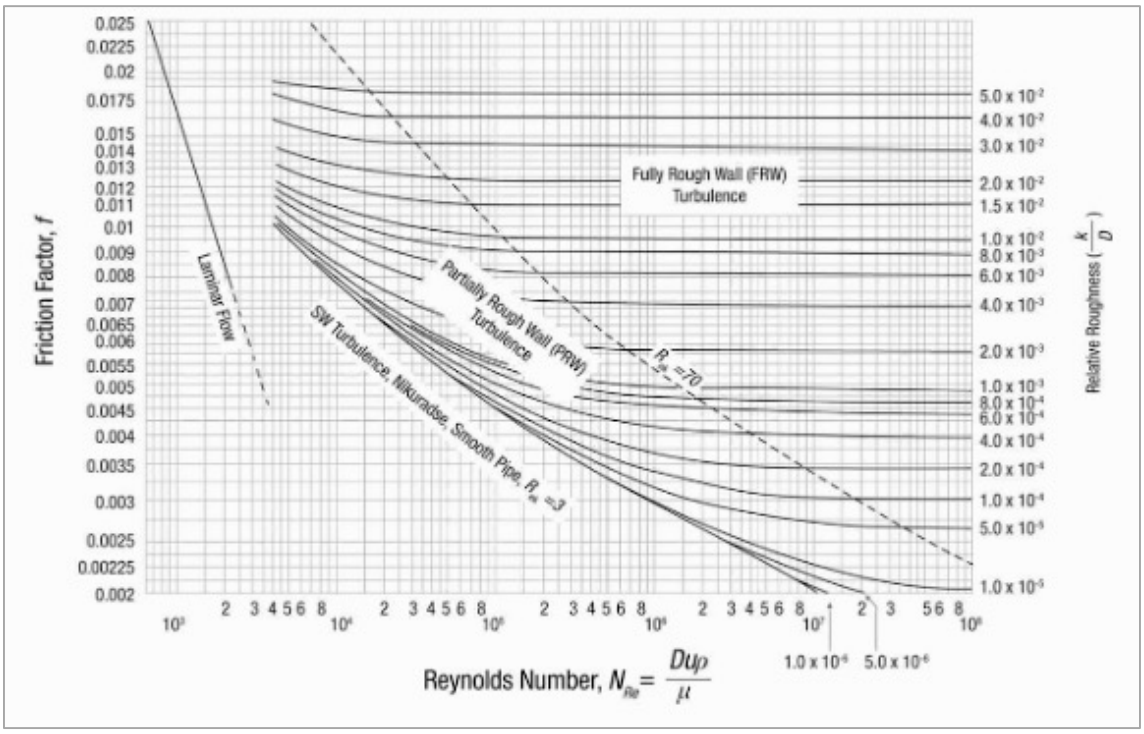

Figure 10 Moody friction factor diagram

Source: Reprinted with permission from Economides et. al. (2013)

3. SUBSURFACE AND SURFACE COUPLING MECHANISMS

Integration of the models in this study is carried out by a method called coupling. The general concept of coupling is to connect both subsurface and surface models by exchanging their controlled parameters. Three coupling schemes are being used to couple subsurface and surface simulations in the industry. The schemes are explicit coupling, implicit coupling, and fully implicit coupling. They basically differ in how two models are being treated, how the coupling parameters, for example, bottomhole flowing pressure is calculated, and how the models' convergence takes place. In this section, we will show how the coupling is performed, and the advantages and disadvantages of each scheme.

3.1. Explicit Coupling Scheme

Explicit coupling works by considering subsurface and surface simulations as different domains. The subsurface and surface models are solved sequentially and the process to get the synchronized controlled parameters is being treated explicitly at the timestep level. The coupled solutions depend on only on the convergence of reservoir equations. The balancing is being performed at the beginning of the time step to calculate the bottomhole pressure for subsurface model by using production rate from the previous time step. When subsurface model converges providing pressure and saturations in the grid blocks, the bottomhole pressure of each well obtained from equation 23 is sent to the surface model to solve for a new production rate. With new production rate, grid block conditions changes; thus, subsurface simulation is carried out to find the new bottomhole

pressure to pass to the surface model. This process is being carried out iteratively until the end of the simulation. The pre-selection of timestep size is also one of the critical parameters. Large step size leads to a faster calculation but may result in an instability of the results due to dynamics of the system were not fully accounted. The procedure of explicit coupling scheme is exhibited as a flowchart in Figure 11.

Since the balancing between subsurface and surface model takes place only at the beginning of the timestep, this method requires fewer computational effort. However, being unable to predict the reservoir states at the time of flowrate calculation leads to inaccurate results. Explicit coupling scheme is applicable with most of the commercial software since no source code modification is required.

3.2. Implicit Coupling Scheme

The implicit scheme or being called a partially implicit method works similarly to the explicit method, but the coupling is being operated at Newton iteration level. Due to nonlinearity of the reservoir discretization equations presented in the previous section, the Newton-Raphson is introduced to linearize the system allowing the system to be solved by linear solvers. The solutions are also based on the convergence of the reservoir equations. The iterative process is being carried out until the Newton iteration is converged. Newton linearization introduces the use of Jacobian matrix which is a set of partial derivatives of the unknown parameters' residual terms. The general structure of Newton linearization is $\partial x = J^{-1}R$ where ∂x represents the solution vector from the

linearization, J^{-1} represents the submatrix of Jacobian matrix, and R accounts for the residual vector.

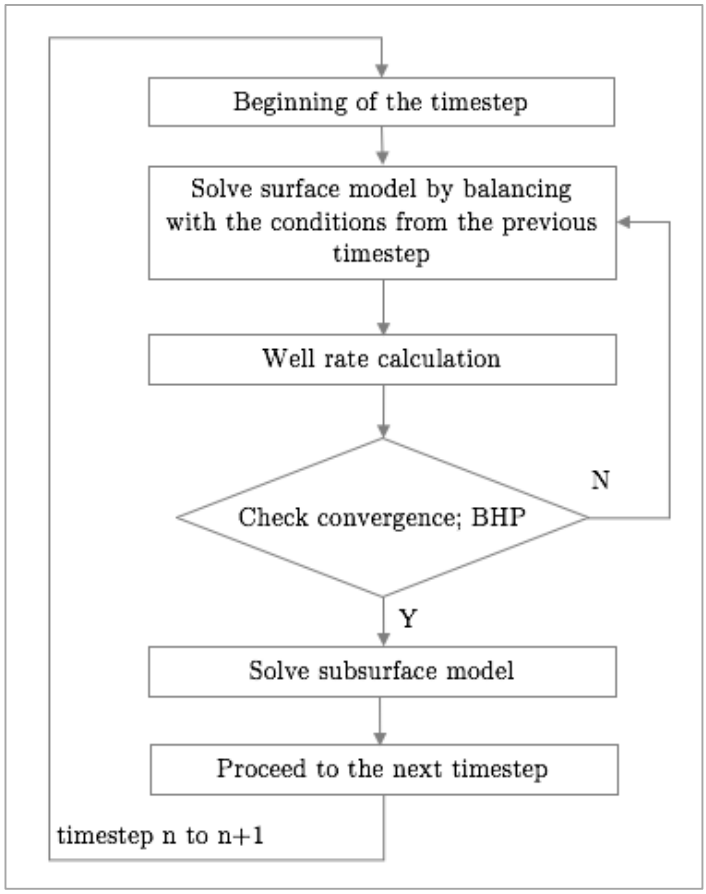

Figure 11 Explicit coupling flowchart

Source: Adapted from Gao (2014)

To solve the nonlinear reservoir system, we present the residual of oil, water, and gas discretization equations and well flowing equations in this subsection while the details of Newton-Raphson linearization method will be discussed in the latter part of this section.

To this end, the residual of reservoir oil discretization equation is:

$$
\begin{aligned}
R_{ro} = \; & \frac{1}{\Delta x_i}\left(\lambda_{o_{i+\frac{1}{2},j,k}}\frac{p_{o_{i+1,j,k}} - p_{o_{i,j,k}}}{\Delta x_i^+} + \lambda_{o_{i-\frac{1}{2},j,k}}\frac{p_{o_{i-1,j,k}} - p_{o_{i,j,k}}}{\Delta x_i^-}\right) \\
& + \frac{1}{\Delta y_i}\left(\lambda_{o_{i,j+\frac{1}{2},k}}\frac{p_{o_{i,j+1,k}} - p_{o_{i,j,k}}}{\Delta y_i^+} + \lambda_{o_{i,j-\frac{1}{2},k}}\frac{p_{o_{i,j-1,k}} - p_{o_{i,j,k}}}{\Delta y_i^-}\right) \\
& + \frac{1}{\Delta z_i}\left(\lambda_{o_{i,j,k+\frac{1}{2}}}\frac{p_{o_{i,j,k+1}} - p_{o_{i,j,k}}}{\Delta z_i^+} + \lambda_{i,j,k-\frac{1}{2}}\frac{p_{o_{i,j,k-1}} - p_{o_{i,j,k}}}{\Delta z_i^-}\right. \\
& \left. - \lambda_{o_{i,j,k+\frac{1}{2}}}\gamma_{o_{i,j,k+\frac{1}{2}}}\frac{z_{i,j,k+1} - z_{i,j,k}}{\Delta z_i^+} - \lambda_{o_{i,j,k-\frac{1}{2}}}\gamma_{o_{i,j,k-\frac{1}{2}}}\frac{z_{i,j,k-1} - z_{i,j,k}}{\Delta z_i^-}\right) \\
& - \left[(1 - S_w - S_g)^n(b_o^{n+1}\phi' + \phi^n b_o')\Delta_t p_o - (\phi b_o)^{n+1}\Delta_t S_w - (\phi b_o)^{n+1}\Delta_t S_g\right] \\
& - WI_o(p_{o_{i,j,k}}^{n+1} - p_{wf})
\end{aligned}
\tag{41}
$$

Residual of reservoir water discretization equation is presented in the same fashion as:

$$
\begin{aligned}
R_{rw} = & \frac{1}{\Delta x_i}\left(\lambda_{w_{i+\frac{1}{2},j,k}}\frac{p_{o_{i+1,j,k}} - p_{o_{i,j,k}}}{\Delta x_i^+} + \lambda_{w_{i-\frac{1}{2},j,k}}\frac{p_{o_{i-1,j,k}} - p_{o_{i,j,k}}}{\Delta x_i^-}\right) \\
& + \frac{1}{\Delta y_i}\left(\lambda_{w_{i,j+\frac{1}{2},k}}\frac{p_{o_{i,j+1,k}} - p_{o_{i,j,k}}}{\Delta y_i^+} + \lambda_{w_{i,j-\frac{1}{2},k}}\frac{p_{o_{i,j-1,k}} - p_{o_{i,j,k}}}{\Delta y_i^-}\right) \\
& + \frac{1}{\Delta z_i}\left(\lambda_{w_{i,j,k+\frac{1}{2}}}\frac{p_{o_{i,j,k+1}} - p_{o_{i,j,k}}}{\Delta z_i^+} + \lambda_{w_{i,j,k-\frac{1}{2}}}\frac{p_{o_{i,j,k-1}} - p_{o_{i,j,k}}}{\Delta z_i^-}\right. \\
& \left. - \lambda_{w_{i,j,k+\frac{1}{2}}}\gamma_{w_{i,j,k+\frac{1}{2}}}\frac{z_{i,j,k+1} - z_{i,j,k}}{\Delta z_i^+} - \lambda_{w_{i,j,k-\frac{1}{2}}}\gamma_{w_{i,j,k-\frac{1}{2}}}\frac{z_{i,j,k-1} - z_{i,j,k}}{\Delta z_i^-}\right) \\
& - \left[S_w^n[b_w^{n+1}\phi' + \phi^n b_w']\Delta_t p_o + [\phi^{n+1}b_w^{n+1}]\Delta_t S_w\right] - WI_w(p_{w_{i,j,k}}^{n+1} - p_{wf})
\end{aligned}
\tag{42}
$$

And finally, the residual of reservoir gas discretization equation is:

$$
\begin{aligned}
R_{rg} = \; & \frac{1}{\Delta x_i}\left((R_s\lambda_o)_{i+\frac{1}{2},j,k}\frac{p_{o_{i+1,j,k}}-p_{o_{i,j,k}}}{\Delta x_i^+}+(R_s\lambda_o)_{i-\frac{1}{2},j,k}\frac{p_{o_{i-1,j,k}}-p_{o_{i,j,k}}}{\Delta x_i^-}\right)\\
& +\frac{1}{\Delta y_i}\left((R_s\lambda_o)_{i,j+\frac{1}{2},k}\frac{p_{o_{i,j+1,k}}-p_{o_{i,j,k}}}{\Delta y_i^+}+(R_s\lambda_o)_{i,j-\frac{1}{2},k}\frac{p_{o_{i,j-1,k}}-p_{o_{i,j,k}}}{\Delta y_i^-}\right)\\
& +\frac{1}{\Delta z_i}\left((R_s\lambda_o)_{i,j,k+\frac{1}{2}}\frac{p_{o_{i,j,k+1}}-p_{o_{i,j,k}}}{\Delta z_i^+}+(R_s\lambda_o)_{i,j,k-\frac{1}{2}}\frac{p_{o_{i,j,k-1}}-p_{o_{i,j,k}}}{\Delta z_i^-}\right.\\
& -(R_s\lambda_o)_{i,j,k+\frac{1}{2}}\gamma_{o_{i,j,k+\frac{1}{2}}}\frac{z_{i,j,k+1}-z_{i,j,k}}{\Delta z_i^+}\\
& \left.-(R_s\lambda_o)_{i,j,k-\frac{1}{2}}\gamma_{o_{i,j,k-\frac{1}{2}}}\frac{z_{i,j,k-1}-z_{i,j,k}}{\Delta z_i^-}\right)\\
& +\frac{1}{\Delta x_i}\left(\lambda_{g_{i+\frac{1}{2},j,k}}\frac{p_{o_{i+1,j,k}}-p_{o_{i,j,k}}}{\Delta x_i^+}+\lambda_{g_{i-\frac{1}{2},j,k}}\frac{p_{o_{i-1,j,k}}-p_{o_{i,j,k}}}{\Delta x_i^-}\right)\\
& +\frac{1}{\Delta y_i}\left(\lambda_{g_{i,j+\frac{1}{2},k}}\frac{p_{o_{i,j+1,k}}-p_{o_{i,j,k}}}{\Delta y_i^+}+\lambda_{g_{i,j-\frac{1}{2},k}}\frac{p_{o_{i,j-1,k}}-p_{o_{i,j,k}}}{\Delta y_i^-}\right)\\
& +\frac{1}{\Delta z_i}\left(\lambda_{w_{i,j,k+\frac{1}{2}}}\frac{p_{o_{i,j,k+1}}-p_{o_{i,j,k}}}{\Delta z_i^+}+\lambda_{w_{i,j,k-\frac{1}{2}}}\frac{p_{o_{i,j,k-1}}-p_{o_{i,j,k}}}{\Delta z_i^-}\right.\\
& \left.-\lambda_{w_{i,j,k+\frac{1}{2}}}\gamma_{w_{i,j,k+\frac{1}{2}}}\frac{z_{i,j,k+1}-z_{i,j,k}}{\Delta z_i^+}-\lambda_{w_{i,j,k-\frac{1}{2}}}\gamma_{w_{i,j,k-\frac{1}{2}}}\frac{z_{i,j,k-1}-z_{i,j,k}}{\Delta z_i^-}\right)\\
& -\{\{(1-S_w-S_g)^n[(b_o^{n+1}\phi'+\phi^n b_o')R_s^n+R_s'(\phi b_o)^{n+1}]\\
& +S_g^n[b_g^{n+1}\phi'+\phi^n b_g']\}\Delta_t p_o-R_s^{n+1}(b_o\phi)^{n+1}\Delta_t S_w\\
& +[(b_g\phi)^{n+1}-R_s^{n+1}(b_o\phi)^{n+1}]\Delta_t S_g\}-WI_g\left({p_g}_{i,j,k}^{n+1}-p_{wf}\right)\\
& -\;R_s^{n+1}WI_o\left({p_g}_{i,j,k}^{n+1}-p_{wf}\right)
\end{aligned}
\tag{43}
$$

In addition, the residual of well flowing equation can be described by the Peaceman's equation and the derivation of oil phase is:

$$R_{Wo} = q_o^* - WI_o(p_{o_{wc}}^{n+1} - p_{wf}) \tag{44}$$

while the residual of well water flowing equation is:

$$R_{Ww} = q_w^* - \ WI_w(p_{w_{wc}}^{n+1} - p_{wf}) \tag{45}$$

And in the similar fashion, the residual of well gas flowing equation can be presented as:

$$R_{Wg} = q_g^* - R_s^{n+1} WI_o\big(p_{o_{wc}}^{n+1} - p_{wf}\big) - WI_g(p_{g_{wc}}^{n+1} - p_{wf}) \tag{46}$$

As mentioned earlier, the bottomhole pressure is the coupling parameter between surface and subsurface models, we show the residual of the well bottomhole pressure equation as:

$$R_{BHP} = p_{wf} - p_{t1} \tag{47}$$

where p_{t1} is pressure of tubing at the bottomhole that connected to the reservoir.

Although this approach gives more accurate results due to the frequency of the synchronization, it requires more computational effort and thus, computational time. There are also some challenges in the implicit coupling compatibility between the commercial subsurface and surface models owing to the differences in the governing equations computation. The procedure of partially implicit coupling scheme is exhibited as a flowchart in Figure 12.

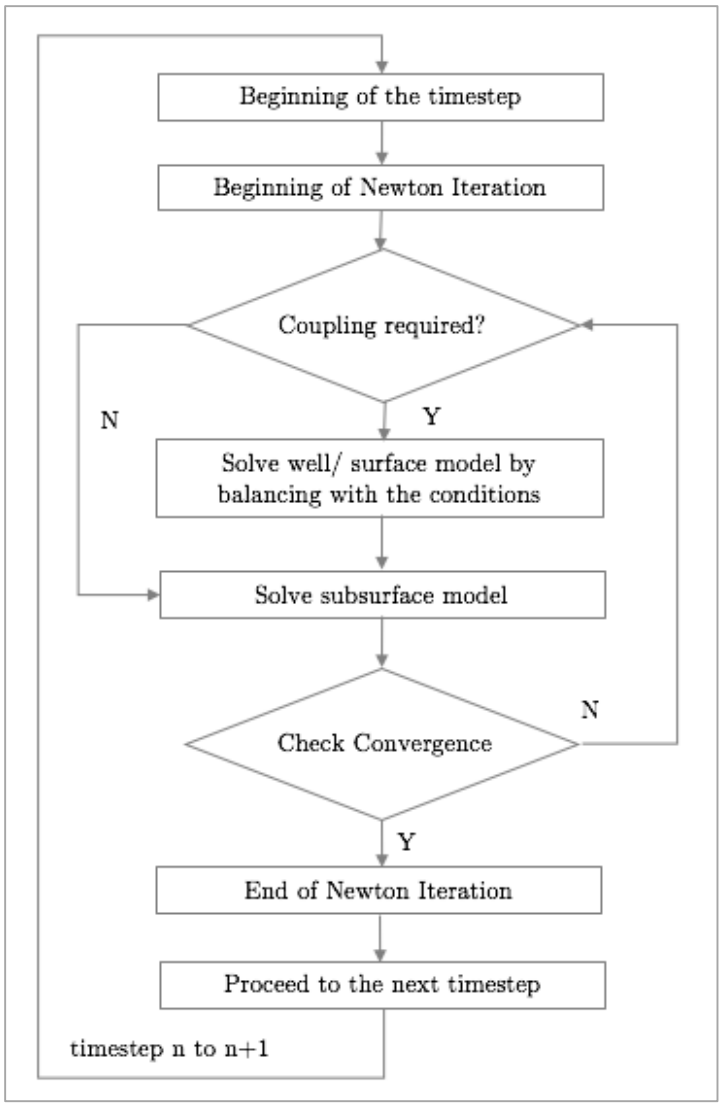

Figure 12 Implicit coupling flowchart

Source: Adapted from Gao (2014)

3.3. Fully Implicit Coupling Scheme

Unlike the partially coupling schemes, the fully implicit method treats subsurface and surface models as a single model, and the convergence of both reservoir and surface facilities equations is taking place simultaneously. Surface equations are consolidated into reservoir equations as an extended grid block of the reservoir domain. It can be said that instead of solely calculating pressure and saturations in the grids, mass conservation and energy balance in the surface network are also being calculated. The convergence of the combined set of equations is taking place at the Newton iteration level as same as implicit method. The compatibility challenges we face in the implicit method are solved since the configuration of the equations is generalized to one system. The combined equations to solve flow in porous media and surface facilities system are also nonlinear and need to be linearized in the same manner as the reservoir fluid flow equations. The surface network equations are added into the reservoir Newton iteration structure; thus, the general structure of the fully coupled subsurface and surface system is:

$$\begin{bmatrix} \partial x_{res} \\ \partial x_{sur} \end{bmatrix} = \begin{bmatrix} A_{\underset{res}{res}} & A_{\underset{sur}{res}} \\ A_{\underset{res}{sur}} & A_{\underset{sur}{sur}} \end{bmatrix}^{-1} \begin{bmatrix} R_{res} \\ R_{sur} \end{bmatrix}$$

where R_{res} and R_{sur} are the residual vectors of reservoir and surface models. The elements in Jacobian matrix represent a derivative of the residual to variable factor; for example, $A_{\underset{sur}{res}}$ is a derivative of the residual of the reservoir equations to the variable vector of the surface equations. ∂x_{res} and ∂x_{sur} represent the solution vectors for reservoir (subsurface) and surface domain, respectively. The procedure of fully implicit coupling scheme is

exhibited as a flowchart in Figure 13. The construction of the coupled set of subsurface and surface equations and the Newton-Raphson linearization method are discussed in this section.

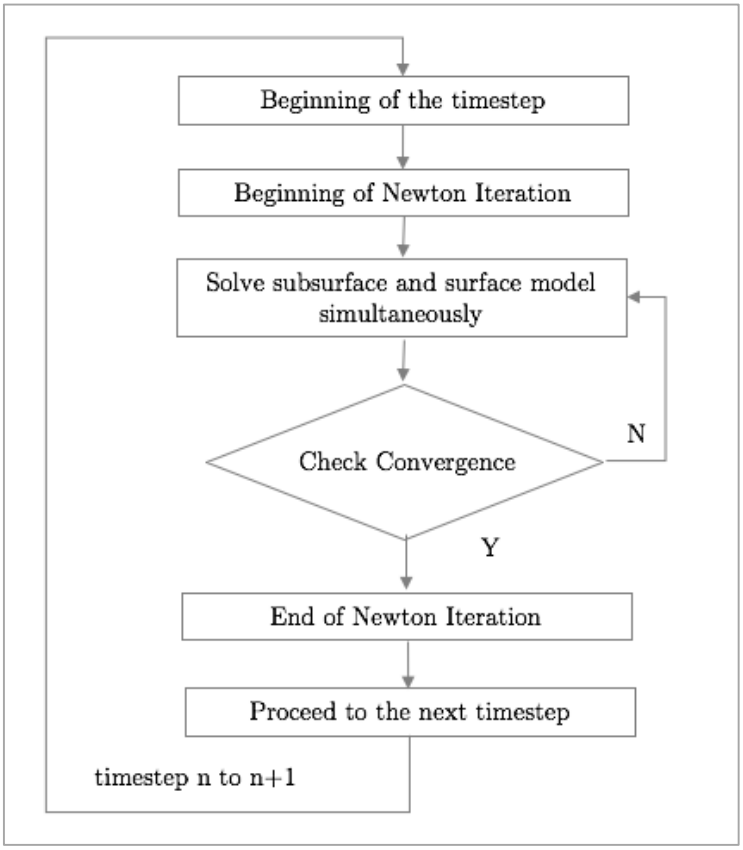

Figure 13 Fully implicit coupling flowchart

Source: Adapted from Gao (2014)

3.3.1. Construction of Coupled Governing Equations

The governing equations are a combination of the subsurface (reservoir) equations and surface facilities equations. These equations are connected by exchanging the controlled parameters, such as bottomhole pressure, and flowrate. These nonlinear equations are complex and related to many parameters. As mentioned in the previous section, the network in this study is considered as steady-state. This implies that the flowrate of each phase equals to flowrate at the bottomhole q^*. The residual of surface flowing equations with steady-state assumption can be written as:

Residual of tubing/ surface piping oil flow equation

$$R_{sur,o} = q^{n+1}_{sur,o_i} - q^{*n+1}_{o} \tag{48}$$

Residual of tubing/ surface piping water flow equation

$$R_{sur,w} = q^{n+1}_{sur,w_i} - q^{*n+1}_{w} \tag{49}$$

Residual of tubing/ surface piping gas flow equation

$$R_{sur,g} = q^{n+1}_{sur,g_i} - q^{*n+1}_{g} \tag{50}$$

Residual of energy conservation equation

$$R_{sur,p} = p^{n+1}_{sur_{i+1}} - p^{n+1}_{sur_i} - \Delta p^{n+1}_{sur_j} \tag{51}$$

Equation 51 shows the pressure losses along segment j of the tubing and surface piping while i indicates the properties at node i. Multiphase flow correlations are used to calculated these pressure terms. In this study, the boundary condition of the coupled model is a separator pressure; thus, we get the residual of boundary condition equation as:

$$R_{bc} = p_{sur_i}^{n+1} - p_{constrain} \tag{52}$$

3.3.2. Newton-Raphson Linearization

The Newton-Raphson method is used to linearize the nonlinear subsurface and surface governing equations to allow the system to be solved by linear solver. Newton-Raphson is general linearization procedure which can be used in various implementations. It is noted that the partially implicit coupled model is also solved by using the Newton-Raphson method but, the construction of residual equations, unknown parameters, and Jacobian matrix is solely based on the reservoir equations presented in section 3.2. The implementation flowchart of Newton-Raphson method is shown in Figure 14.

After the residual of all the equations and parameters were set, the Jacobian matrix can be calculated. The residual and unknown parameters used in fully implicit scheme are defined and categorized into two parts; reservoir and well equations, and tubing and surface piping equations. The residual vectors are:

$$R_{res} = (R_{ro}, R_{rw}, R_{rg}, R_{Wo}, R_{Ww}, R_{Wg}, R_{BHP})^T$$

$$R_{sur} = (R_{sur,o}, R_{sur,w}, R_{sur,g}, R_{sur,p}, R_{bc})^T$$

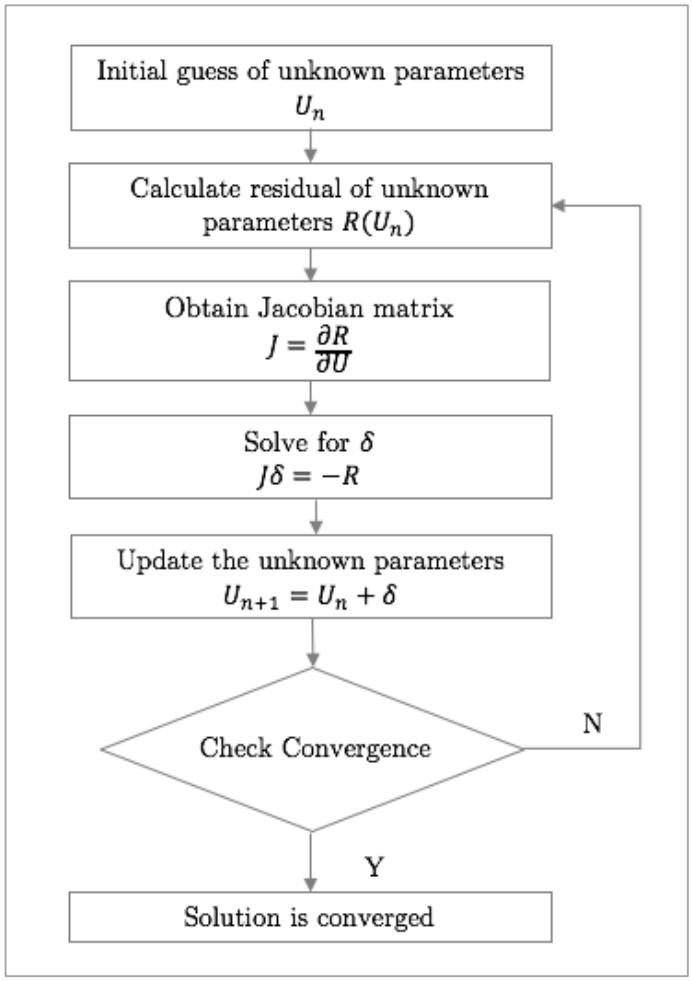

Figure 14 Newton-Raphson method flowchart

Source: Adapted from Iemcholvilert (2013)

while the unknown parameters are:

$$U_{res} = (p_{res}, S_w, S_g, R_s, q_o, q_w, q_g, p_{wf})^T$$

$$U_{sur} = (p_{sur}, q_{sur,o}, q_{sur,w}, q_{sur,g})^T$$

With the fully implicit system, the Jacobian matrix becomes:

$$J = \frac{\partial R}{\partial U} = \begin{bmatrix} \frac{\partial R_{res}}{\partial U_{res}} & \frac{\partial R_{res}}{\partial U_{sur}} \\ \frac{\partial R_{sur}}{\partial U_{res}} & \frac{\partial R_{sur}}{\partial U_{sur}} \end{bmatrix} \tag{53}$$

The Newton-Raphson iteration proceeds for unknown parameters update as:

$$J^k \delta U = -R^k \tag{54}$$

$$U^{k+1} = U^k + \delta U^k \tag{55}$$

where k is the Newton-Raphson iteration that is controlled by the convergence criteria set by the users.

The Newton-Raphson is iteratively carried out until the solutions are converged. The convergence can be based on only reservoir discretization equations or combined reservoir and surface equations depending on the coupling method. It can be seen that the size of the Jacobian matrix of the fully coupled model shown in equation 53 is significantly larger than the partially coupled case where the only unknown parameters and residuals are calculated in only the reservoir part i.e. U_{res}, and $\frac{\partial R_{res}}{\partial U_{res}}$. The fully combination of the reservoir equations and surface equations matrix leads to much more expensive computations.

The indication of the convergence is that the value of the residual equation approaches zero and in the defined tolerance. A typical Newton Raphson solution path taken from INTERSECT technical description (Schlumberger (2015)) is shown in Figure 15 where $R(x)$ represents the residual vector and x is the solution vector.

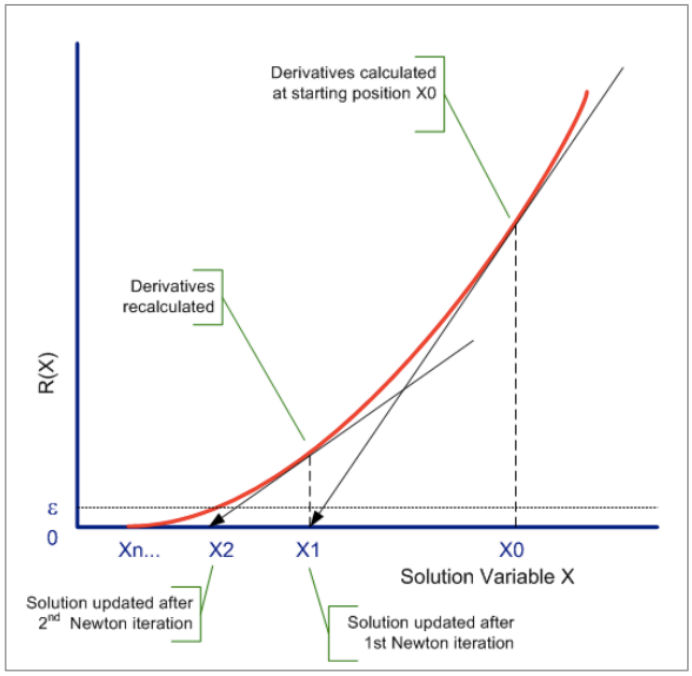

Figure 15 Newton-Raphson solution path

Source: Reprinted from INTERSECT Technical description (Schlumberger (2015))

The Newton-Raphson linearization is used on both partially implicit and fully implicit method; however, the fully implicit method and a combination of two sets of equations were exhibited to show how tight the subsurface and surface integration can be. We also

discussed advantages and disadvantages of each scheme. We believe that choosing how tight the coupling is can be one of the keys to achieving the optimal goals.

4. MODEL DEVELOPMENT AND NUMERICAL SIMULATIONS

The main objective of this thesis is to assess the potential of integrated field optimization, including subsurface, surface, and economic models. Therefore, we develop optimization strategies and evaluate the effects of coupling on the optimal field development scenario.

In what follows, we introduce the benchmark case and all the components of the surface network system. We also present the economic model for further use in this study. We implement the coupling mechanism using a set of commercial software, test each of the coupling mechanisms and perform several numerical studies regarding the coupling mechanism.

4.1. Development of UNISIM-I-D Reservoir Model

A synthetic model was created from data of Namorado Field, Campos Basin, Brazil. The original model: UNISIM-I-R contains high-resolution geological data with over 3 million active cells. The model was constructed based on structural, facies, and petrophysical models utilizing well log data, core samples data, and 3D seismic lines and horizons. The objective of the benchmark models is to provide a model with known properties for the purpose of development methodologies testing and comparison (Avansi and Schiozer (2013)).

UNISIM-I-D reservoir model was upscaled from UNISIM-I-R model with uncertainties for an exploitation strategy selection. UNISIM-I-D model is divided into 81 x 58 x 20 grid

blocks and has approximately 36,000 active cells. The porosity map of UNISIM-I-D reservoir model with four production history matching wells is shown in Figure 16. The original oil in place volume of UNISIM-I-D model is 130 million m^3. The oil density is 28 ºAPI and the fluid model is Black Oil. There is a sealing fault which leads to two different equilibration regions. Waterflooding was chosen as a pressure maintenance methodology, and no gas injection will be implemented (Avansi and Schiozer (2013) and Gaspar et. al (2015)).

The objective of UNISIM-I-D deterministic approach study is to maximize economic indicators, such as Net Present Value (NPV) by optimizing a field development strategy selection. Assumptions and constraints of the case were provided (Gaspar et. al. (2015)); thus, the design and controlled variables should be optimized with honor to the data. Production system data were also given to evaluate a production system integration. An initial oil production development strategy is an expected result of the model.

Apart from four given vertical wells, another ten horizontal producers and eleven water injectors were added to the model with reference UNISIM-I-H model designated for history matching and uncertainties reduction (Maschio et. al. (2015)). Well location selection was performed with the guideline in Botechia et. al. (2013) which they introduced well indicators to represent the complexity of parameters relating to oil field development and production strategy optimizations.

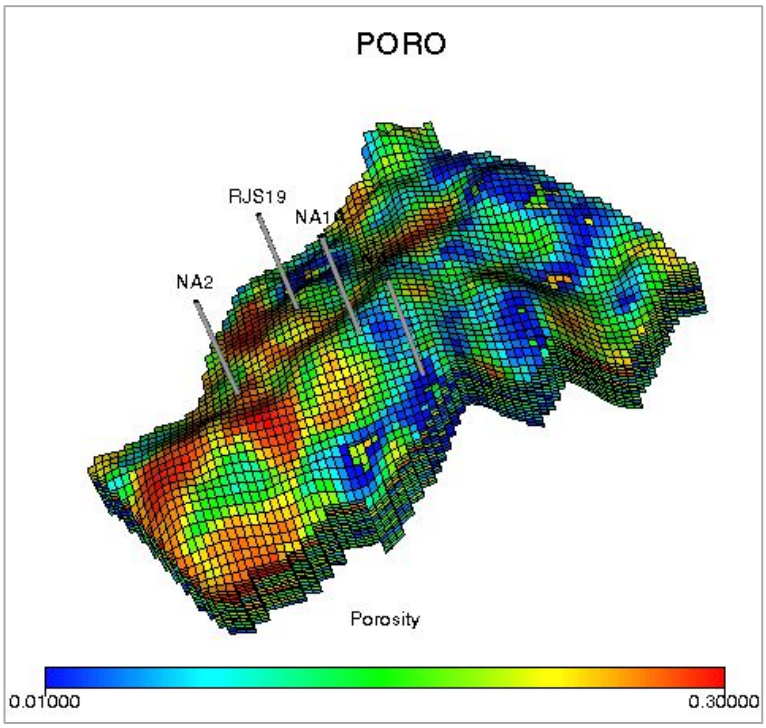

Figure 16 UNISIM-I-D model – Porosity map with four vertical wells

Some modifications were made on the well configurations to avoid inactive blocks in the reservoir. All additional wells are horizontal with 500 m horizontal length. Horizontal producers were completed in between layer 2 to layer 8 while injectors were completed in between layer 9 to layer 15. The first well is scheduled to be opened on July 1st, 2018. The rest of the wells are scheduled to be opened with a minimum 30-day interval between each opening. The last day of the production forecast period is May 31st, 2043. Well data and operating conditions were defined in Gaspar et. al. (2015) and used as controlled parameters in reservoir simulations, as listed in Table 1. UNISIM-I-D porosity map and the base case well placement are shown in Figure 17. Well names were not included to ease the visualization.

Table 1 Well data and operating conditions

Type	Vertical Producer	Horizontal Producer	Horizontal Injector
Max water rate (m^3/d)	-	-	5000
Min oil rate (m^3/d)	20	20	-
Max liquid rate (m^3/d)	2000	2000	-
BHP (bar)	Min 190	Min 190	Max 350
Well radius (m)	0.0762	0.0762	0.0762
Max GOR (m^3/m^3)	200	200	-

ECLIPSE 100 reservoir simulator (Schlumberger (2014)) was used to model a UNISIM-I-D base case model. ECLIPSE 100 is a commercial reservoir simulation software applicable for black oil fluid type developed by Schlumberger. ECLIPSE 100 simulates the flow of oil, gas, and water with changes in reservoir properties. In extensive reservoir simulations, wells are controlled at the bottomhole, thus, the only well deliverability calculation is based on well inflow performance calculation. UNISIM-I-D reservoir with 14 producers and 11 injectors was run on ECLIPSE 100 simulator. In this case, only reservoir inflow performance relationship was used; thus, the wells were controlled at the bottomhole as stated in Table 1.

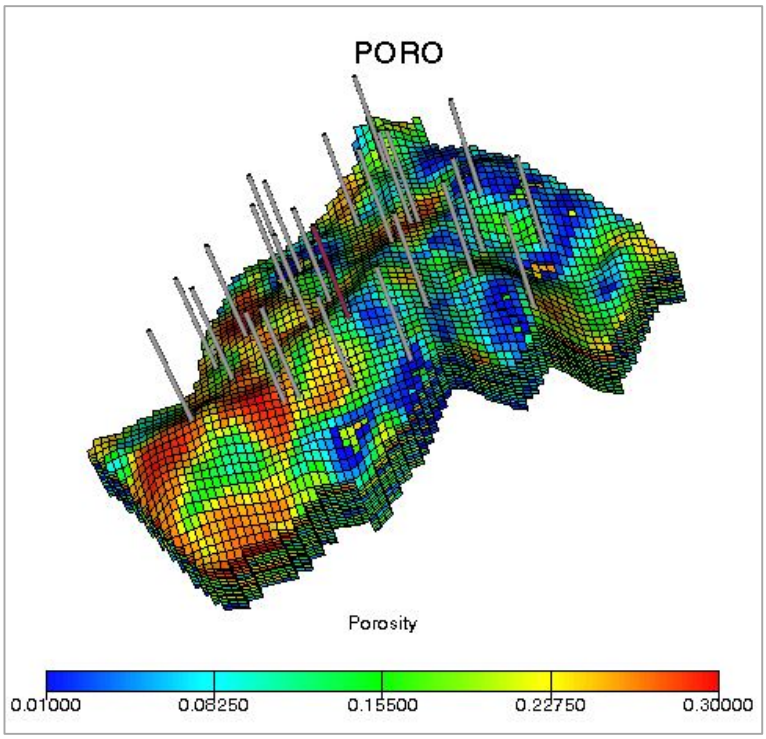

Figure 17 UNISIM-I-D reservoir model and well placement

Controlling well's operating conditions at the bottomhole is not a very practical task. Most of the time, wells are monitored at the surface, either at the wellhead (tubing head) or the gathering facilities. Moreover, not considering the effects of flows in wellbore and surface facilities would lead to an overestimation in the recovery, thus, affecting the economic performance of the production. ECLIPSE 100 has an ability to perform a well deliverability calculation by getting an intersection between reservoir inflow performance relationship (IPR) and outflow performance relationship (OPR) or as being called as a well's vertical flow performance (VFP) as shown in Figure 1.

The IPR represents what reservoir can deliver while the VFP represents what the wells can produce. The intersection of the two curves yields the expected production rate and bottomhole flowing pressure. The VFP is incorporated into ECLIPSE 100 in a table form. VFP table is a calculation of pressure losses in the production tubing for various liquid flowrate, water cut, and GOR. VFP table can be generated from well simulation software or network simulation software such as PROSPER, Petrel, and PIPESIM.

Gaspar et. al. (2015) presented a data set for production system integration into UNISIM-I-D benchmark model. All the wells are satellite wells which connected to the platform. Environment data and well's operating conditions were provided to evaluate the production system integration and are shown in Table 2 and 3, respectively. In this study, VFP tables were generated in PIPESIM by configuring the wells with respect to the ECLIPSE well data.

Table 2 Environment and reservoir data

Data	Value	Unit
Reservoir depth	2900-3400	m
Water depth	166	m
Coastline distance	80	km
Geothermal gradient	0.020: $<$ 200m 0.023: $>$ 200 m	ºC/m

Table 2 Continued

Data	Value	Unit
Water temperature	20 to 16 linear	ºC
Sea current	0.5	m/s

Table 3 Well data and operating conditions for production system integration

Type	Vertical Producer	Horizontal Producer	Horizontal Injector
Max water rate (m^3/d)	-	-	5000
Min oil rate (m^3/d)	20	20	-
Max liquid rate (m^3/d)	2000	2000	-
Min THP (bar)	15	15	-
Max BHP (bar)	-	-	350
Max GOR (m^3/m^3)	200	200	-

4.2. Development of a Surface Network Model

PIPESIM is a steady-state multiphase flow simulator developed by Schlumberger. The application of PIPESIM covers a broad range in oil and gas production, for example, well

and network modeling, nodal analysis, artificial lift design and optimization, pipeline design, equipment sizing, etc. (Schlumberger (2015)). In this project, PIPESIM is used to generate vertical flow performance (VFP) tables and calculate the pressure drop through the surface facility system for coupling purpose.

In the surface network modeling, producers and injectors are treated separately. It is assumed that the source of injected water is abundant and no limitation in surface pumping exists, thus, water injectors are controlled at the bottomhole. As a result, injectors are not included in the network model. Injection flowlines and risers are fixed at 6-inch size since the calculated velocity laid in the recommended limit for water injection flowline (API RP 14E: Recommended Practice for Design and Installation of Offshore Production Platform Piping Systems). Well productivity index of the given production history matching wells were plotted. Among four wells, NA1A, NA2, NA3D, and RSJ19, NA2 gave the highest productivity index; thus, the platform was placed at the location of the NA2 well. Flowlines and risers are installed to connect the satellite wells to the platform. Table 4 shows details of wells and connections from well to platform of vertical producers, horizontal producers, and horizontal injectors. It is assumed that the pressure losses across surface piping from the end of the riser to the inlet separator are negligible. All the wells are on the seabed with 166 m water depth; thus every well's riser length is 166 m.

Well and connections data in Table 4 were used as inputs of PIPESIM network simulation. Production flowline and riser network generated in PIPESIM is shown in Figure 18.

Table 4 Tubing, flowline and riser data for UNISIM-I-D producers and injectors

Well Name	Tubing Size (in)	Bottomhole Depth (m)	Flowline Size (in)	Flowline Length (m)	Riser Size (m)	Riser Length (m)
NA1A	5 1/2"	3074.5	6	1700	6	166
NA2	5 1/2"	3088.5	6	0	6	166
NA3D	5 1/2"	3084.4	6	2404	6	166
RJS19	5 1/2"	3081	6	1345	6	166
PROD005	5 1/2"	3009.4	6	1921	6	166
PROD008	5 1/2"	3030.6	6	447	6	166
PROD009	5 1/2"	3046.3	6	849	6	166
PROD010	5 1/2"	3041	6	1700	6	166
PROD012	5 1/2"	2956.4	6	2773	6	166
PROD014	5 1/2"	2977.3	6	3312	6	166
PROD021	5 1/2"	3032.8	6	922	6	166
PROD023A	5 1/2"	3140	6	4535	6	166
PROD024A	5 1/2"	3090.5	6	4001	6	166
PROD025A	5 1/2"	3059	6	3764	6	166

Table 4 Continued

Well Name	Tubing Size (in)	Bottomhole Depth (m)	Flowline Size (in)	Flowline Length (m)	Riser Size (m)	Riser Length (m)
INJ003	5 1/2"	3048.4	6	3225	6	166
INJ005	5 1/2"	3052.9	6	2147	6	166
INJ006	5 1/2"	3074.4	6	2700	6	166
INJ007	5 1/2"	3024.7	6	4205	6	166
INJ010	5 1/2"	3063.6	6	3423	6	166
INJ015	5 1/2"	3055	6	1616	6	166
INJ017	5 1/2"	3043.7	6	1204	6	166
INJ019	5 1/2"	3115.8	6	1063	6	166
INJ021	5 1/2"	3058.5	6	671	6	166
INJ022	5 1/2"	2992.6	6	3890	6	166
INJ023	5 1/2"	3052.4	6	2970	6	166

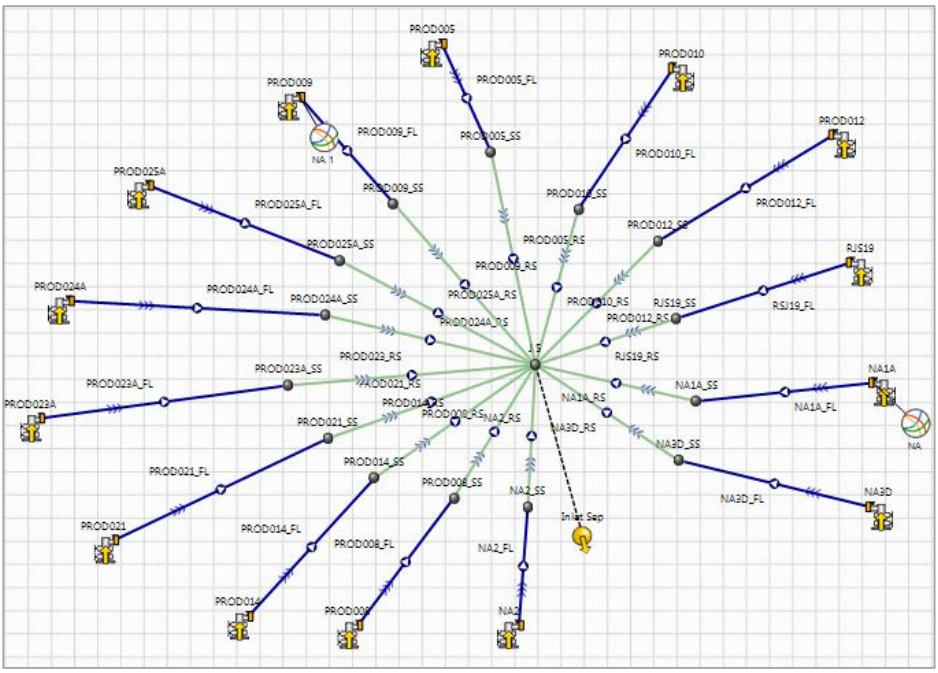

Figure 18 PIPESIM Network for UNISIM-I-D Producers

4.3. Development of Economic Model

Net Present Value (NPV) is one of the most common objective functions used in petroleum industry's economic optimizations. Gaspar et. al. (2015) provided a set of equations to calculate major investments, net cash flow, and the Net Present Value of UNISIM-I-D benchmark model. Table 5 shows fiscal assumptions to be used in the UNISIM-I-D economic model. Some equations had also been developed from the description of the model and are presented in this section.

Table 5 UNISIM-I-D fiscal assumptions

Variable	Value
Corporate tax rate (%)	34.0
Social taxes rate - charge over gross revenue (%)	9.25
Royalties rate - charge over gross revenue (%)	10.0

4.3.1. Net Present Value (NPV) Calculation

NPV is defined as a sum of the cash flows which are discounted at a discount rate at the given time. NPV calculation is shown in equation 56. The annual discount rate used in this calculation is 9.00%. Net cash flow is obtained from a calculation of investments and revenue. The detailed calculation is presented in next subsection.

$$NPV = \sum_{m=1}^{N_t} \frac{NCF_m}{(1+d)^{t_m}} \tag{56}$$

where NPV is an asset's Net Present Value, NCF_m is a net cash flow at period m, m is period indexing which depends on specified timestep, N_t is a total number of calculation timestep, d is discount rate, and t_m is time of period m related to the analysis date.

Despite the fact that reservoir simulation utilizes an adaptive timestep and the timestep varies among study cases, in the economic calculation, the calculation is carried out on a monthly basis.

4.3.2. Net Cash Flow Calculation

In UNISIM-I-D benchmark case (Gaspar et. al. (2015)), project net cash flow at specific time is calculated by following simplified equation based on the Brazilian fiscal regime as shown in equation 57.

$$NCF = [(R - Roy - ST - OC) \times (1 - T)] - Inv - AC \tag{57}$$

where NCF is the net cash flow, R is gross revenue from oil selling, Roy is royalties that charged over gross revenue, ST is social taxes on gross revenue, OC is an operational cost (associated with the oil and water production, and water injection), T is corporate tax rate, Inv is a summation term of investments on equipment and facilities (platform, wells, drilling and completion, flowlines, surface networks, etc.), and lastly AC is an abandonment cost which is charged on the drilling and completion investment. Oil price, production and injection costs, and some economic parameters are shown in Table 6.

Table 6 UNISIM-I-D economic parameters

Variable	Value	Unit
Oil price	314.5	USD/m^3
Oil production cost	62.9	USD/m^3
Water production cost	6.29	USD/m^3
Water injection cost	6.29	USD/m^3
Abandonment cost - charge over drilling	8.20	%
Annual discount rate	9.00	%

4.3.3. Investments Calculation

Major investments in oil field development in this project comprise of platform investment, drilling and completion investment, and well-platform connection investment. The equation to calculate platform investment was given in UNISIM-I-D model description (Gaspar et. al. (2015)) and is shown in equation 58. It is noted that no gas production or gas injection terms are present in the equation. It is stated that the gas production cost is included in the calculation of oil processing facilities and we assume that there is no gas injection in this field development.

$$Inv_{plat} = 417 + (16.4 \times Cp_o + 3.15 \times Cp_w + 3.15 \times Ci_w + 0.1 n_w) \tag{58}$$

where Inv_{plat} is an investment on platform in million USD, Cp_o is oil processing capacity which equals to liquid processing capacity (in 1000 m3/day), Cp_w is the water processing capacity (in 1000 m3/day), Ci_w is water injection capacity (in 1000 m3/day), and n_w is a total number of wells.

Drilling and completion investment involve on type and number of wells. Well can be vertical, horizontal, and intelligent well with inflow control valve (ICV) installed. Drilling and completion in horizontal part is a more difficult task than in the vertical one; thus, the unit cost of the drilling and completion are different. The investment depends on the production tubing size as well. The investment in drilling and completion of vertical and horizontal wells can be calculated by using equation 59 and 60, respectively. Related parameters used to calculate drilling and completion cost are shown in Table 7.

$$\begin{aligned} Inv_{drill,ver} = &(Production\ column\ length \times Tubing\ unit\ cost) \\ &+ Fixed\ vertical\ drilling\ and\ completion \end{aligned} \tag{59}$$

$$\begin{aligned} Inv_{drill,hor} = &(Production\ column\ length \times Tubing\ unit\ cost) \\ &+ (Horizontal\ part\ length \times Horizontal\ drilling\ cost) \\ &+ \ Fixed\ horizontal\ drilling\ and\ completion \end{aligned} \tag{60}$$

Table 7 Drilling and completion parameters

Variable	Dimension	Value	Unit
Production column (Tubing size)	2 7/8”	221	USD/m
	3 1/2"	234	USD/m
	4 1/2"	250	USD/m
	5 1/2"	270	USD/m
Fixed vertical drilling and completion	-	20.90	million USD
Horizontal drilling and completion/ length	-	21185	USD/m hor
Fixed horizontal drilling and completion	-	25.66	million USD

Well-platform connection investment consists of investment in flowline and riser. Investment of flowline and riser depends on the size and length. Riser is a vertical pipe that connects the flowline from the seabed level to the platform. Flowline length is determined by the location of the well and distance from the well to platform while the length of riser is related to water depth. The well-platform connection investment is calculated by using equation 61 while the parameters are shown in Table 8.

$$Inv_{conn} = (Flowline\ length \times Flowline\ unit\ cost) + (Riser\ length \times Riser\ unit\ cost) + Fixed\ riser\ and\ flowline\ installation \quad (61)$$

Table 8 Well-platform connection parameters

Variable	Dimension	Value	Unit
Production/ Injection Flowline	4”	411	USD/m
	6”	768	USD/m
	8”	1976	USD/m
Riser	4”	879	USD/m
	6”	1513	USD/m
	8”	2597	USD/m
Riser and flowline installation	-	11.70	million USD

With the assumption that no well conversion and recompletion is planned in this stage, the total investment is a summation of the three portions mentioned above which can be presented in the equation form as:

$$Inv = Inv_{plat} + Inv_{drill} + Inv_{conn} \tag{61}$$

It is noted from UNISIM-I-D case description that the platform and all of the drilling and completion are invested at the early stage while the well-platform connection investment is accounted at the time the connection is taking place. The project timeline will be visualized in the next section for better understanding.

4.3.4. Project Development Timeline

According to Gaspar et. al. (2015), there are some mandatory date and times that we need to consider in calculating the Net Present Value. The period of production history is not included in this study since no well was connected to the production facility and we cannot perform a subsurface-surface coupling. Important field timeline and cash flow timeline are presented in Table 9 and 10, respectively. Figure 19 taken from UNISIM-I-D case description Annex A (Gaspar et. al. (2015)) depicts the field and cash flow timeline regarding the information in Table 9 and 10.

Table 9 Field timeline

Event	Date
End of production history period Beginning of drilling and completion	05/31/17
End of drilling and completion Beginning of production forecast period Opening of the first well	07/01/2018
Opening of the second well	07/31/2018
End of production forecast	05/31/2043

Table 10 Cash flow timeline

Event	Date
Present date	05/31/17
Investment in platform/ facilities	07/01/2018
Investment in drilling and completion	
Investment in the first connection	07/01/2018
Cost of field abandonment	05/31/2043

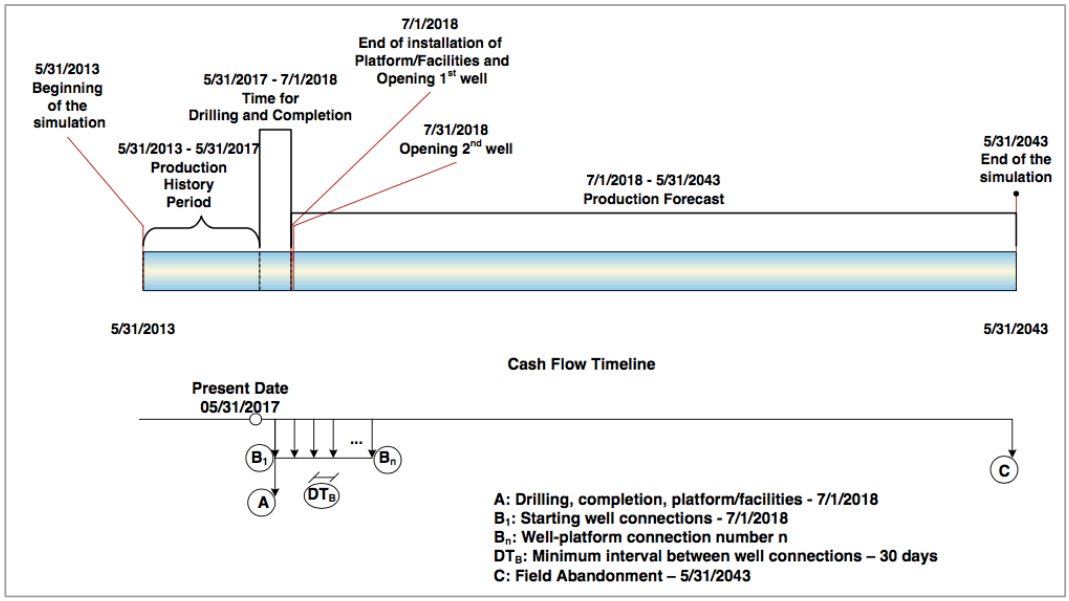

Figure 19 UNISIM-I-D field and cash flow timeline

Source: Reprinted from Gaspar et. al. (2015)

It can be seen in this section that most of the values used in the calculations are related to development strategy and production data; thus, those data will be obtained from the simulations. Integrating economic scenarios into the coupled model improves the capability to cope with the dynamics of the business.

4.4. Effect of Surface Facility Limits on Uncoupled Reservoir

We developed four study cases to show the effect of surface constraints to the production. Different control points between the bottomhole and tubing head are utilized to exhibit the simple coupling between reservoir and well model. It is noted that this study operates all the simulations automatically using MATLAB codes. MATLAB is a high-level programming language developed by MathWorks aiming to be used in engineering and sciences field of works. It can be integrated with other programming languages, enabling us to develop more complicate procedures and algorithms (MathWorks (2016)). Initiation of study cases is done in MATLAB, then MATLAB will call the commercial software and run the cases. After the run on commercial software finishes, MATLAB retrieves the results for further calculation. The workflow used to run uncoupled ECLIPSE reservoir simulator is depicted in Figure 20. The predefined timestep employed in the reservoir simulations is 15 days while imposing adaptive timestep at the beginning of the simulation. It should be noted, however, that the NPV calculation is being performed on a monthly basis referring to the general practice of the industry.

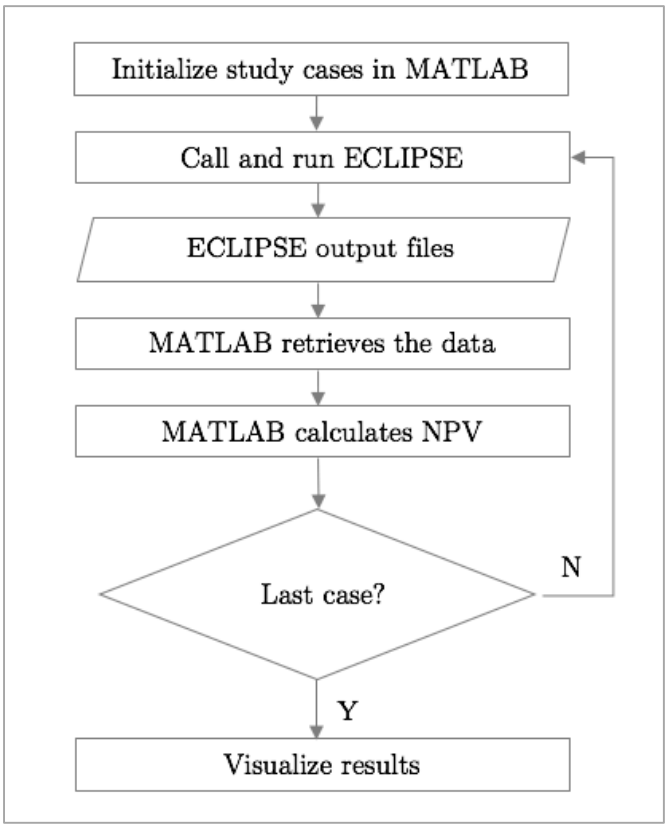

Figure 20 Flowchart for MATLAB-ECLIPSE operation

Four study cases designed to see the effect of process facilities constraints and difference in bottomhole and tubing head control are listed as

1. Bottomhole pressure control with no surface facilities limitation
2. Tubing head pressure control with no surface facilities limitation
3. Bottomhole pressure control with surface facilities limitation
4. Tubing head pressure control with surface facilities limitation

Surface facilities limitation in this context refers to a platform capacity to process oil, total liquid, produced water, and water injection. In case 3 and 4, we use the values

specified in Maschio et. al. (2015) for the group control conditions for production prediction. The values are shown in Table 11.

Table 11 Group controls from UNISIM-I-H case

Group Name	Max Liquid (Sm^3/d)	Max Oil (Sm^3/d)	Max Water (Sm^3/d)
Producer	15500	15500	13950
Injector	-	-	21700

All of the cases were run on ECLIPSE, and the results were calculated in MATLAB. The field production and injection rates are constrained by the group control values. The guide rate control is used when the total rates exceed the limit. The group's guide rate is set at the beginning of each timestep and the allocation is based on the well production potential. The well potential is defined as the flowrate that the well would initially have in the absence of any constraints (Schlumberger (2015)). Each well can have both flow and pressure constraints due to the group control rates and the individual control pressures.

The first observation from plotting the field oil recovery results in Figure 21 is that the bottomhole pressure control case is more sensitive to the limitation in the processing facilities than the tubing head pressure control. Both the bottomhole pressure control and the tubing head pressure control recover a smaller amount of oil in the cases with surface

limitation comparing to the cases with no process limit. However, when comparing asset's Net Present Value shown in Figure 22, we found that case 1, 2, and 4 give almost the same results.

Although case 1 and 2 provide higher oil recovery, they require higher investment in the surface facilities since the investment depends on the production and injection rates. Without limitation, wells try to produce as much as the reservoir can deliver, thus the production profile peaks at one point in time and rapidly decline. This represents a flaw in estimating recoverable reserves and making a decision without taking process facilities limit into account. On the other hand, imposing surface facilities limits and guide rate control lead to less water production and injection rate which affects the initial investment and the operational costs and eventually asset's Net Present Value.

Oil production rate, water production rate, and water injection rate are plotted in Figure 23, 24, and 25, respectively. Oil production results shown in Figure 23 reveal that there is a reduction in the oil production rate after the peak production period in the tubing head pressure control cases leading to lower oil recovery comparing to the bottomhole pressure control case. The differences could be a result of changes in the fluid properties along the production period which affecting the pressure drop calculation in the production tubing.

It should be noted that the unusual peaks in case 3 and 4 oil production and water injection are results of the guide rate control in ECLIPSE that works in an explicit fashion; i.e. it takes the previous timestep's flowrate to control the wells.

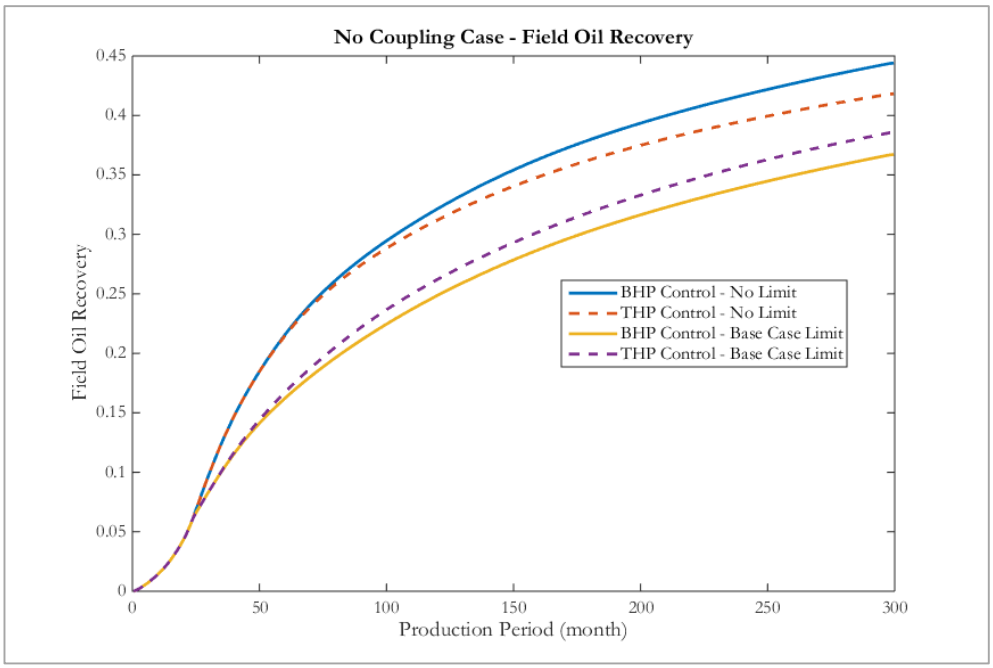

Figure 21 Field oil recovery for no coupling cases

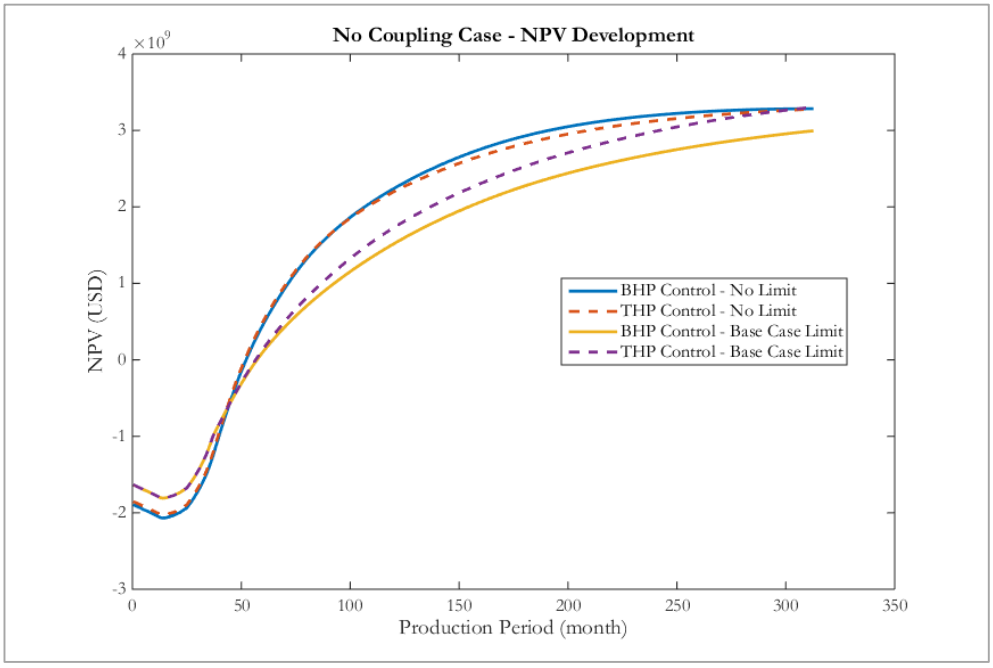

Figure 22 Net Present Value for no coupling cases

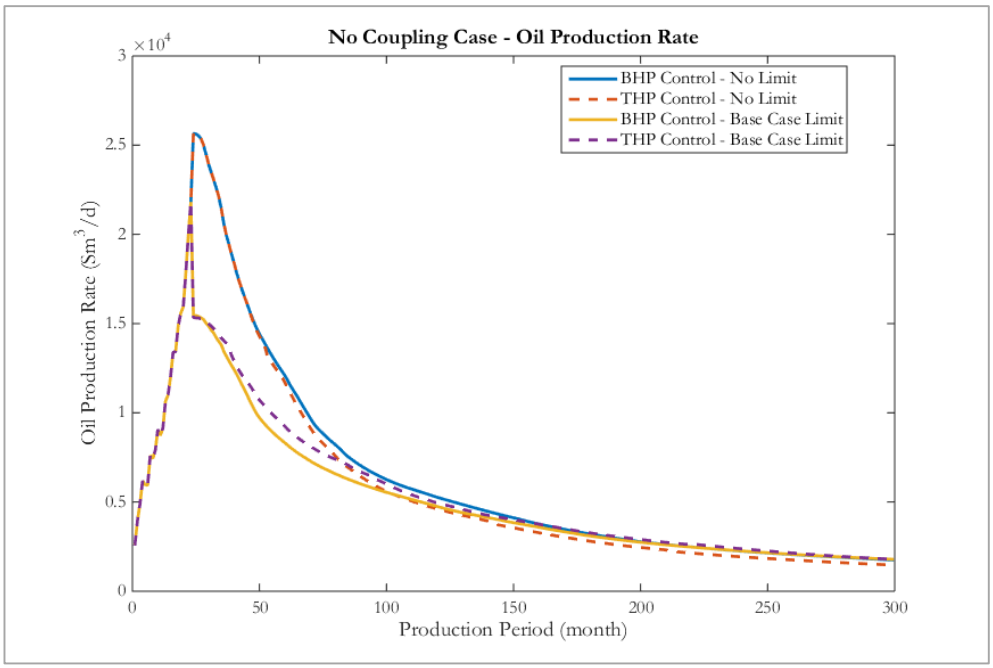

Figure 23 Oil production rate for no coupling cases

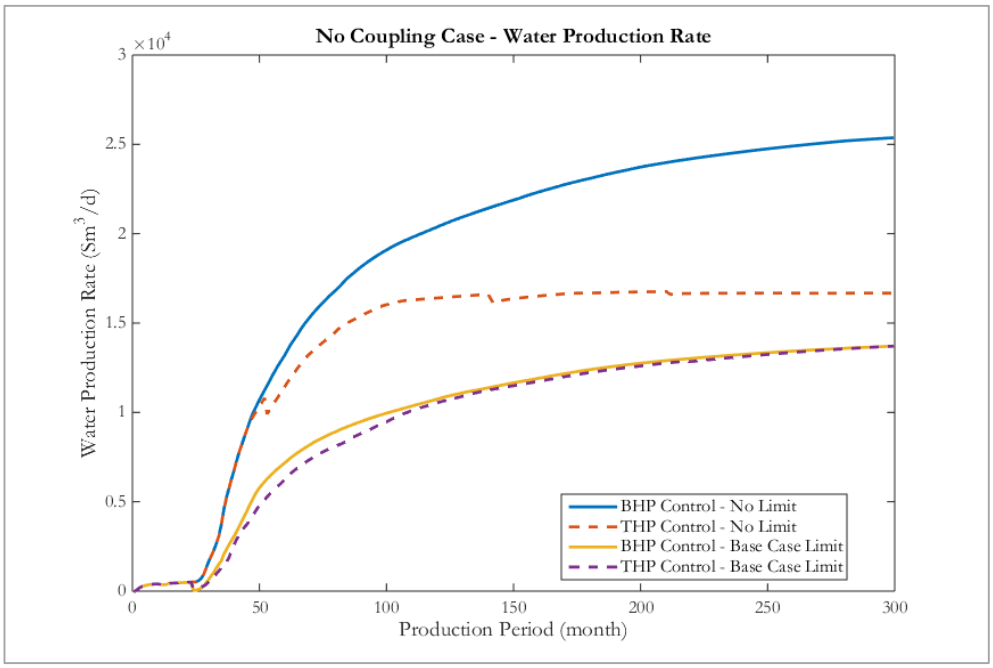

Figure 24 Water production rate for no coupling case

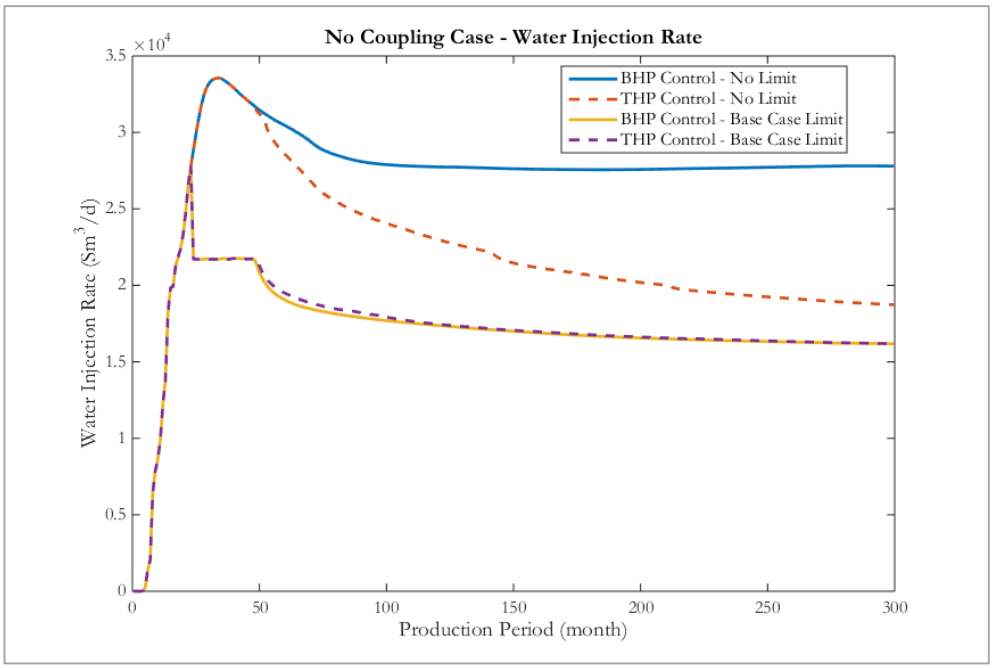

Figure 25 Water injection rate for no coupling cases

As a summary of this section, we can say that the cases with tubing head pressure control provided more realistic results than the bottomhole pressure control cases; thus, this control point is selected to be further used in the project. We can also see that there is a great potential for optimizing and improving the asset's Net Present Value by having surface processing capacities as decision variables. There is around 5% of recovery gap between the tubing head pressure control with and without surface facilities limitation, but both cases gave the same Net Present Value. This implies that if we can improve the recovery by optimizing surface capacity constraints, we will have a better asset's Net Present Value.

4.5. Effect of Coupling Scheme and Coupling Frequency on Subsurface and Surface Coupled Model

In this section, we will demonstrate the impact of coupling scheme and coupling frequency on the UNISIM-I-D case. We introduce three cases which reflects the three types of coupling; namely, the explicit coupling, the implicit coupling with Newton iteration number = 3, and the implicit coupling with Newton iteration number = 10. All the cases in this section are run on INTERSECT simulator which couples ECLIPSE reservoir simulator and PIPESIM network simulator.

INTERSECT is a high-resolution reservoir simulator developed by Schlumberger (Schlumberger (2015)). It contains two nodes which are Reservoir Simulation node and Field Management node. The Reservoir Simulation node works in the same manner as ECLIPSE reservoir simulator. In this study, INTERSECT reservoir is migrated from ECLIPSE data file by using Schlumberger's Migrator. The Field Management system is used to schedule and control the production operations. It captures the ability of the reservoir to deliver fluids and matches with the capability of the surface network. Operational constraints, complex limitations, and economic parameters are considered. It provides predictive scenarios which are useful in field development planning, surface facilities design, and the production optimization process. Details of INTERSECT Field Management node can be found in Guyaguler et. al. (2006).

One of the advantages of INTERSECT field management over other coupling tools; for example, ECLIPSE with network option is that no pre-generated VFP table is used in

the pressure losses calculation; thus, there is no limitation and constraint in the operating windows. This gives flexibility in seamless coupling between subsurface and surface models.

Coupling of subsurface and surface model is carried out by specifying the keyword "NetworkBalanceAction". The keyword works by balancing the reservoir model and surface network model at the coupling location. In this study, "CombinedNetworkBalanceAction" keyword is used to perform a network balance using "NetworkBalanceAction" keyword and a rate allocation using "GuideRateBalanceAction" keyword. Rate allocation in the coupled case is also carried out in the same manner as the uncoupled simulation which is allocated by the well potential. The network balancing or coupling is taking place at the bottom hole. The solutions of the balance are obtained from the intersection of IPR (from INTERSECT Field Management node) and OPR (from surface network) and is passed to the Reservoir Simulation node as boundary conditions. Coupling scheme and frequency can be specified by using the keyword "CouplingProperties". The explicit coupling is called "Periodic" coupling where the coupling action is performed at the timestep level while the partially implicit coupling is called "Iteratively lagged" coupling where the coupling is made at the defined Newton iteration number N_c. Running of these cases are carried out in an automatic manner as the previous section, however, having two inputs from two simulations leads to a difference in workflow as shown in Figure 26.

Three cases were run on INTERSECT. No surface facilities limitation was posted on the cases. Cumulative oil production and asset's Net Present Value of all the cases are

visualized in Figure 27 and 28. Oil production rate, water production rate, and water injection rate are plotted in Figure 29, 30, and 31, respectively.

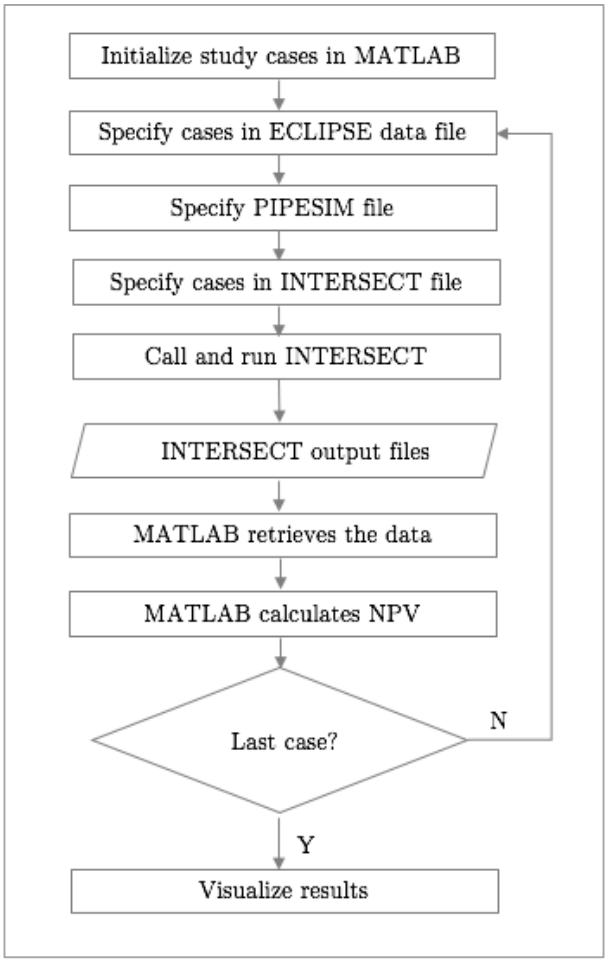

Figure 26 Flowchart for MATLAB-INTERSECT operation

It is observed that although giving the best NPV, the results from the explicit coupling scheme oscillate. This might be a result of rapid conditions changes in complicated reservoir model and surface network, and it indicates that the balancing of subsurface and surface model is not complete. It can be said that the results from the surface network

model cannot represent the controlled parameters at the end of the timestep and reservoir model does not converge in the specified conditions; hence, the results contain large degree of errors. Different coupling frequency also gives the different results as can be seen in the case with Newton iteration number = 3 and Newton iteration number = 10. The differences occur when the production rates sharply decline. In the more frequent coupling cases, we found that more wells were shut since it reaches the limits imposed previously such as; minimum bottomhole pressure, high water production rate. This explains why more coupling frequency is better in capturing the changes in pressure and flowrate and providing the accurate parameters at the coupling point. However, frequent coupling takes longer simulation time; thus, in order to obtain more study cases, we will continue using implicit coupling with Newton iteration number = 3 in the latter part of this work.

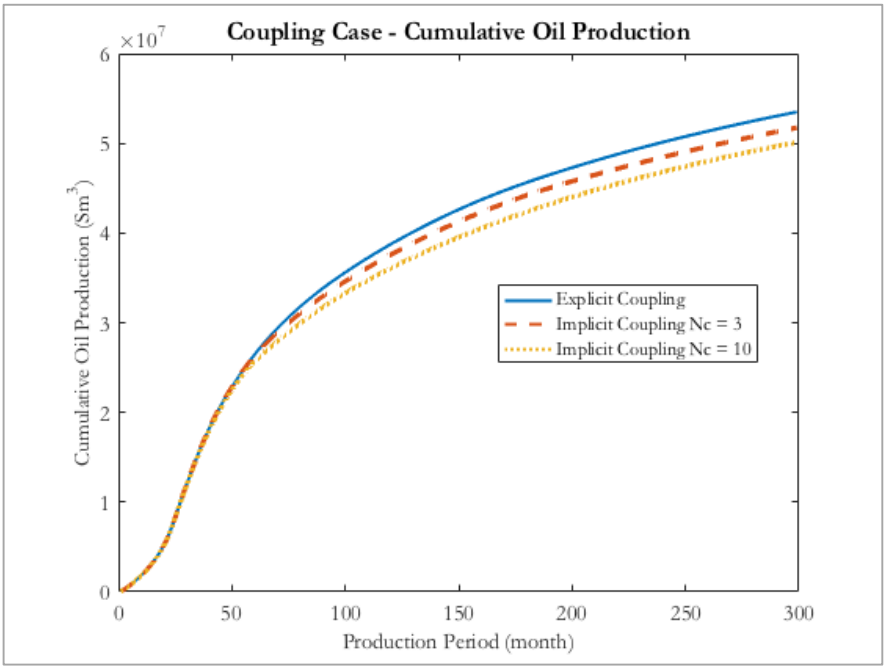

Figure 27 Cumulative oil production for different coupling schemes

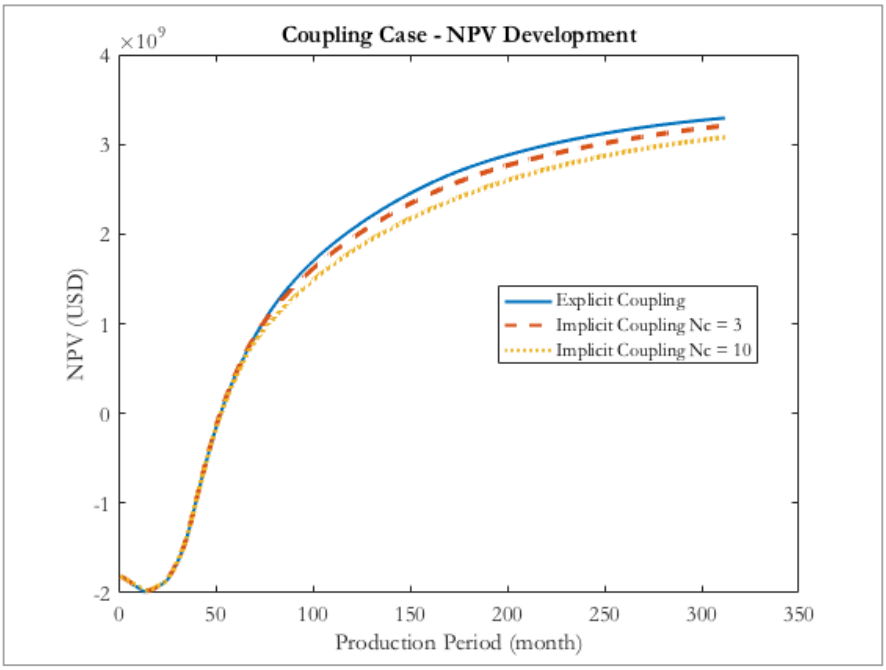

Figure 28 Net Present Value for different coupling schemes

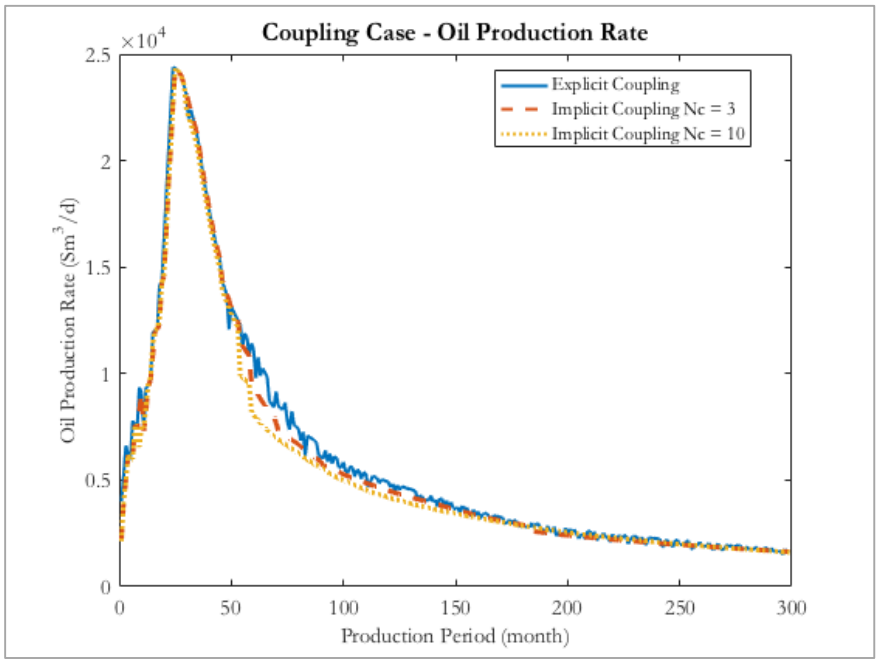

Figure 29 Oil production rate for different coupling schemes

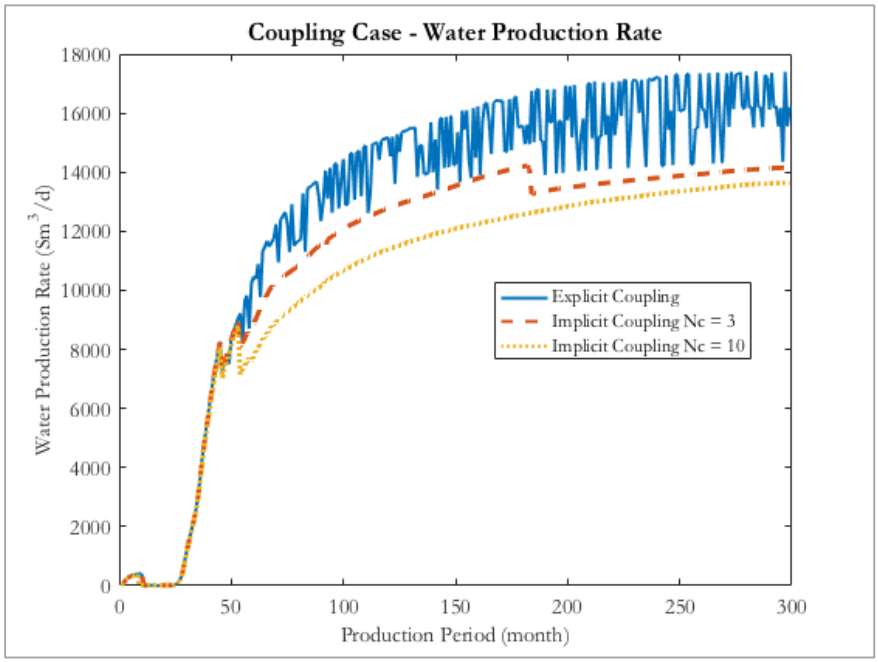

Figure 30 Water production rate for different coupling schemes

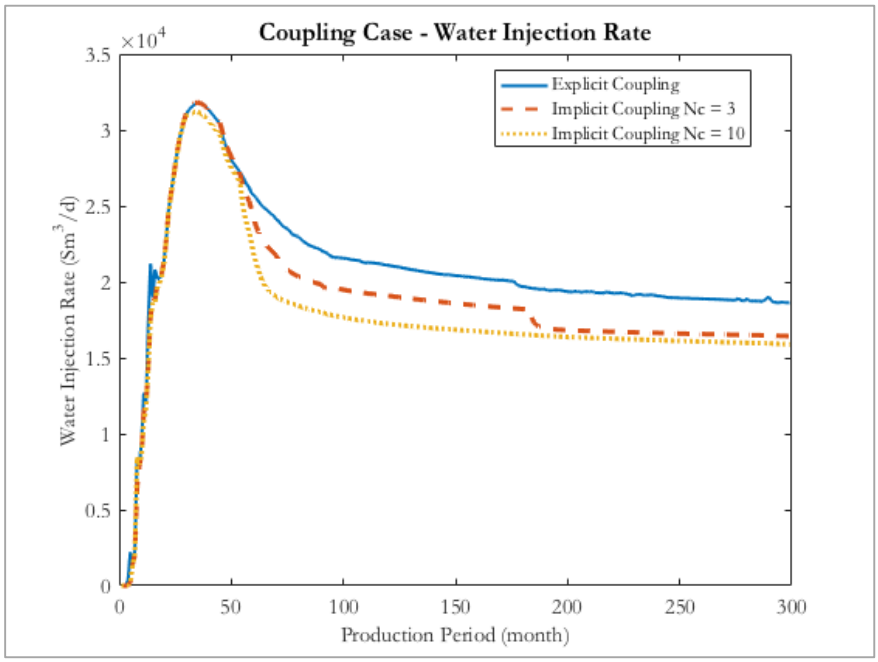

Figure 31 Water injection rate for different coupling schemes

The subsurface and surface models in this section are partially coupled where the surface network model is providing the boundary conditions for the reservoir simulator (which may be solved fully implicitly). It can be concluded that coupling schemes and coupling frequency have significant effect on the production results. Having tighter coupling i.e. implicit scheme leads to more accurate results but may results in increased simulation time as more Newton iterations are required to converge the system. A more frequent coupling case can be further performed to obtain the more accurate results and can be used in acceptable accuracy determination. However, the tighter coupling takes longer simulation time and may not be suitable for an operation optimization. Explicit coupling would be the solution, but proper timestep should be applied to reduce the oscillation. The selection of the proper timestep can be improved by using a concept of PID control (Akakpo and Gildin (2017)).

The end remark of the model development and numerical simulations section is that the commercial software introduced in this study is not able to perform a fully implicit coupling. We attempted to use the open-source MATLAB Reservoir Simulation Toolbox (MRST) developed by SINTEF (Knut-Andreas Lie (2016)) to perform a fully implicit coupling on the UNISIM-I-D case. Unfortunately, the current MRST codes are incompatible with the UNISIM-I-D black oil model. Due to the complexity in geological settings e.g. pinch out, and different equilibriums, MRST is able to perform only the incompressible simulation on the model. The incompressible run was carried out, but the results are significantly different from the results obtained from the commercial software in black oil mode. Since the results from MRST and commercial software are not

comparable, we focus on using the commercial software with partial coupling scheme for the rest of the study.

4.6. Comparison between Uncoupled Base Case and Coupled Base Case

It is one the most important tasks of this study to exhibit the advantages of the reservoir and surface integration. This section aims to show the similarities and differences in the results between UNISIM-I-D uncoupled reservoir and the implicitly coupled UNISIM-I-D reservoir and surface network. The uncoupled case chosen for comparison is the case with the tubing head pressure control. Both uncoupled and coupled cases are run with the base case limitations taken from UNISIM-I-H model (shown in Table 11).

Results of the comparison are plotted in Figure 32 to 38. The red dashed line represents the uncoupled case while blue line represents the coupled case. Cumulative oil production for both uncoupled and coupled cases is plotted in Figure 32. The final cumulative oil production difference is 0.3%. Asset's Net Present Value for both cases is displayed in Figure 33. The NPV difference is 0.6% where the uncoupled case value is 3.30 billion USD and the coupled case value is 3.28 billion USD. Figure 34 - 38 present comparisons of oil production rate, water production rate, cumulative water production, water injection rate, and cumulative water injection, respectively. All the results show no difference between the two cases. It is noted that since in this study, the producing fluid contains only oil and water, changing in pressure and flowrate does not have significant effect on the flow regime and pressure losses. Also the flows are assumed to be in steady-state, the integration of the surface pipeline network does not show significant difference in this

stage. However, when the pressure declines and gas production occurs, the coupled model will give the more accurate results than the uncoupled one.

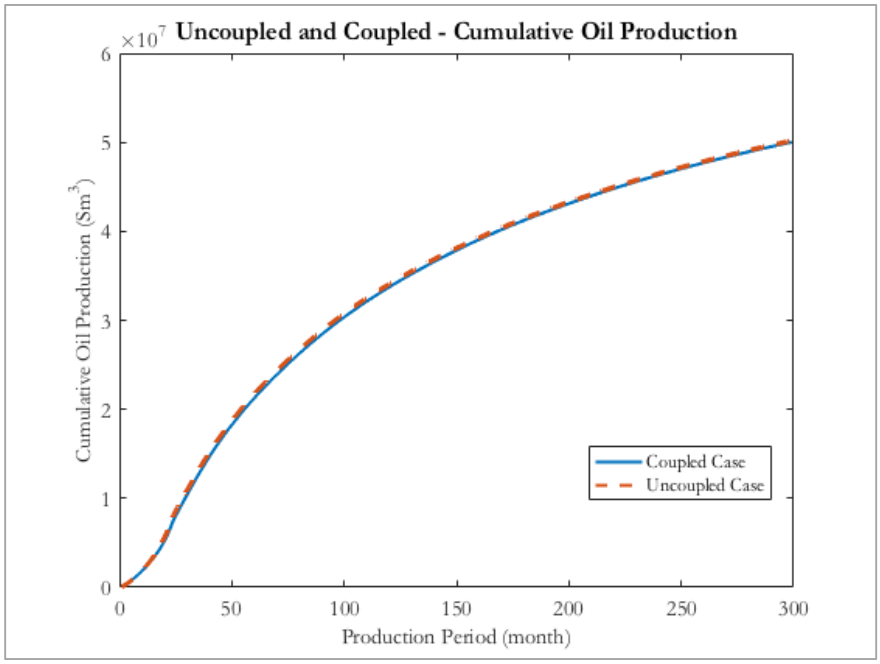

Figure 32 Cumulative oil production for uncoupled and coupled case

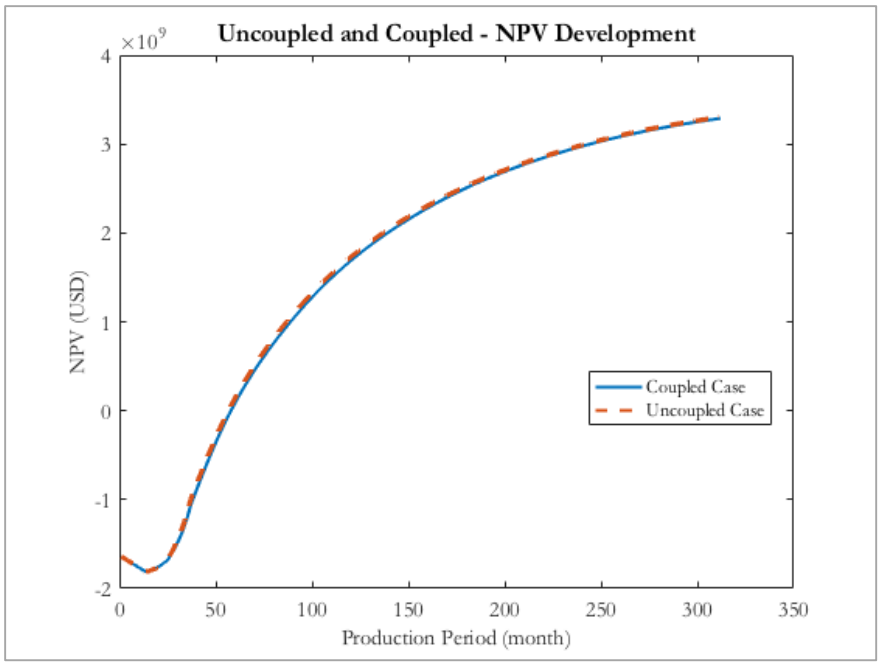

Figure 33 Net Present Value for uncoupled and coupled case

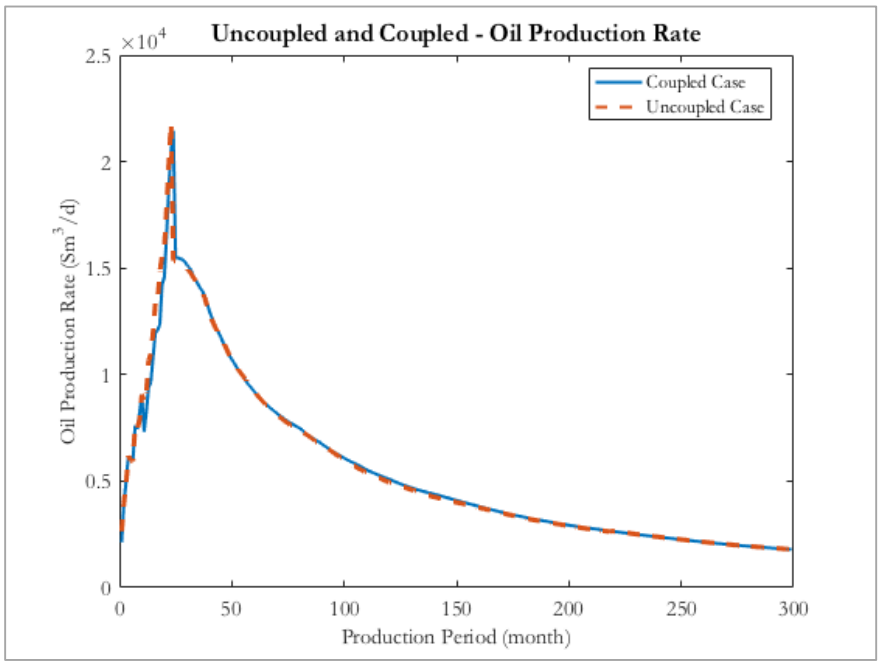

Figure 34 Oil production rate for uncoupled and coupled case

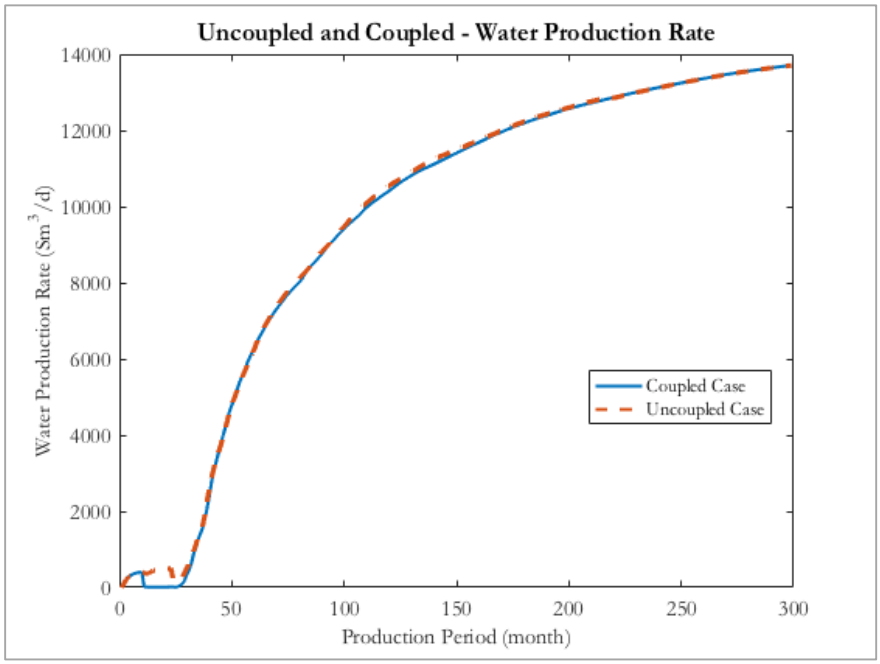

Figure 35 Water production rate for uncoupled and coupled case

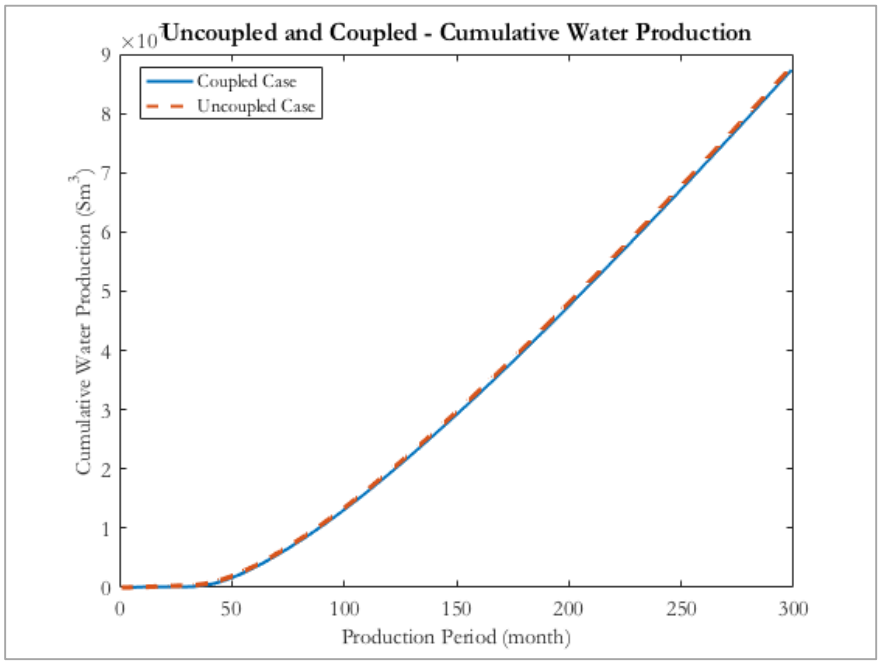

Figure 36 Cumulative water production for uncoupled and coupled case

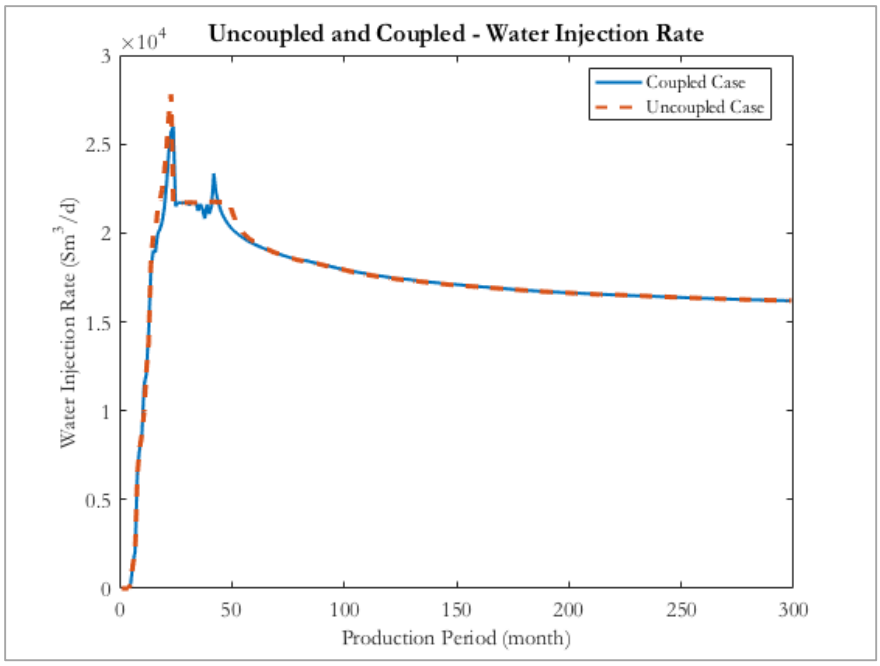

Figure 37 Water injection rate for uncoupled and coupled case

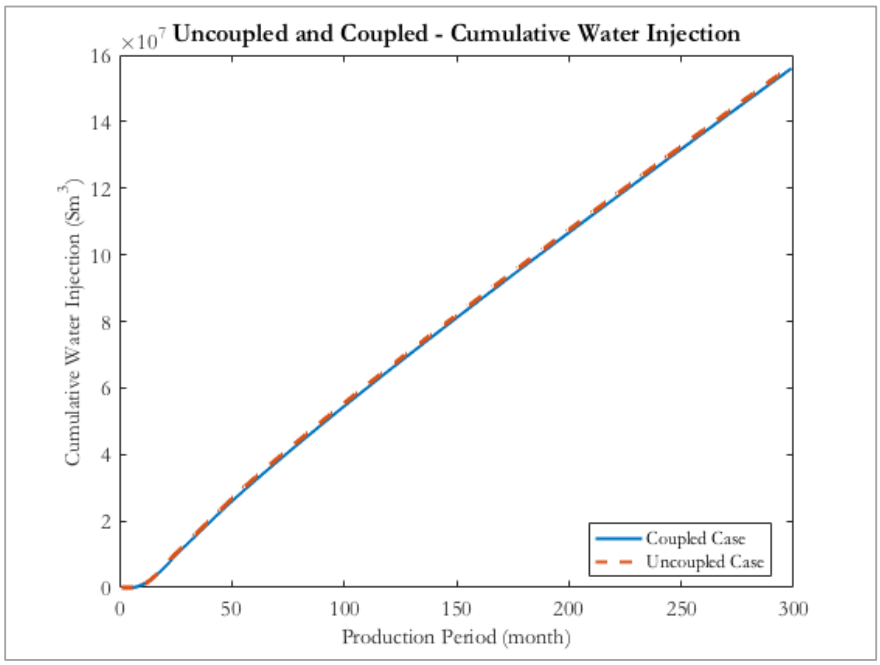

Figure 38 Cumulative water injection for uncoupled and coupled case

5. OPTIMIZATION AND NUMERICAL STUDY

As discussed in the previous sections, that the integrated model provides a holistic understanding of the petroleum production system and, thus, optimization of the integrated model enhances the efficiency of field development and planning, and in turn, maximizes recovery and asset's Net Present Value. This section gives an overview of the optimization on the coupled subsurface and surface model where theories and procedures to obtain the optimal results will be explained. Theoretical descriptions in the area of optimization can be found in Nocedal and Wright (2006). We will also demonstrate the benefits of optimization using the UNISIM-I-D benchmark case.

5.1. Optimization Model Components

Optimization is an important tool used in decision making. The optimization methods and techniques were introduced to help decision makers to identify the possibility that best-fit with their goals. The optimization problem can be presented by one or more mathematical models. The model should be formulated and constructed to describe the problem in a simple but detailed manner. The optimization model comprises of three main components, e.g. objective function, decision variables, and constraints. Once having a model, an optimization algorithm can be used to find its solutions. Selection of the optimization algorithm, number of decision variables and constraints, and characteristics of the objective function are crucial as they affect the numerical and computational efficiency to obtain the solution or would not be able to achieve the solution at all.

In general, the task of optimization is to maximize or minimize an Objective Function that is a qualitative measure of the system's performance. The Objective Function can be mathematically defined as a function of Decision Variables. Limitations and restrictions of the Decision Variables are called Constraints. In a mathematical point of view, maximization and minimization can be solved in the same manner by imposing the negative sign to the objective function equation. The formulation of optimization model is shown in equation 62.

$$\min_{x \in R^n} J(x) \qquad subject\ to\ c_i(x) \geq b_i, i = 1, \ldots, m \tag{62}$$

where $J(x)$ is an objective function, x represents decision variables, $c_i(x)$ represents the constraint functions of variable x, and b_i is the constraint value.

The objective of this study is to maximize the asset's Net Present Value (NPV). NPV is a function of investment, revenues from selling hydrocarbons, and the operational costs accounted with oil/ water/ gas handling from the reservoir to the surface process. The formulation and details of NPV calculation were shown in Section 4.3: Development of an economic model. Several parameters are affecting the value of NPV. In this study, we choose oil and water processing capacity and water injection capacity as decision variables to predict longer term effects on the production rather than controlling each well's production rate. The optimization is treated as a nonlinear problem which the solutions of the problem require an iterative process to establish a direction of search.

5.2. Optimization Methods and Algorithms

The optimization problem can be classified by the nature of the objective function and constraints i.e. linear, and nonlinear programming problem. The optimization problem can also be categorized in various manners, for example, unconstrained and constrained, global and local, and stochastic and deterministic optimization. Here we briefly introduce the concept of global and local optimization.

In nonlinear optimization problems, there may exist multiple local solutions, points that the objective function is smaller than the surrounding feasible points, but among all of these local optimum, there exists only one point that gives the highest or lowest objective function; this point is called a global solution. Finding a global solution poses a challenging task; and in practice, getting a local optimum is acceptable if the search area is large. Two optimization methods that are being used to iteratively solve for the optimal solution are:

- Gradient-based algorithms: these algorithms utilize the gradient (first derivative) and Hessian (second derivative) of the objective functions to find the search direction. They are computationally efficient and provide robust solutions, but to achieve that, they require knowledge of the system source codes to obtain the accurate gradient information. The other disadvantage of the gradient-based method is that the optimizer would be trapped in the local solution if the initial guess is not appropriate.

- Gradient-free algorithms: these algorithms use the information from the previous iteration to estimate the next one. The advantage of these methods is that they do not require reservoir simulation gradient and can treat the reservoir as a black box.

Although having an ability to obtain the global solutions without requiring detailed knowledge of the reservoir simulation, gradient-free method, e.g. genetic algorithm method, requires significantly more computations. UNISIM-I-D coupled model may take weeks to run the optimization cases, to perform model verification, and to obtain results validation on the office computer; thus, we use gradient-based method algorithms to optimize the computational time of this study. It is noted that although the results may be trapped in the local solutions, the optimizer improves the performance of the field development project.

5.3. Sensitivity Analysis

This study is assumed to be carried out in the field development phase where the surface capacity limitation is set. It should be noted that each implicit coupling simulation runs for 26 years of production, takes around 4 hours while the uncoupled ECLIPSE reservoir simulation takes less than 4 minutes. Therefore, due to limitations in hardware resources available, the uncoupled cases were run to visualize parameters sensitivity analysis.

Facilities limitations of UNISIM-I-H case presented in Table 11 are used in a base case calculation. NPV of the base case is 3.30 billion USD. Decision variables in the base case

are perturbed by having one parameter changing at a time to exhibit the amplitude of effect from each variable. To scope down the optimization cases, the upper and lower boundaries are set for each decision variable and are shown in Table 12.

Table 12 Boundaries for decision variables sensitivity analysis

Variable	Lower Boundary (Sm^3/d)	Upper Boundary (Sm^3/d)
Oil Processing Capacity	13000	26000
Water Processing Capacity	13000	26000
Water Injection Capacity	13000	26000

The parameter sensitivity results are summarized in Table 13. The results are also visualized in a form of tornado chart in Figure 39.

Table 13 Sensitivity analysis results

Variable	Base NPV (USD)	Min NPV (USD)	Max NPV (USD)	Increment (%)
Oil Processing Capacity	3.30E+09	3.30E+09	3.39E+09	2.7
Water Processing Capacity	3.30E+09	3.26E+09	3.30E+09	0
Water Injection Capacity	3.30E+09	3.28E+09	3.52E+09	6.7

The bar colors indicate the relation between the sensitivity analysis value and the base case objective function. Red color shows that the cases give lower NPV than the base case while blue shows that the cases give higher NPV than the base case. The results indicate that the water injection capacity has the strongest effect on the asset's NPV while water processing capacity has the smallest effect. The highest NPV increment was obtained by changing the water injection capacity. The NPV increase 6.7% from the base case by changing only water injection capacity.

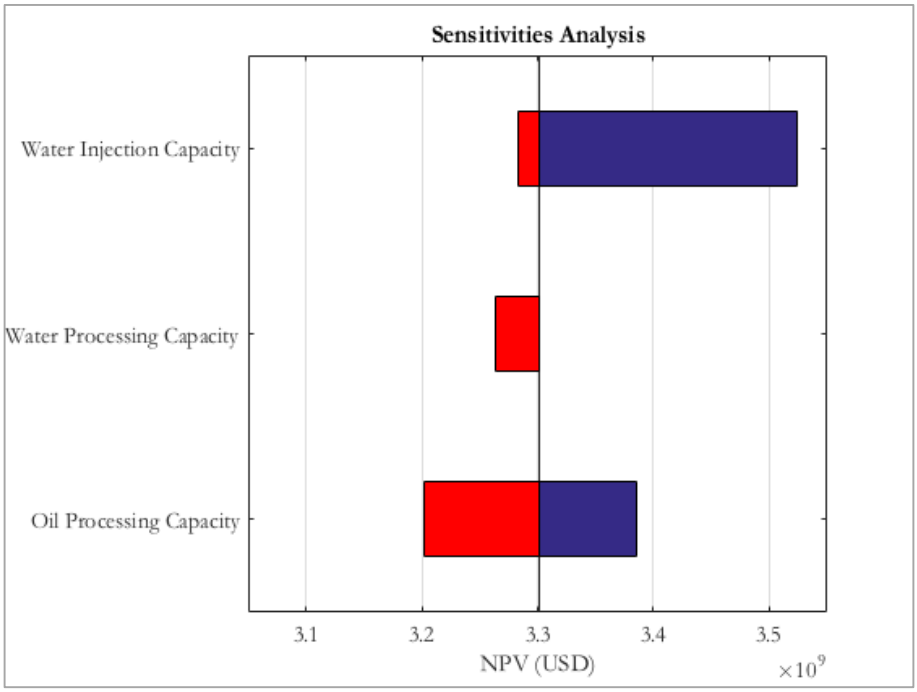

Figure 39 Tornado chart for sensitivity analysis

The results of single parameter sensitivity analysis are plotted in Figure 40, 41, and 42 for changing in oil processing capacity, water processing capacity, and water injection capacity, respectively.

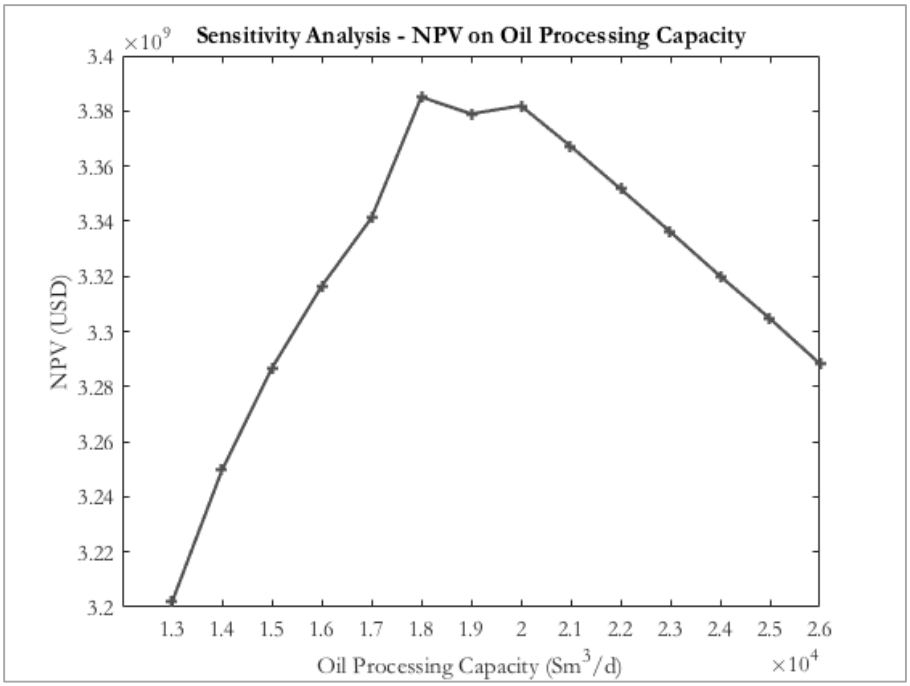

Figure 40 Single parameter analysis on oil processing capacity

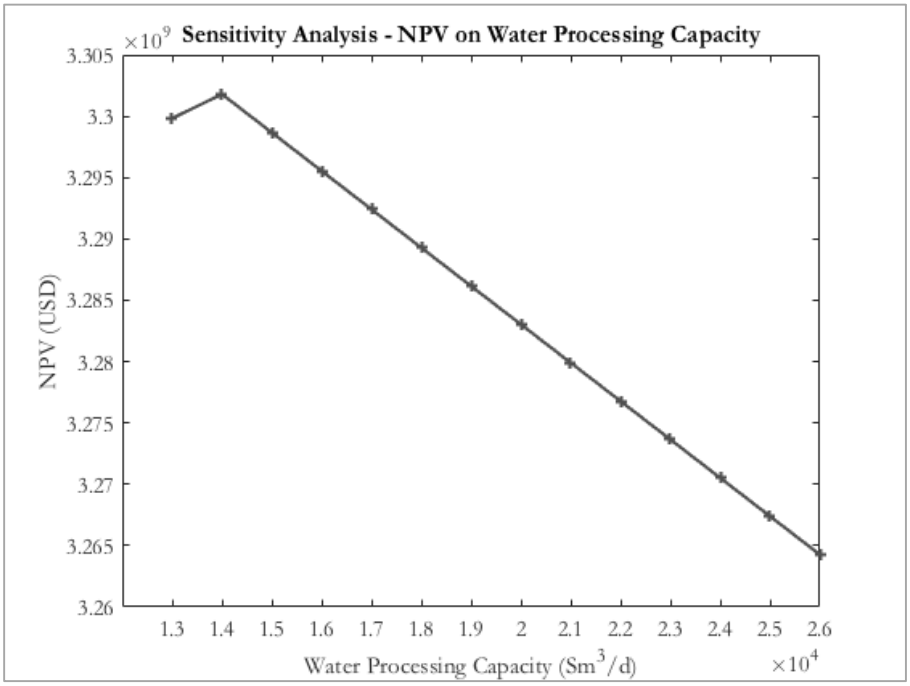

Figure 41 Single parameter analysis on water processing capacity

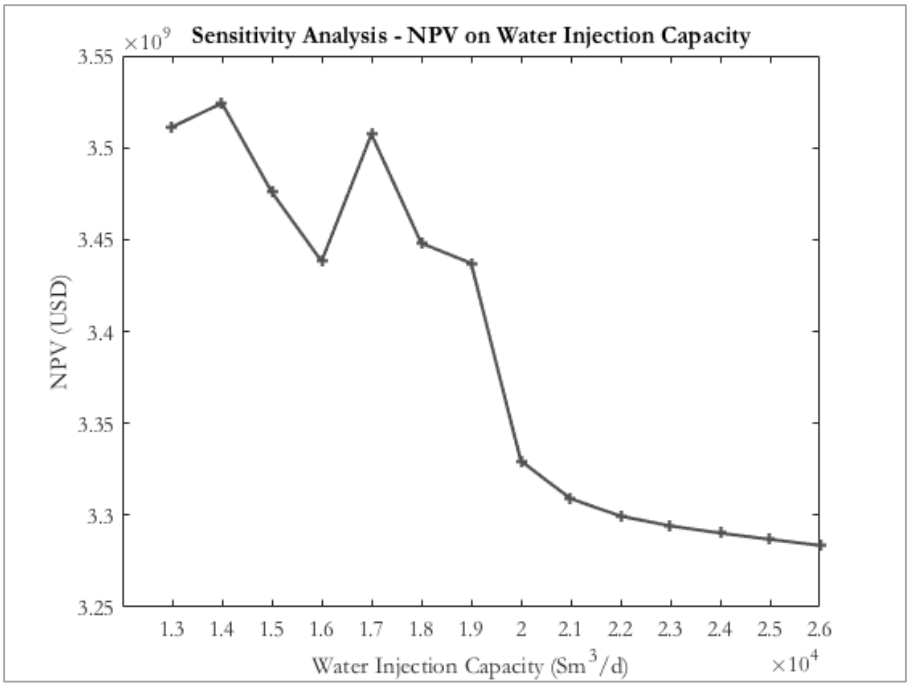

Figure 42 Single parameter analysis on water injection capacity

A total of 1,176 discrete cases were run in order to present the effect of each decision variable. Boundaries of oil processing capacity and water processing capacity used in the two-parameter analysis runs are the same as stated in Table 12 while the lower boundary for the water injection facility used in the two-parameter analysis runs is 20000 Sm^3/d. The increment of each discrete parameter is 1000 Sm^3/d. Surface parameter analysis shows the NPV results when two parameters are changing simultaneously. The results of the surface parameter analysis are displayed in Figure 43 and 44.

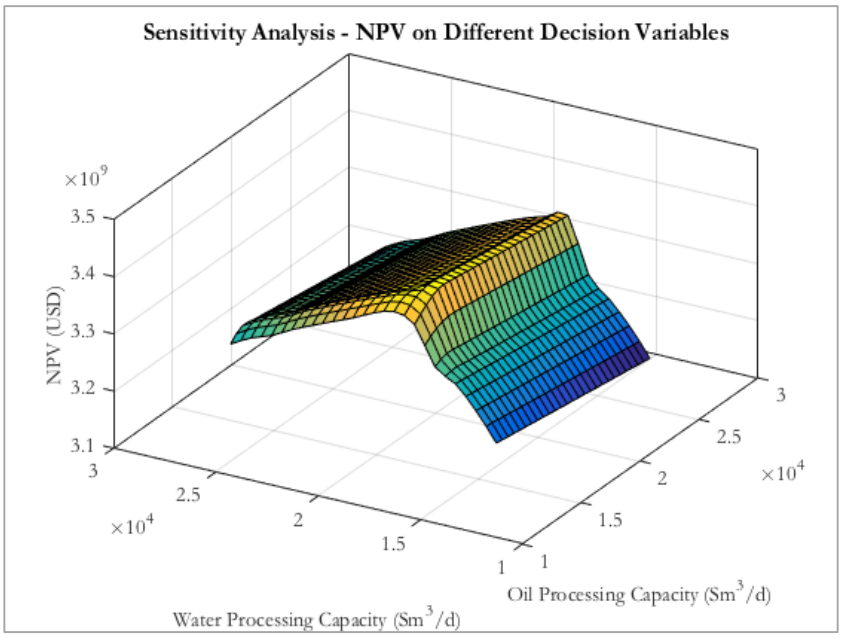

Figure 43 Surface parameter analysis between oil processing capacity and water processing capacity

From the sensitivity analysis, it can be said that the optimization has a clear potential for improving asset's Net Present Value. However, the results from single parameter sensitivity analysis cannot be directly applied to the optimization problem since the combination of the parameters gives the different optimal solution. The optimization algorithms introduced in the previous section will be applied of maximizing the asset's Net Present Value in the next section.

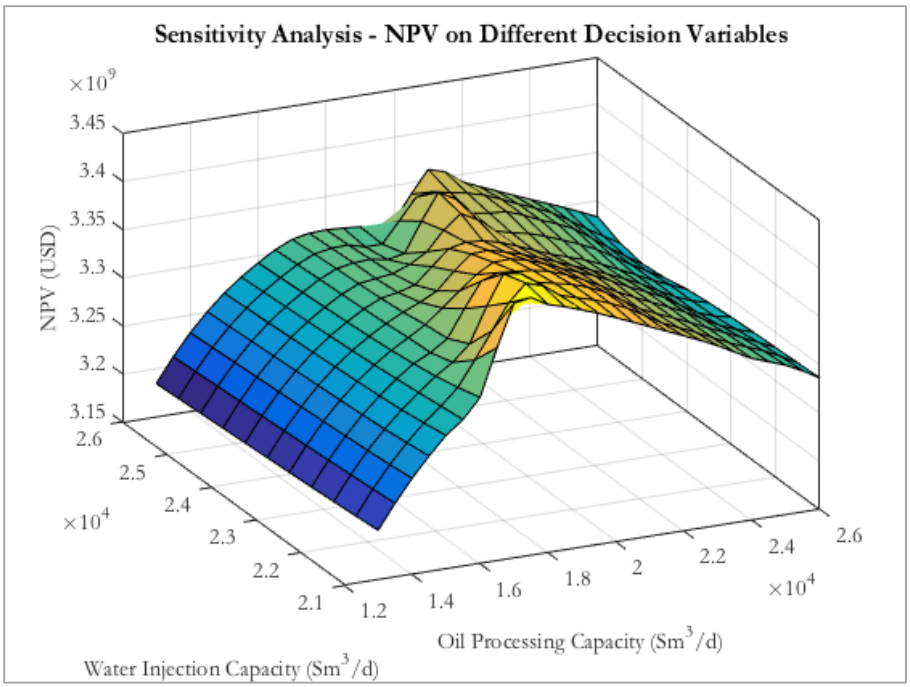

Figure 44 Surface parameter analysis between oil processing capacity and water injection capacity

5.4. Optimal Field Development Results

In the general petroleum production optimization problem, the decision variables are always tangible parameters that can be modified during operations. They are usually related to well rates and bottomhole flowing pressure, while in the coupled subsurface and surface model, the controlled parameters are chosen based on surface parameters.

MATLAB Optimization Toolbox™ (MathWorks (2016)) is introduced into the optimization part of this study. The toolbox contains functions to obtain the minimum or maximum objective function while honoring all the constraints. Functions in MATLAB

Optimization Toolbox™ are able to achieve the solutions without user-supplied gradient; however, the computation will be faster if the user supplies a gradient and a Hessian for the solvers.

5.4.1. Optimal Results for the Uncoupled Case

In this section, optimization is carried out in two different manners. One is treating decision variables as discrete parameters and perform objective function calculation using every single discrete value. The results of this calculation are used to compare with the results from gradient-based optimization algorithm and are used to exhibit the sensitivity analysis in the previous subsection.

The second way is to utilize MATLAB Optimization Toolbox™. In this case, "fmincon" solver is used to find the optimal oil and water processing capacity and water injection capacity of UNISIM-I-D model. "fmincon" is a solver designed to solve a constrained minimization problem. The algorithm defaulted in "fmincon" solver is 'interior-point' algorithm. 'interior-point' algorithm is recommended since it can handle a large-scale problem and requires lower memory usage compared to the other four algorithms available in "fmincon" method. The detailed algorithms and implementation can be found in Nocedal and Wright (2006). The algorithm satisfies boundaries at all iterations and can manage the "not-a-number" or "infinite" results.

Optimization options can be set using "optimoptions" keyword. Gradient can be supplied to the solver to improve the speed and reliability of the solver by setting 'SpecifyObjectiveGradient' to be 'true. To improve the speed of the optimization, Parallel

Computing was initiated in MATLAB by setting 'UseParallel' to be true. Further details on MATLAB Optimization Toolbox™ can be found in the document section in MATLAB (MathWorks (2016)).

Production capacities from the UNISIM-I-H were used as initial values for the solver. The optimization constraint for each decision variable follows the boundaries set in Table 12. Results from each optimization technique are shown in Table 14.

Table 14 Optimization results for UNISIM-I-D uncoupled reservoir

Case	Oil Processing (Sm^3/d)	Water Processing (Sm^3/d)	Water Injection (Sm^3/d)	NPV (USD)
Base Case	15500	13950	21700	3.30E+09
Discrete	16000	15000	21000	3.42E+09
fmincon interior-point	15463	12248	20000	3.31E+09

It can be seen in Table 14 that the NPV from "fmincon" solver with 'interior-point' algorithm is lower than the value obtained from a discrete run. It confirms that "fmincon" solver was trapped in the local solutions. Different algorithm and initial points were used to repeat the optimization with "fmincon". Although 'interior-point' algorithm is recommended to be run in the first place, MATLAB suggests that the results can be

slightly less accurate than the other algorithms due to the internal calculations. The other algorithm used in "fmincon" solver for comparison is 'sqp' or Sequential Quadratic Programming.

The new initial values are the values giving the highest NPV in the single parameter analysis. The new initial oil processing capacity is 18000 Sm^3/d, water processing capacity is 14000 Sm^3/d, and the water injection capacity is 14000 Sm^3/d. The NPV result using a different algorithm and initial values are shown in Table 15. All the optimization completes because the objective function is non-decreasing in the feasible directions. The other three optimization runs give the same solutions and objective function values. Performance of each optimization runs is also displayed in Table 15.

Table 15 Comparison between different initial values and algorithms

Case	Initial Value / **Optimized Value** (Sm^3/d)			NPV (USD)	Iteration/ Function Count
	Oil Processing	Water Processing	Water Injection		
1 – fmincon interior-point	15500 **15463**	13950 **12248**	21700 **20000**	3.31E+09	9 / 116
2 – fmincon interior-point	18000 **13000**	14000 **13000**	14000 **13000**	3.54E+09	7 / 67

Table 15 Continued

Case	Initial Value / **Optimized Value** (Sm^3/d)			NPV (USD)	Iteration/ Function Count
	Oil Processing	Water Processing	Water Injection		
3 - fmincon	15500	13950	21700	3.54E+09	4 / 51
sqp	**13000**	**13000**	**13000**		
4 - fmincon	18000	14000	14000	3.54E+09	2 / 12
sqp	**13000**	**13000**	**13000**		

The results from the optimization in the uncoupled case give the better NPV value comparing to the results from the sensitivity analysis. The increment of NPV from the base case is 7.3%. It is observed that the gain of NPV is from a reduction of the water injection capacity. This shows an opportunity on the injection well placement to obtain more sweeping and recover more oil.

The base case results of the uncoupled and coupled cases are identical as exhibited in section 4.6. As it is one the most important tasks of this study to exhibit the advantages of the reservoir and surface integration, this section aims to obtain the uncoupled optimal solution as a reference for the coupled case optimization in the next subsection. The results will be used to confirm the pros and cons of the subsurface and surface integration.

5.4.2. Optimal Results for Coupled Case

The optimization of the integrated model is carried out in MATLAB utilizing the same optimization method and algorithm as the uncoupled case. Only 'interior-point' algorithm is used in the optimization of the coupled case. Although 'sqp' algorithm may provide the faster results, MATLAB recommends starting the "fmincon" optimization with the defaulted 'interior-point' algorithm. The initial values are set at the UNISIM-I-H limitations. Optimization results of the coupled case are shown in Table 16.

Table 16 Optimization results for UNISIM-I-D coupled reservoir

Case	Oil Processing (Sm^3/d)	Water Processing (Sm^3/d)	Water Injection (Sm^3/d)	NPV (USD)
Base Case	15500	13950	21700	3.28E+09
fmincon interior-point	13000	13000	13000	3.39E+09

The increment of asset's Net Present Value in the optimal coupled UNISIM-I-D reservoir is 3.4% comparing to the base case while the cumulative oil production of the optimal case decreases by 6.6% from the base case. The NPV development and accumulated oil production of the base case and the optimized case are shown in Figure 45 and 46.

Figure 47 – 52 show the comparison between coupled base case and optimal case in oil production rate, liquid production rate, water production rate, cumulative water production, water injection rate, and cumulative water injection. Although getting less cumulative oil production, the optimal case has the better NPV from the longer oil production plateau, and significant lower cumulative water production and cumulative water injection.

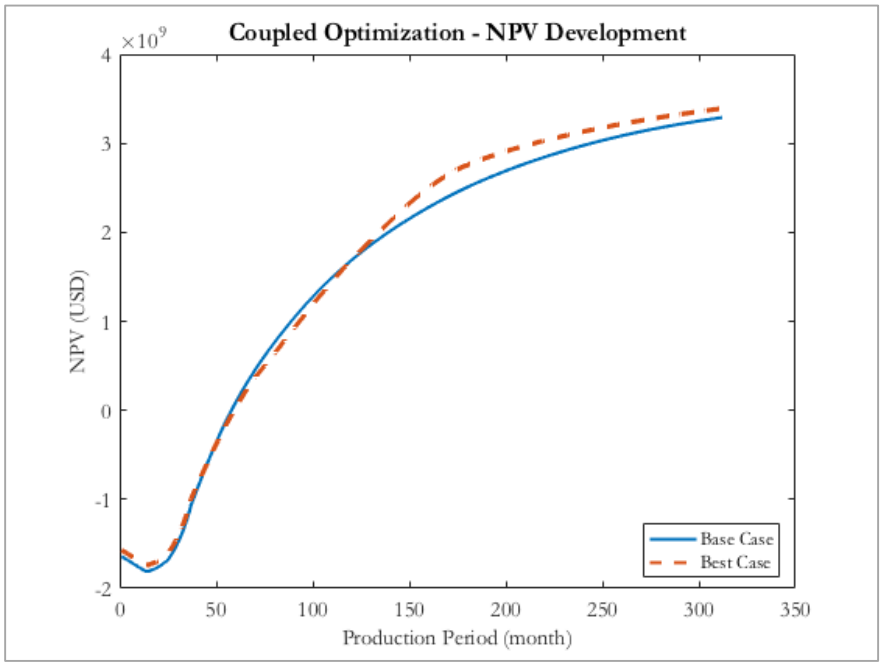

Figure 45 NPV development for the coupled base case and optimal case

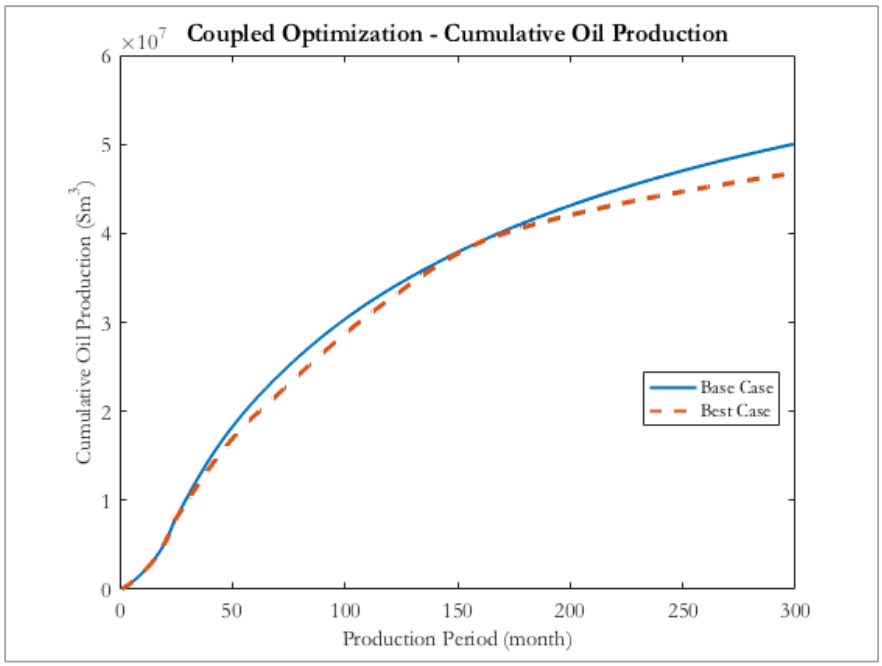

Figure 46 Cumulative oil production for the coupled base case and optimal case

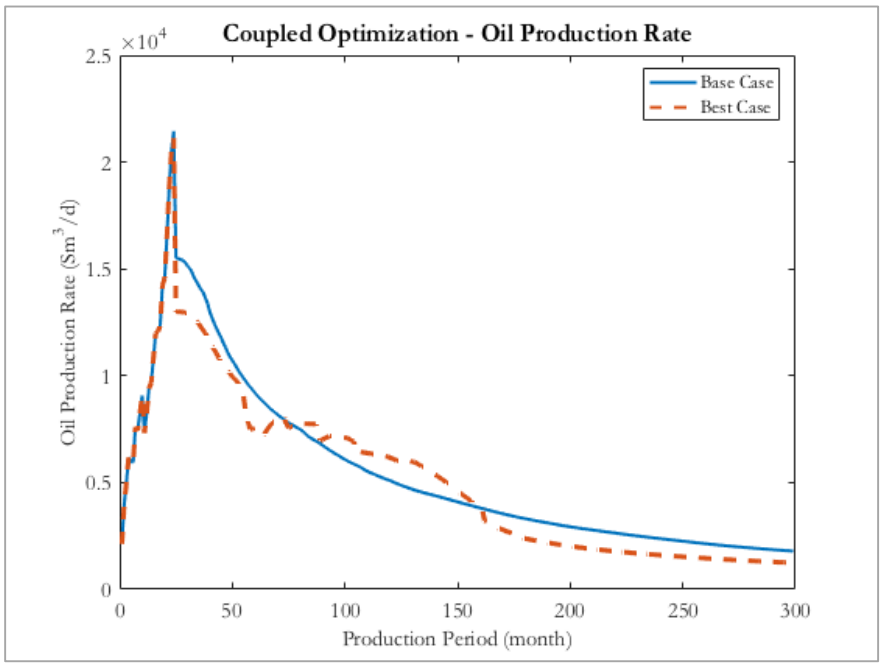

Figure 47 Oil production rate for the coupled base case and optimal case

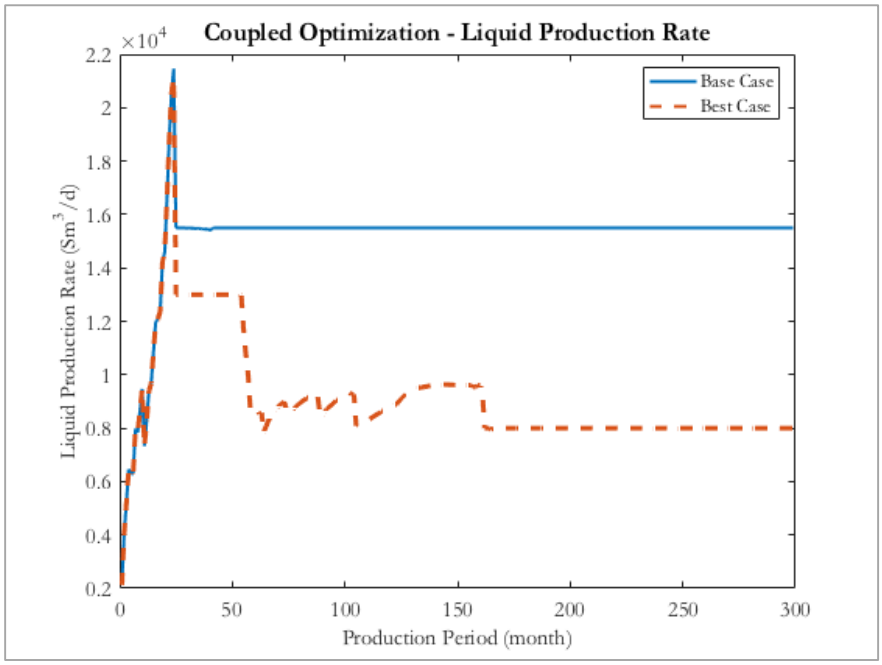

Figure 48 Liquid production rate for the coupled base case and optimal case

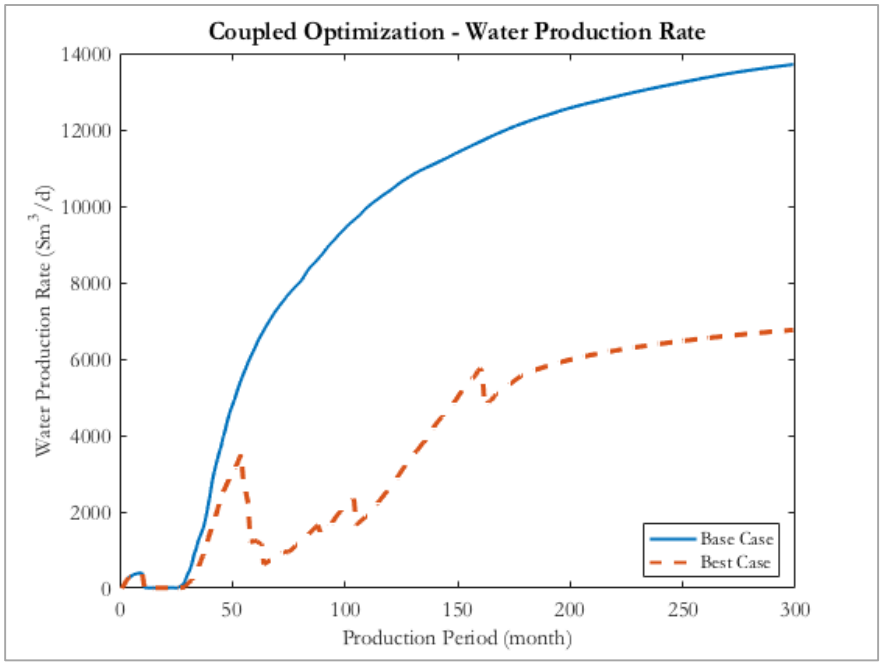

Figure 49 Water production rate for the coupled base case and optimal case

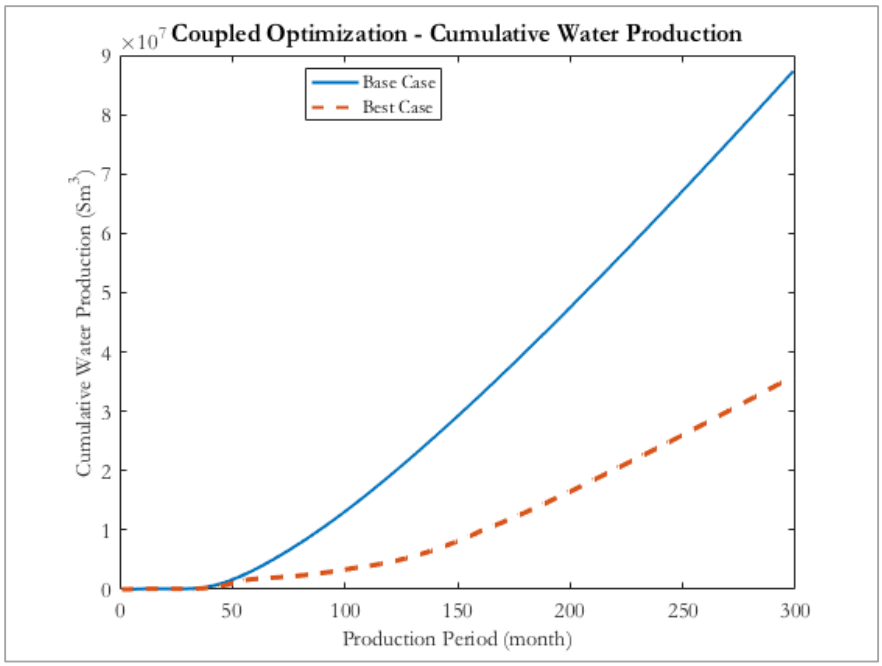

Figure 50 Cumulative water production for the coupled base case and optimal case

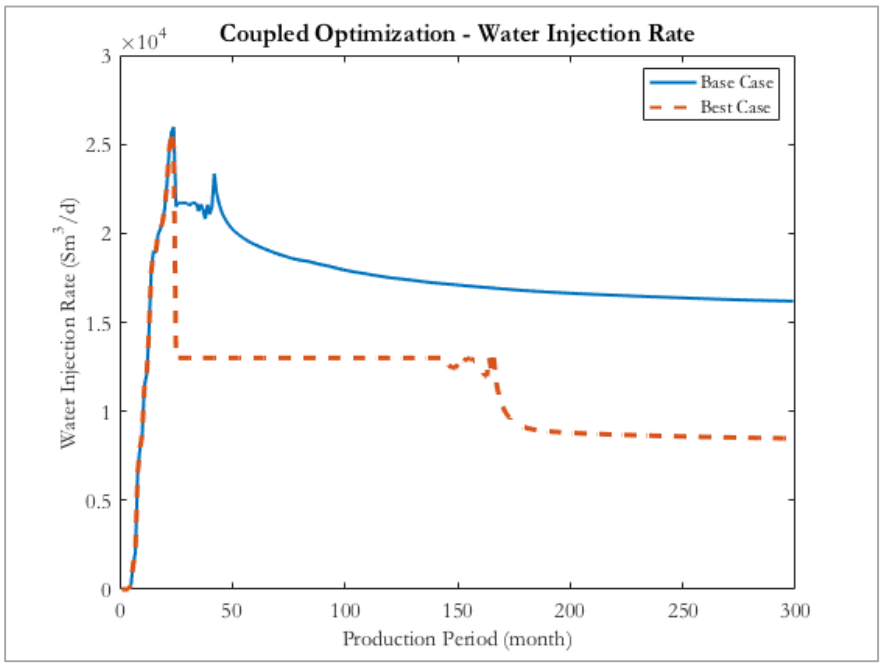

Figure 51 Water injection rate for the coupled base case and optimal case

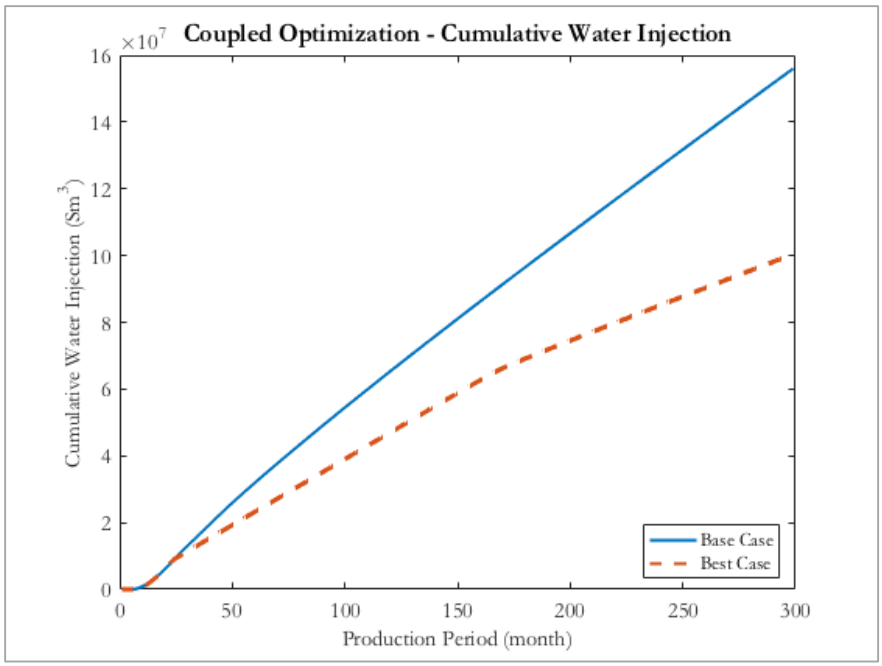

Figure 52 Cumulative water injection for the coupled base case and optimal case

Although having the same optimal solutions, the asset's Net Present Value which is our objective function from the uncoupled and coupled cases is different. The NPV increment from the uncoupled case is 7.3% while the increment from the coupled case is 3.4%. While the base case results give the identical NPV, it proves that the integration has an effect on the optimal results.

The reduction of the field oil recovery is expected to relate with the individual well's pressure control. In the uncoupled model, all the wells are able to produce at the same minimum tubing head pressure while in the coupled model, the wells are producing at the back pressure that is influenced by the other wells. That tubing head pressure is higher than the specified tubing head pressure to honor the constraint, thus, leading to the lower

production from the well. This issue can be rectified by applying choke valves into each well and perform the optimization on the choke network.

It is noted that since the producing fluid contains only oil and water without free gas and the flow system is treated in steady-state, changing in pressure and flowrate does not have significant effect on the flow regime and pressure losses, thus, the integration of the surface pipeline network does not show great difference in this stage. However, when the pressure declines and gas production occurs, the coupled model will give the more accurate results than the uncoupled one due to the account of intermittent flow in the gas-liquid system.

5.5. Effect of Economic Parameters on Optimal Solutions

UNISIM-I-D benchmark case is also designed for a probabilistic study. Economic uncertainties are defined in three case, namely, the most likely scenario that we have been using in the earlier parts of this study, the optimistic scenario, and the pessimistic economic scenario. This section aims to demonstrate the effect of economic parameters on the optimal solutions. The calculations are performed by using all the equations shown in section 4. Parameters for optimistic and pessimistic economic scenarios are shown in Table 17 to 19.

Table 17 Optimistic and pessimistic economic parameters

Variable	Optimistic	Pessimistic	Unit
Oil price	440.30	251.60	USD/m^3
Oil production cost	81.80	52.40	USD/m^3
Water production cost	8.18	5.24	USD/m^3
Water injection cost	8.18	5.24	USD/m^3
Platform Investment	1.25 x Base	0.80 x Base	million USD

Table 18 Optimistic and pessimistic drilling and completion parameters

Variable	Dimension	Optim.	Pessim.	Unit
Production column (Tubing size)	2 7/8”	276	193	USD/m
	3 1/2"	292	205	USD/m
	4 1/2"	313	219	USD/m
	5 1/2"	337	236	USD/m
Fixed vertical drilling and completion	-	26.38	18.28	million USD
Horizontal drilling and completion/ length	-	26481	18537	USD/m hor
Fixed horizontal drilling and completion	-	32.07	22.77	million USD

The base cases with UNISIM-I-H surface facilities limits are run to present a baseline of the optimization. The results are displayed in Table 20. The optimal results using MATLAB "fmincon" solver with 'sqp' algorithm and solver performances are shown in Table 21. The pessimistic case gives the highest NPV improvement from the base case which is 8.6%. This confirms that the field development optimization is a crucial tool to achieve the better asset management and maximize the asset's Net Present Value.

Table 19 Well-platform connection parameters

Variable	Dimension	Optim.	Pessim.	Unit
Production/ Injection Flowline	4"	514	360	USD/m
	6"	960	672	USD/m
	8"	2470	1729	USD/m
Riser	4"	1098	769	USD/m
	6"	1892	1324	USD/m
	8"	3247	2273	USD/m
Riser and flowline installation	-	14.63	10.24	million USD

Table 20 Base case results for various economic scenario

Case	Oil Processing (Sm^3/d)	Water Processing (Sm^3/d)	Water Injection (Sm^3/d)	NPV (USD)
Most likely	15500	13950	21700	3.30E+09
Optimistic	15500	13950	21700	5.22E+09
Pessimistic	15500	13950	21700	2.44E+09

Table 21 Optimization results for various economic scenario

Case	Oil Processing (Sm^3/d)	Water Processing (Sm^3/d)	Water Injection (Sm^3/d)	NPV (USD)	% Increase	Iteration/ Func Count
Most likely	13000	13000	13000	3.54E+09	7.3	4/51
Optimistic	13000	13000	13000	5.50E+09	4.4	3/46
Pessimistic	13000	13000	13000	2.65E+09	8.6	4/51

The optimization results on various economic scenario show that the optimal surface facilities capacities are the same for all cases. One observation has been made that the operational costs and investment are higher with the higher oil price. Although getting

more NPV value in the optimistic case, the optimal surface facilities limits are at the lower boundary we have set. This may be a result of a bottleneck in the well performances. The issue should be rectified during well type, size, and location picking.

The coupled optimization will also benefit the field development with the scheduled facilities expansion, for example, the forecast water production rate can have a significant effect on the investment. The decision can be made on the facilities design to delay the water production or to produce constant amount of water and that reflects the different processing facilities investment. The coupled model can be used to handle the unforeseen economic uncertainties, identify the production bottlenecks, decide well and connections to shut-in, perform feasibility study of the major debottlenecking, etc.

Although providing an increment in the asset's NPV, the optimization on the integrated model takes significantly high computational effort and time. Running one implicit coupling case optimization on the standard laptop takes 5 hours. Applying parallel computing on the commercial software and MATLAB may save one to two hours for each run. As a result, an optimization run can easily take an order of weeks to obtain the optimal solutions. This computational effort and time should be reduced, for example, the reservoir model reduction methodology should be applied in the integrated case. There is also an opportunity to modify the Python source code of the INTERSECT field management but the framework is not commercially available yet (Zhou, personal communication, March 17, 2017). The modification would incorporate the complex optimization techniques and improve the efficiency of the subsurface and surface coupling. Unfortunately, the editable source code was not provided during the time of this study.

Apart from surface facilities limitation, other parameters can also be optimized, for example, tubing size, flowline size, production rate, and injection rate. Different field development schemes can also be proposed and studied; i.e. gas reinjection, Water Alternate Gas injection (WAG), artificial lifts, etc. Choke should also be added to all the wells to have a better well rate allocation control. The integrated model developed in this study can be modified to get those results. The model can also be extended to cover the complex processing facilities which users will be able to manipulate between oil, gas, and water production based on the market demand and price.

6. CONCLUSIONS

In the volatile oil and gas business situations, optimization is one of the important tools that are being employed to maximize the financial value and improve the return on investment. Hydrocarbons extraction and production heavily depend upon the inner works of two major components: reservoir (subsurface) and production facilities (surface). In this thesis, we have performed an integration between subsurface reservoir simulator and the surface network simulator. Reservoir model used in this study is the UNISIM-I-D benchmark case developed by a research group at the University of Campinas, Brazil while we have generated the surface network model containing 14 producers and 11 injectors. The location of the platform was selected based on the location of the history matching well that gives the highest productivity index.

Commercial software has been used to model the reservoir, the network, and perform an integration; namely, ECLIPSE reservoir simulator, PIPESIM steady-state flow simulator, and INTERSECT field management node. MATLAB programming language has been used as an executor. MATLAB is able to initiate the study case, call the commercial simulators, and analyze the results after the runs have finished.

Based on the work performed in this thesis, we can conclude:

- There is a potential to maximize asset's Net Present Value by optimizing the surface facilities capacity. It can be seen that simulation run without surface limitations gives higher field oil recovery than the case run with base case surface

facilities capacity, but both give the same asset's Net Present Value. Imposing the limits provides stand-out results on produced water handling. It delays water breakthrough and gives better control on produced water.

- The optimal coupling scheme is a partially implicit coupling with the Newton Iteration Number = 3. Explicit coupling gives the fluctuation in the system due to the complexity in the equations convergence. Higher Newton Iteration Number provides more accurate results, but requires longer simulation run time; therefore, to optimize the run time with the available computational resources, Newton Iteration Number = 3 is used.
- The results obtained from the uncoupled and coupled simulation with base case limits are identical. The difference in the Net Present Value is 0.6%. The difference is not significant due to the fact that the fluids in the system are only oil and water without free gas and the flow system is treated in steady-state. As a result, no phase change that would affect the total pressure losses and flow performance. Intermittent flow that usually occurs in the gas-liquid system is also not taken into account.
- Sensitivity analysis shows the effects of individual parameters. It indicates that water injection capacity has the most impact on the asset's NPV. This guides us that the water injection wells placement can be improved and water injection capacity can be increased to gain more oil recovery.
- Optimization technique selected in this study is gradient-based optimization. The optimization has been carried out on MATLAB Optimization Toolbox™ using "fmincon" method with 'interior-point' and 'sqp' algorithm. The results confirm

the potential in field development optimization which resulting in the maximization of the asset's Net Present Value.

- Optimal results from uncoupled and coupled cases are different although having the same solutions. This confirms the importance of the subsurface and surface integration. It can be concluded that in the field development phase, integrated model gives the more accurate results compare to the individual simulations.
- Economic uncertainties have no effect on the optimal surface facilities capacity values. This shows that the bottleneck is at the production and injection wells, therefore, well location, well type, and tubing and flowline size should be redefined to further improve the asset's NPV. The improvement of NPV is higher in the case with lower oil price, thus, confirming the important of the field development optimization.

6.1. Future Work

- The coupled reservoir and choke model optimization should be performed to manage the back pressure from the gathering system. It is expected that with choke valves, we will see the better oil production from the high potential well while having less or delayed water production and the better NPV as a final result.
- Results from the explicit coupling case oscillate due to the improper selection of the timestep leading to the convergence issue. Any type of oscillation mitigation should be applied to the coupled model to obtain the suitable timestep; thus, getting the more accurate results from the explicit coupling. There is an effort

already taking place, which introduced a controller based on the PID scheme to reduce the oscillation (Akakpo and Gildin (2017)).

- The coupled model requires extensive computation since the coupled numerical model is bigger than the uncoupled one. Model reduction is expected to be applied to reduce the time required to solve the model.
- MATLAB codes in this study provide workflows on the calculation of economic parameters which closely link to some of the widely used simulators. Its ability is expected to be able to extend to cover the full field model i.e. including complicated surface facilities process and export. It should also be able to perform probabilistic cases to take uncertainties into account.
- This study works in the field development phase where the calculations and decision making can take a significant amount of time. Although the optimization of the integrated model requires high computational resources, it is still realistic to perform this optimization. However, once the model is used as a production optimization tool, the better computational tools, for example, High Performance Computing should be applied to overcome the simulations bottleneck.

REFERENCES

A.R. Hasan, and C.S. Kabir. 2002. Fluid Flow and Heat Transfer in Wellbores. Richardson, Texas, USA: SPE Textbooks Series, Society of Petroleum Engineers (Reprint).

A.S. Cullick, David Heath, Keshav Narayanan, Jay April, and James Kelly. 2003. Optimizing Multiple-Field Scheduling and Production Strategy with Reduced Risk. Proc., 2003 SPE Annual Technical Conference and Exhibition, Denver, Colorado, October 5-8, 2003. SPE 84239

A.T.F.S. Gaspar, G.D. Avansi, A.A. Santos, J.C.V. Hohendorff Filho, and D.J. Schiozer. 2015. UNISIM-I-D: Benchmark Studies for Oil Field Development and Production Strategy Selection (in International Journal of Modeling and Simulation for the Petroleum Industry 9 (1): 9.

Aleksander Juell, Curtis H. Whitson, and Mohammad Faizul Hoda. 2009. Model-Based Integration and Optimization - Gas Cycling Benchmark. Proc., 2009 SPE EUROPEC/EAGE Annual Conference and Exhibition, Amsterdam, The Netherlands, June 8-11, 2009. SPE 121252

Ana Teresa Gaspar, Alberto Santos, Célio Maschio, Guilherme Avansi, João Hohendorff Filho, Denis Schiozer. 2015. Study Case for Reservoir Exploitation Strategy Selection based on UNISIM-I Field, UNICAMP, Campinas (May 7, 2015).

Avansi, Guilherme D., and Schiozer, Denis J. 2015. UNISIM-I: Synthetic Model for Reservoir Development and Management Applications (in International Journal of Modeling and Simulation for the Petroleum Industry 9 (1): 10.

B. Guyaguler, and K. Ghorayeb. 2006. Integrated Optimization of Field Development, Planning, and Operation Proc., 2006 SPE Annual Technical Conference and Exhibition, San Antonio, Texas, U.S.A., September 24-27, 2006. SPE 102557

Célio Maschio, Guilherme Avansi, Denis Schiozer, ans Alberto Santos. 2015. Study Case for History Matching and Uncertainties Reduction based on UNISIM-I Field, UNICAMP, Campinas (April 14, 2015).

Cenk Temizel, and Aditya Tiwari. 2016. Integrated Asset Modeling through Multi-Reservoir Optimization of Offshore Fields using Next-Generation Reservoir Simulators. Proc., Offshore Technology Conference, Houston, Texas, USA, May 2-5, 2016. OTC-26981-MS

Chunhong Wang, Gaoming Li, and A.C. Reynolds. 2007. Optimal Well Placement for Production Optimization. Proc., 2007 SPE Eastern Regional Meeting, Lexington, Kentucky, USA, October 11-14, 2007. SPE 111154

D. Echeverría Ciaurri, O.J. Isebor, L.J. Durlofsky. 2012. Application of derivative-free methodologies to generally constrained oil production optimization problems (in ICCS 2010 1 (1): 10.

Dall'aqua, Marcelo Jacques. 2016. Application of Simple Smart Logic for Waterflooding Reservoir Management. Master of Science, Texas A&M University, College Station, Texas, USA (December 2016).

Dany Akakpo, and Eduardo Gildin. 2017. A Control Perspective to Adaptive Time-Stepping in Reservoir Simulation. Proc., SPE Reservoir Simulation Conference, Montgomery, Texas, USA, February 20-22, 2017. SPE-182601-MS

David Echeverría Ciaurri, Andrew R. Conn, Ulisses T. Mello, and Jerome E. Onwunalu. 2012. Integrating Mathematical Optimization and Decision Making in Intelligent Fields. Proc., SPE Intelligent Energy International, Utrecht, The Netherlands, March 27-29, 2012. SPE 149780

Denis J. Schiozer, and Cristina C. Mezzomo. 2003. Methodology for Field Development Optimization with Water Injection. Proc., SPE Hydrocarbons Economics and Evaluation Symposium, Dallas, Texas, USA, April 5-8, 2003. SPE 82021

Ertekin, Turgay, Abou-Kassem, J.H., and King, G.R. 2001. Basic Applied Reservoir Simulation. Richardson, Texas, USA: SPE Textbook Series, Society of Petroleum Engineers (Reprint).

Feroney Serbini, Low Kok Wee, Lee Hin Wong, and Nicolas Gomez. 2009. Integrated Field Development - Improved Field Planning and Operation Optimization. Proc., International Petroleum Technology Conference, Doha, Qatar, December 7-9, 2009. IPTC 14010

G. Gokhan Hepguler, and Kunal Dutta-Roy. 1997. Applications of a Field Surface & Production Network Simulator Integrated with a Reservoir Simulator. Proc., SPF Reservoir Simulation Symposium, Dallas, Texas, June 8-11, 1997. SPE 38007

G. Gokhan Hepguler, Santanu Barua, and Wade Bard. 1997. Integration of a Field Surface and Production Network with a Reservoir Simulator (in SPE Computer Applications: 6.

Gao, Mengdi. 2014. Reservoir and Surface Facilities Couples Through Partially and Fully Implicit Approaches. MS thesis, Texas A&M University, College Station, Texas (December 2014).

Iemcholvilert, Sevaphol. 2013. A Research on Production Optimization of Coupled Surface and Subsurface Model. MS thesis, Texas A&M University, College Station, Texas (August 2013).

Isebor, Obiajula J. 2013. Derivative-Free Generalized Field Development Optimization. Proc., SPE Annual Technical Conference and Exhibition, New Orleans, Louisiana, USA, September 30 - October 2, 2013. SPE 167633-STU

Jialing Liang, and Barry Rubin. 2014. A Semi-Implicit Approach for Integrated Reservoir and Surface-Network Simulation (in SPE Reservoir Evaluation & Engineering: 13.

Jorge Nocedal, and Stephen J. Wright. 2006. Numerical Optimization. New York, USA: Springer Series in Operation Research and Financial Engineering, Springer (Reprint).

Lianlin Li, and Behnam Jafarpour. 2012. A variable-control well placement optimization for improved reservoir development (in Computational Geosciences 16 (4): 19.

Lie, Knut-Andreas. 2016. An Introduction to Reservoir Simulation Using MATLAB: User Guide for the MATLAB Reservoir Simulation Toolbox (MRST). Oslo, Norway, SINTEF ICT, Department of Applied Mathematics (Reprint).

Marcio Augusto Sampaio Pinto, Mohammadreza Ghasemi, Nadav Sorek, Eduardo Gildin, and Denis José Schiozer. 2015. Hybrid Optimization for Closed-Loop Reservoir Management. Proc., SPE Reservoir Simulation Symposium, Houston, Texas, USA. SPE-173278-MS

MathWorks. 2016. MATLAB Documentation. In, ed MathWorks Inc.

Michael J. Economides, A. Daniel Hill, Christine Ehlig-Economides, Ding Zhu. 2013. Petroleum Production Systems, 2nd edition. Upper Saddle River, New Jersey, USA, Pearson Education, Inc. (Reprint).

Michael Litvak, Brian Gane, Glyn Williams, Mark Mansfield, Patrick Angert, Chris Macdonald, Lesley Mcmurray, Roger Skinner, and Greg J. Walker. 2007. Field Development Optimization Technology. Proc., 2007 SPE Reservoir Simulation Symposium, Houston, Texas, USA, February 26-28, 2007. SPE 106426

Michael Litvak, Jerome Onwunalu, and Josh Baxter. 2011. Field Development Optimization with Subsurface Uncertainties. Proc., SPE Annual Technical Conference and Exhibition, Denver, Colorado, USA, October 30 - November 2, 2011. SPE 146512

Pallav Sarma, and Wen H. Chen. 2008. Efficient Well Placement Optimization with Gradient-Based Algorithms and Adjoint Models. Proc., 2008 SPE Intelligent Energy Conference and Exhibition, Amsterdam, The Netherlands, February 25-27, 2008. SPE 112257

R. Moraes, R.M. Fonseca, M. Helici, A.W. Heemink, J.D. Jansen. 2017. Improving the Computational Efficiency of Approximate Gradients Using a Multiscale Reservoir Simulation Framework. Proc., SPE Reservoir Simulation Conference, Montgomery, Texas, USA, February 20-22, 2017. SPE-182620-MS

Sara Scaramellimi, Paolo Cerri, Amalia Bianco, and Silvia Masi. 2015. Short-term Production Operation Management: Continuous Application of an Innovative Integrated Production Optimization Tool. Proc., SPE Annual Technical Conference and Exhibition, Houston, Texas, USA, September 28-30, 2015. SPE-174915-MS

Schlumberger. 2014. ECLIPSE Reference Manual. In ECLIPSE Industry-reference reservoir simulator, ed Schlumberger.

Schlumberger. 2015. INTERSECT User Guide. In INTERSECT High-resolution reservoir simulator, ed Schlumberger.

Schlumberger. 2015. PIPESIM User Guide. In PIPESIM Steady-state multiphase flow simulator, ed Schlumberger.

Schlumberger. 2015. INTERSECT Technical Description. In INTERSECT High-resolution reservoir simulator, ed Schlumberger.

Silvya Dewi Rahmawati, Curtis Hays Whitson, Bjarne Foss, Arif Kuntadi. 2010. Multi-Field Asset Integrated Optimization Benchmark. Proc., SPE EUROPEC/EAGE Annual Conference and Exhibition, Barcelona, Spain, June 14-17, 2010. SPE 130768

Silvya Dewi Rahmawati, Curtis Hays Whitson, Bjarne Foss, Arif Kuntadi. 2012. Integrated field operation and optimization (in Journal of Petroleum Science and Engineering 81: 10.

Silvya Dewi Rahmawati, Mohammad Faizul Hoda, Daniel Wagner, and Arif Kuntadi. 2014. Mix-n-match Reservoir Coupling in Integrated Modeling and Optimization. Proc., International Petroleum Technology Conference, Kuala Lumpre, Malaysia, December 10-12, 2014. IPTC-17727-MS

Trick, M.D. 1998. A Different Approach to Coupling a Reservoir Simulator with a Surface Facilities Model. Proc., 1998 SPE Gas Technology Symposium, Calgary, Alberta, Canada, March 15-18, 1998. SPE 40001

V.E. Botechia, A. T. Gaspar, and D.J. Schiozer. 2013. Use of Well Indicators in the Production Strategy Optimization Process. Proc., EAGE Annual Conference &

Exhibition incorporating SPE Europec, London, United Kingdom, June 10-13, 2013. SPE 164874

Z.X. Ding, and R.A. Startzman. 1996. A Software System for Oilfield Facility Investment Minimization (in SPE Computer Applications: 6.

Zhou, Wentao. (2017, March 17). E-mail. IX Coupling Meeting.